

Consortium of Universities for the Advancement of Hydrologic Science, Inc.

TECHNICAL REPORT 14
October 9th, 2017



OWP | OFFICE OF
WATER
PREDICTION



National Water Center
Innovators Program
Summer Institute Report 2017

National Water Center Innovators Program

Summer Institute Report 2017

Editors:

J. Michael Johnson
James M. Coll
David R. Maidment
Sagy Cohen
Jim Nelson
Fred Ogden
Sarah Praskiewicz
Edward P. Clark

Prepared in cooperation with the Consortium of Universities for the Advancement of Hydrologic Science, Inc. and the National Water Center

CUASHI Technical Report No. 14

DOI: 10.4211/technical.20171009

Version 1.02

October 9th, 2017

Suggested Citation:

Johnson J. M, Coll J M, et al. 2017. National Water Centers Innovators Program Summer Institute Report. Consortium of Universities for the Advancement of Hydrologic Science, Inc. Technical Report No 14.

Contents

| | |
|--|----|
| Preface: | 2 |
| Project Summary: | 4 |
| Chapter 1: ADHydro Introduction and Workflow | 6 |
| Chapter 2: Comparison of Coarse and high-resolution Hydrologic Modeling in Mountainous Areas | 14 |
| Chapter 3: Hyper-resolution Modeling in Urban Landscapes | 23 |
| Chapter 4: Evaluating the Performance of a Hyper-resolution Model in a Low Gradient Watershed..... | 32 |
| Chapter 5: Integrity Check of Synthetic Rating Curves for HAND Inundation Mapping | 39 |
| Chapter 6: Comparing NWM Inundation Predictions with Hydrodynamic Modeling | 49 |
| Chapter 7: Framework for Statistical Analysis and Visualization of the National Water Model Streamflow Product | 58 |
| Chapter 8: Using the National Water Model Forecasts to Plan for and Manage Ecological Flow and Low-Flow during Drought | 66 |
| Chapter 9: Using Public Input to Create a Better Online Flood Mapping Framework | 75 |
| Chapter 10: FloodImpact: A Web Application to Identify Flood Extent and Community Vulnerabilities for Real-time Weather Forecasts..... | 85 |
| Appendix: | 95 |

Preface:

The Consortium of Universities for the Advancement of Hydrologic Science, Inc. (CUAHSI) consists of 110 member universities in the U.S. This NSF-funded consortium exists to advance hydrologic science through broad initiatives across the academic community. The Office of Water Prediction of the NOAA National Weather Service has established a National Water Center on the Tuscaloosa campus of the University of Alabama to serve as the hub for the building of a National Water Model of the United States. NOAA has also established a National Water Center Innovators Program with CUAHSI to engage the academic community in research to advance the mission of the NOAA National Weather Service Office of Water Prediction at the National Water Center.

The key activity of the Innovators Program is a seven week Summer Institute at the National Water Center, bringing graduate students and faculty advisors together with National Water Center staff to conduct group projects that involve rapid prototyping of new ideas. The intent is to create an innovation incubator where students from many universities can exchange ideas and advance concepts that, although developed over a short timeframe and study areas, are illustrative of issues that affect the functioning of the National Water Model across the continental United States. This year's Summer Institute was held from June 6th to July 28th, 2017, and involved 32 graduate students drawn from 25 universities.

The first activity of the Summer Institute was an all-day focus on emergency response, highlighted by the Mayor of Tuscaloosa, Walter Maddox, describing his experiences in responding to the 2011 tornado that devastated Tuscaloosa. Rob Robertson, Emergency Management Coordinator for Tuscaloosa County, and Whitney Henson of the National Water Center led a flood emergency response exercise. The students took on the roles of Police, Fire, Public Works and Non-Governmental Organizations in a simulation of a breach of the Northport Levee and the resulting flooding of the City of Northport, which lies just on the other side of the Black Warrior River from the National Water Center. First response personnel gave a field demonstration of a water rescue from a nearby creek using a ladder truck. These experiences gave the students a first-hand impression of the activities that first responders undertake during actual flood emergencies.

The 2017 Summer Institute was led by five theme coordinators: Fred Ogden of the National Water Center and the University of Wyoming, Jim Nelson of Brigham Young University, Sagy Cohen and Sarah Praskiewicz of the University of Alabama, and David Maidment of the University of Texas at Austin. Two Student Coordinators helped with organization and execution of the projects: Jim Coll from the University of Kansas and Mike Johnson from the University of California, Santa Barbara. Several National Water Center staff provided guidance for particular projects: Ed Clark, Trey Flowers, Fernando Salas, Nathan Swain, Brad Bates and Whitney Henson. During the first week of the Summer Institute, fieldwork experiences for the students were assisted by operation of a rainfall simulator by Edward Kempema of the University of Wyoming, and of stream measurement equipment by John Sloat of WaterCube, Daniel Wagenaar of SonTek, Inc (Xylem), and Lisa Landry of YSI, Inc. (Xylem). In addition, Jim Coll demonstrated operation of a drone and Sarah Praskiewicz demonstrated operation of a high precision survey-grade GPS.

Educational and technical support for the hyper-resolution modeling theme was provided by Chuck Downer and Steve Turnbull of the US Army Corps of Engineers, Engineer Research and

Development Center, who led a three-day GSSHA modeling workshop. Ehab Meselhe of the Water Institute of the Gulf assisted with student projects related to numerical modeling of open channel hydraulics. Bob Steinke and Nels Frazier of the University of Wyoming held a three-day ADHydro model workshop, and provided technical support of student projects, and helped the students run jobs on the Univ. of Wyoming Advanced Research Computing Cluster, and the NCAR-Wyoming Yellowstone supercomputer. Project guidance and organization were guided by the USGS Center for Integrated Data Analytics which included Alison Appling, Jordan Read, Emily Reed, Jordan Waker, and David Watkins. Additional expertise was provided by Bill Guertal, John McNary, and Marie Peppler. Jon Nania of the Iowa USGS office also contributed his guidance and expertise to the student projects.

It can be appreciated that an activity of this magnitude involves a great deal of organization. Jerad Bales and Emily Clark of CUAHSI, and Pamela Harvey of the University of Alabama, were the main people who helped with the institutional arrangements and with travel, housing, and living arrangements in Tuscaloosa. University of Alabama Students Dinuke Munasinghe and James Misfeldt assisted with field activities and student projects. The contribution from all Univ. of Alabama support is greatly appreciated.

A key to the success of the National Water Center Innovators Program is the support it receives through the voluntary collaboration of the academic community, along with commercial and government partners. David Maidment wishes to acknowledge that his contribution to this research was supported by the University of Texas at Austin, and by the Kisters water data management firm. Altogether, over the three Summer Institutes held since the inaugural event in 2015, more than one hundred graduate students have had the experience of working together at the National Water Center in group research projects. Aside from the technical progress that they make, equally important are the friendships formed and professional networks established among the Summer Institute participants that they carry with them into the future. This is a unique and valuable professional experience, and we express our appreciation to the NOAA National Weather Service for hosting and supporting this innovative activity and this opportunity to contribute to the enhancement of water prediction for our nation.

David Maidment, Sagy Cohen, Jim Nelson, Fred Ogden, Sarah Praskiewicz
Theme Leaders, National Water Center Innovators Program Summer Institute 2017

Project Summary

In August of 2016, the National Water Model became operational marking an unprecedented effort that rightfully challenges the way research can be done and the way hydro-intelligence can benefit society. This modeling framework has also introduced ways in which interdisciplinary research surrounding water resources can be done. By providing river forecasts for 2.7 million reaches within CONUS, the NWM provides a nerve center in which two previously distinct groups - ‘data generators’ and ‘data users’ - can unite to answer new questions in a time where population pressures and a changing climate make water management more paramount.

‘Data generators’ have traditionally included the modeling community, who are interested in ensuring the data is as accurate as possible in as many places as possible, and ‘data users’ are those who use this data to communicate, plan, and study emerging properties grounded in water resources. With the NWM serving as common platform to both generate and provide data, these groups can interact in ways that result in a more accurate models and more robust applications. Capitalizing on this opportunity, the third Summer Institute at the National Water Center brought together 32 students from 25 universities ranging from California to New York with backgrounds across a breadth of fields. Through an intensive seven week stretch, these students, with the help of theme leaders, industry professionals, and government researchers, demonstrated how these two previously distinct groups can not only come together under the framework of the NWM, but how their knowledge and experience can integrate, supplement, and improve each other’s work. In total, nine projects were executed that can thematically be grouped under the domains of hyper-resolution modeling, flood inundation mapping, and communicating NWM results. Combined, they explore questions relating to the implementation of hyper resolution models, how output data be leveraged and validated, and how outputs can be leveraged to serve society.

Chapter 1 of this report introduces a new hyper-resolution (sub-100 m horizontal resolution) model called the “ADaptive Hydrological model”, or ADHydro for short. This quasi-3D model, which was developed to simulate large watersheds on a supercomputer and operates on an unstructured mesh providing variable resolution across the modeling domain. In total 10 students worked closely with the development team from the University of Wyoming to evaluate this model. At the end of the summer these groups mark the first individuals to successfully generate meaningful results from ADHydro and helped showcase its potential in three specific areas that are traditionally hard to model. **Chapter 2** illustrates a case study in Colorado’s Animas basin which tests how ADHydro performs in comparison to NWM in areas dominated by snowmelt and steep terrain. They were particularly interested in evaluating the effect of spatial resolution on snow water equivalent and discharge over the watershed. The authors of the **chapter 3** focused their efforts on an urban watershed in Baltimore which takes into account building footprints, and **chapter 4** investigated ADHydro’s performance in a watershed with low topographic relief in Southern Louisiana.

Another group of students evaluated methods for converting forecasted discharge into inundation maps. The authors of **chapter 5** picked up on the previous work for HAND inundation mapping using synthetic rating curves and developed a framework that not only validates these synthetic curves across the spatial domain of CONUS but also proposes a suite of correction methodologies to improve the terrain derived rating curves in underperforming areas. The authors of **chapter 6** were interested in improving flood inundation predictions from the National Water Model and

hypothesized the NWM would not accurately capture the backwater effects of Hurricane Matthew along the Neuse river. Instead they implemented a steady state model, SPRNT, to generate discharge and stage values. They used the HAND method to generate flood inundation maps from both SPRNT and NWM discharge values and validated them against a remotely sensed image acquired through a new approach for detecting floods.

Two groups worked to evaluate the accuracy and applications of the first 23-year retrospective run of NWM v1.0. The authors of **chapter 7** approached the retrospective data from a statistical vantage point and built a Tethys application to compare the retrospective data to USGS station data. Their application offers both a graphical representation of the data along with a suite of statistical metrics to assess how well the model is performing, both at an individual reach and CONUS-wide. The authors of **chapter 8** took a more applied approach and created a Tethys application which uses the NWM long-range forecasts to visualize and warn of potential low flow conditions, whose definitions are derived from the retrospective record. They also created a package in R for processing retrospective data and evaluating model performance.

The final two groups focused on communicating and understanding how communities and individuals understand and can respond to the information. **Chapter 9** administered a set of surveys to the public to better understand public perceptions surrounding floods and flooding risk. Feedback from each survey helped produce a conceptual framework for a set of inundation maps for Baton Rouge, LA and Dallas, TX. In the end, they proposed a map structure that public believed to be more concise and effective than current products. The authors of **Chapter 10** developed a web-based application that integrates flood forecasts with potential social impacts. The application uses GSSHA to model inundation based on real-time precipitation forecasts, and a Tethys-based front-end to display on-the-fly estimates of the people and places potentially threatened by an impending flood.

The students of the 2017 Summer Institute have been an absolute pleasure to work with and all successes are a testament to their work ethic, ability to collaborate, and dedication to spend their summer away from family. The breadth of their work and respective backgrounds highlights the impact a community model can have on bringing scientist together. They have all contributed towards a goal of changing how water resources research is carried out and how citizens can engage with their water circumstance. More so their relationships have brought the academic domain a bit closer through relationships that will last a career.

The reports published here represent the culmination of seven weeks of research, and present a platform not only for these students to continue pushing forward with their advisors, each other and the NWC, but for the rest of the community, whether ‘data-generators’ or ‘data-users’, to become more engaged in the development of the NWM.

J Michael Johnson

Student Coordinator, National Water Center Innovators Program Summer Institute 2017
Department of Geography, University of California, Santa Barbara

James M. Coll

Student Coordinator, National Water Center Innovators Program Summer Institute 2017
Department of Geography and Atmospheric Sciences, University of Kansas

Chapter 1

ADHydro Introduction and Workflow

Jason Chang¹, Irene Garousi-Nejad², Lauren Grimley³, Siwei He⁴, Mariam Khanam⁵, Tyler Madsen⁶, Qicheng Tang⁷, Eddie Tiernan⁸, Danielle Tijerina⁹, Chris Turnipseed¹⁰

¹ University of Florida, snjason@ufl.edu

² Utah State University, i.garousi@aggiemail.usu.edu

³ University of Iowa, lauren.grimley@uiowa.edu

⁴ University of Wyoming, she@unyo.edu

⁵ University of Alabama, mkhanam@crimson.ua.edu

⁶ Iowa State University, madsen@iastate.edu

⁷ Pennsylvania State University, qut9@psu.edu

⁸ University of Texas at Austin, etiernan@utexas.edu

⁹ Colorado School of Mines, dtijerina@mines.edu

¹⁰ Louisiana State University, christopherturnipseed@gmail.com

Academic Advisors: Wendy Graham, *University of Florida*; David Tarboton, *Utah State University*; Witold F. Krajewski, *University of Iowa*; Noriaki Ohara, *University of Wyoming*; Sagy Cohen, *University of Alabama*; Kristie J Franz, *Iowa State University*; Henry Lin, *Pennsylvania State University*; Ben R Hodges, *University of Texas at Austin*; Reed Maxwell, *Colorado School of Mines*; Clinton S Willson, *Louisiana State University*

Summer Institute Theme Advisor: Fred Ogden, University of Wyoming, fogden@unyo.edu

1. Introduction to the Model

ADHydro is a high-resolution, physics-based, quasi-3D, hydrologic model that utilizes an unstructured mesh. Developed in a parallel computing environment by the CI-WATER research team at the University of Wyoming⁽¹⁾, the characteristics of this model include: 1) an innovative method for modeling vadose zone dynamics, 2) a water management module considering reservoirs, diversions, and irrigation, 3) a coupled scheme to estimate interception, evaporation, and snow processes through the community Noah Land Surface Model (LSM) with multi-parameterization options (Noah-MP)^(2, 3) and 4) the capability to ingest downscaled atmospheric forcing from the Weather Research and Forecasting (WRF) meteorological model using the CHARM++ parallel programming environment. More information on the physical process of ADHydro are summarized in the following sections.

1.1 Interception, Evapotranspiration, and Snowmelt

The interception, evapotranspiration, and snow melt processes are simulated using the Noah-MP model^(2, 3). The Noah-MP model considers biophysical processes such as interactive vegetation canopy, multilayer snow pack and soil, overland runoff, and unconfined aquifers with dynamic water tables for underground storage. Its major components include 1-layer canopy, 3-layer snow, and 4-layer soil. In Noah-MP, precipitation is partitioned into rainfall and snowfall. Using surface-air temperature as a criterion, the canopy water scheme simulates the canopy water interception and evaporation, and the “semitile” sub-grid scheme calculates the skin temperature of the canopy and

snow/soil surface separately using an interactive energy balance method. Snow and soil layer temperatures are used to assess the energy for melting and freezing for the snow and soil layers.

1.2 Routing

The overland flow can be simulated using dynamic wave or diffusive wave shallow water equations (SWEs), which include one mass conservation equation and one momentum equation. In this model, 2D SWEs with the diffusive wave approximation are used for the overland flow routing. Diffusion wave approximation assumes the velocity terms are negligible and it is applicable in situations where Froude number is small.

$$\frac{\partial h}{\partial t} = \frac{\partial}{\partial x} \left(h k \frac{\partial Z}{\partial x} \right) + \frac{\partial}{\partial y} \left(h k \frac{\partial Z}{\partial y} \right) + q_s \quad (1)$$

$$k = \frac{h^{\frac{2}{3}}}{n} \left(\frac{1}{\sqrt{\frac{\partial Z}{\partial s}}} \right) \quad (2)$$

Where δs is in the direction of the maximum slope, and n is Manning's roughness coefficient.

1D SWEs, which are also known as Saint-Venant equations, are used for the channel routing method in this model,

$$\frac{\partial A}{\partial Q} + \frac{\partial Q}{\partial x} = q_x \quad (3)$$

$$\frac{\partial Q}{\partial t} + \frac{\partial Q^2}{A} = -gA \frac{\partial Z}{\partial x} - gAS_f \quad (4)$$

Where A is cross section area of the channel, and Q is volumetric flow rate.

For lakes and reservoirs, the reservoir routing method is used,

$$\frac{dS}{dt} = I - O + R - E - S_p + O_l \quad (5)$$

Where S is volume of storage in the reservoir, I is inflow, O is outflow, R is rainfall, E is evaporation, S_p is seepage, and O_l is lateral overland flow.

1D SWEs, which are also known as Saint-Venant equations, are used for the channel routing method in this model. For lakes and reservoirs, the reservoir routing method is used. 2D overland flow feeds

into 1D channels and the discharge is calculated by an empirical equation that was proposed by Blade et al.⁽⁴⁾ for the natural channels.

$$Q = \begin{cases} KL(z_1 - z_w)\sqrt{2g(z_1 - z_w)}, & \frac{2}{3}(z_1 - z_w) \geq (z_2 - z_w) \\ 2.6KL(z_2 - z_w)\sqrt{2g(z_1 - z_w)}, & \frac{2}{3}(z_1 - z_w) < (z_2 - z_w) \end{cases} \quad (6)$$

z_1 is headwater surface elevation, z_2 is tailwater elevation, and z_w is weir crest elevation, L , is the length of 1D channel element in contact with 2D mesh edge, and K is a constant (generally $0.3 < K < 0.6$)⁽⁵⁾.

1.3 Subsurface Flow

The subsurface flow in this model is simulated with a quasi-3D flow scheme, which includes the 1D infiltration in the unsaturated zone and the 2D horizontal flow in the saturated zone. The 1D infiltration and redistribution method in the discretized moisture content domain (i.e. the unsaturated zone) is the Green-Ampt with Redistribution - Talbot-Ogden, proposed by Ogden et al.⁽⁶⁾ and Talbot and Ogden⁽⁷⁾.

$$\frac{dZ_j}{dt} = \frac{K(\theta_d) - K(\theta_i)}{\theta_d - \theta_i} \left(1 + \frac{|h(\theta)| + h_p}{Z_j} \right) \quad (7)$$

Where Z_j is position of surface wetting front of bin j , θ_i is initial water content or the water content of the first bin that is not fully saturated between the groundwater table to the surface, and θ_d is the water content of the right-most bin in the surface wetting front that contains water. $K(\theta_i)$ and $K(\theta_d)$ are the unsaturated hydraulic conductivity of the θ_i and θ_d bins, respectively, h_p is depth of surface ponding, and $h(\theta_d)$ is the capillary pressure of θ_d bin. The movement of a groundwater wetting front can be described by,

$$\frac{dZ_j}{dt} = \frac{K(\theta_j) - K(\theta_i)}{\theta_j - \theta_i} \left(1 - \frac{|h'(\theta_j)|}{D_j} \right) \quad (8)$$

Flow in the saturated zone is simulated using the 2D unconfined aquifer groundwater governing equation, which is also known as the Boussinesq equation.

$$S_y \frac{\partial h}{\partial t} = \frac{\partial}{\partial x} \left(K_x h \frac{\partial H}{\partial x} \right) + \frac{\partial}{\partial y} \left(K_y h \frac{\partial H}{\partial y} \right) + R \quad (9)$$

Where H is total groundwater hydraulic head, h is groundwater depth, K_x and K_y are hydraulic conductivity, R is the vertical recharge rate to the saturated surface, and S_y is the specific yield.

The interaction between channel and groundwater is simulated by a method that was proposed by Gunduz and Aral⁽⁸⁾, and the flow direction depends on the river water surface elevation and the groundwater head.

$$q_L = \begin{cases} K_r w_r \frac{Z_r - H}{\Delta z_b}, & H > z_b - \Delta z_b \\ K_r W_r \frac{h + \Delta z_b}{\Delta z_b}, & H \leq z_b - \Delta z_b \end{cases} \quad (10)$$

Where K_r is river bottom sediment conductivity, w_r is river bed wetted perimeter, Δz_b is the river bed thickness, Z_r is river water surface elevation, H is groundwater head.

1.4 Water Management

The emphasis of the water management module is placed on the engineered aspects of water management and use. This is where storage reservoirs, diversions, and irrigation are simulated. Statistical based methods and operation rules based optimization methods are used. Typical constraints and rules include maximum and minimum elevations, target elevations for wet and drought seasons, maximum and minimum releases, and contractual, legal, and institutional obligations. Interactions between reservoirs and river/aquifer system are also considered.

2. Pre-Processing

Before ADHydro is run, there is a necessary process to create the triangulated irregular network (TIN) that the model's engine actually computes on. This pre-processing stage of using ADHydro is the most labor-intensive, but the quality of the mesh produced in these steps dramatically affects the effectiveness of the ADHydro model runs. For example, the “wall clock multiplier”, which is a measure of how much faster the model runs than real time, is largely a function of the homogeneity of mesh elements created in the pre-processing stage.

2.1 TauDEM Stream and Catchment Delineation

The initial step of ADHydro preprocessing is stream and catchment delineation, which was completed through the use of TauDEM (Terrain analysis using Digital Elevation Models), within the ArcGIS Toolbox. TauDEM, developed by Tarboton et al.⁽⁹⁾ extracts and manipulates data from Digital Elevation Maps (DEM) for utilization in hydrologic and hydraulic modeling. Features include the removal of pits, and computation of flow direction and contributing area in DEMs. The outputs of TauDEM are the initial catchment and stream network shape files (.shp).

2.2 ArcGIS smoothing

These initial catchment, stream network, and NHD waterbodies files are then refined in ArcGIS through the use of the Topological Tool. The refining process includes steps to ensure the catchment and shape files have no geometric gaps and do not overlap. This creates contiguous shapefiles which in aggregate form a complete watershed. Also, through ArcGIS specific regions of a watershed can be refined further for a higher resolution in the subsequent mesh. It is in this step that the “mesh resolution” is set. That is, for a specific resolution, ArcGIS removes or interpolates vertices in the shapefile that are less spatially discrepant than the resolution tolerance. In this way, the minimum triangle edge possible is the resolution tolerance. The outputs of the ArcGIS smoothing are the initial files for the mesh creation.

2.3 Triangle Mesh Creation

The refined catchment, waterbody, and stream network files are then used in the creation of a 2D, unstructured mesh (**Figure 1**) through a program called Triangle. Triangle, developed by Shewchuk⁽¹⁰⁾, creates several ASCII files which define the triangular elements and their relations. These ASCII files are then utilized by ADHydro as a computational domain, which the subsequent meteorological forcing data is applied over. However, before a simulation, physical parameters must be interpolated onto the newly created mesh. The parameters include a digital elevation map (DEM) from the National Elevation Dataset (NED), land use maps from the National Land Cover Database (NLCD), and soil data from the Natural Resources Conservation Service (NRCS).

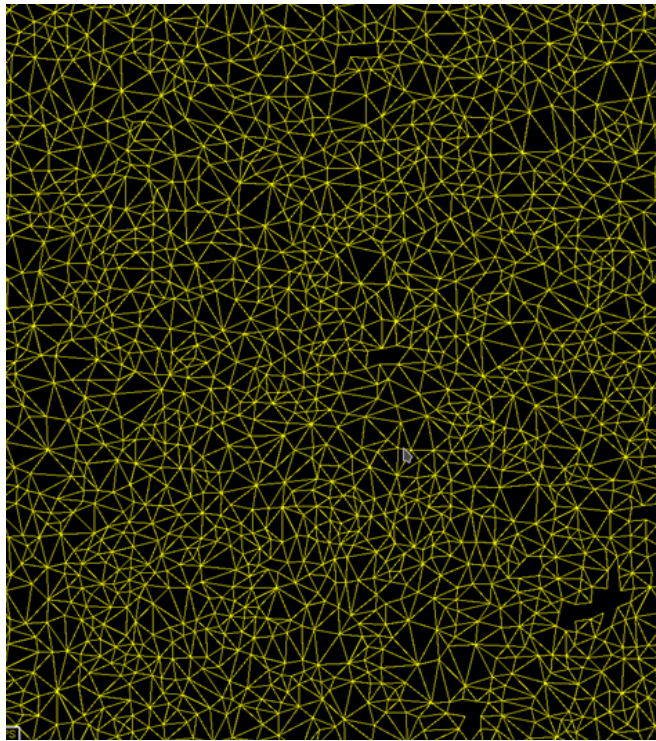


Figure 1. Example of a mesh created by Triangle program, Mermentau River Basin.

3. Processing

The workflow for running a simulation with ADHydro is still under development, and the modeling software itself does not yet have an ordained processing graphical user interface. The distributed nature of ADHydro causes outputs to be computationally expensive to obtain, and as a consequence ADHydro is most effectively run by parallelizing the I/O and operations within a supercomputing environment. Traditionally, supercomputing environments are driven by command line prompts and not executions within a GUI, which helps explain why the development of a graphical platform for ADHydro has not been a priority. A number of existing platforms and methods must be employed to initially create the distributed network that ADHydro will run on, as well as myriad custom-made scripts. A disclaimer that must be at this juncture is the conspicuous lack of a parameter calibration process once the mesh is created and before the model is run. That due diligence process would be

necessary for a publication-worthy hydrologic study, but was not included in the tests of ADHydro described in the following chapters.

3.1 Mesh Massage

After the cumbersome pre-processing steps have been completed, and the triangle meshes with joined elevation, soils, and land cover data are organized within an ASCII folder, the procedure for actually running the ADHydro model may commence. In the model command script, called a "superfile", the ASCII mesh files are set as inputs, and a model setting called "mesh massage" is activated. The purpose of this, additional, pre-modeling step is to ensure that each triangle catchment has somewhere to drain, and warnings are thrown if any catchments are behaving as "digital dams" from which water cannot escape. If these digital dams are occurring, there is likely an error in the triangle creation, and the pre-processing steps must be revisited. By doing this check before putting any water into the modeled system, much computational headache and confusion can be avoided. The mesh massage is the initial step of what is essentially a four-stage model running methodology⁽⁵⁾.

3.2 Drain Down

The second step of the model running methodology is to synthetically introduce a groundwater moisture initial condition into the system. Creating this groundwater initial condition can dramatically decrease the amount of "spin-up" time a model needs before it can output trustworthy data. This groundwater moisture initialization step is called the "drain down" step, and is conducted similarly to the mesh massage, with a model setting activated within the job superfile. A key difference, however, is that the drain down accepts, as inputs, the geometry and parameter NetCDF files containing the mesh information created in the mesh massage stage (converted from ASCII format), and its output is updating the state and display NetCDF files, as well as copying over the geometry and parameter files into the output directory. Another difference is that, in order to successfully run the drain down, forcing data must be provided. The implementation of forcing data in the drain down phase is a little counter-intuitive; the drain down takes the forcing data (sans precipitation) from the first-time instance, and assumes that forcing state persists for two days. Additionally, the drain down setting artificially saturates the catchment at the beginning of the simulation. In this way, the drain down can isolate two modules of the ADHydro model, infiltration and evapotranspiration, such that water is only leaving the catchment, and a plausible groundwater moisture condition is left behind. Time is allowed to "advance" only in the model, without any calendar advancement of forcing data occurring⁽⁵⁾.

3.3 Spin-Up

The second to last step of the ADHydro modeling workflow is a critical, correctional step known as the spin-up. A spin-up period is commonly used in the modeling world to ensure that the initial conditions are as realistic as possible. While the drain down helps create a physically real groundwater condition, that cannot be assumed to accurately represent the initial condition of the catchment before the storm event of interest. Several studies have shown model sensitivity to initial conditions such that removing uncertainty in those conditions is now considered an important step in any modeling process. The spin-up is computationally identical to the actual model step (in terms of using forcing as the impetus for run-off), with the sole difference being that the output, updated state and display NetCDF files, aren't considered valid approximations of the catchment behavior. A rule of thumb for spin-up duration is two weeks, but there is no general consensus for this rule and more studies on

the sensitivity of initial conditions to spin-up duration are needed. When the amount of spin-up time required exceeds the forcing data available, one potentially useful strategy is to feed the preliminary spin-up output back into the same forcing loop, and repeat until convergence is reached⁽⁵⁾.

3.4 Model Runs

Once appropriate initial conditions have been approximated, the actual storm period can be simulated (**Figure 2**). This simulation duration can be as long as necessary to fully capture the catchment response behavior. The model run step has the same format as the spin-up, accepting the output of the spin-up as the initial conditions, and a continuation of the forcing data to drive the model. The output of the model run is once again update state and display NetCDF files. After the model is run and the output data is obtained, useful results can be visualized using a number of conversion scripts and different visualization platforms⁽⁵⁾.

4. Post-Processing

Post-processing of ADHydro output can take many forms depending upon what the user's desired result is. However, the three groups collaborating on this workflow were primarily interested in streamflow behavior at the outlet of their respective catchments, so hydrographs were the desired deliverable. A python script was used to read the streamflow from the state NetCDF output and plot the data over time.

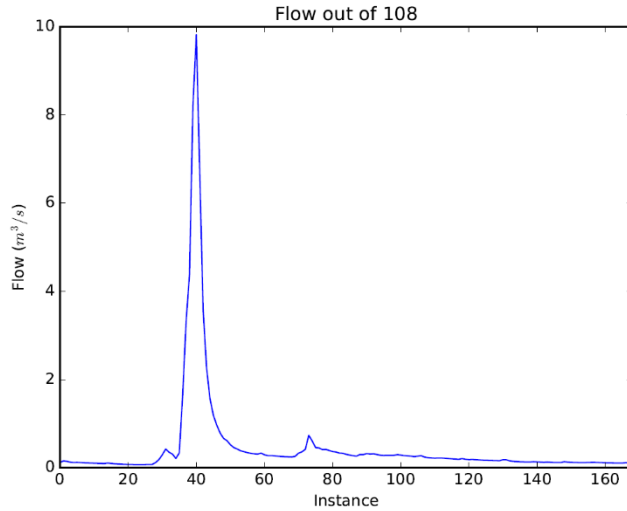


Figure 2. Example of the output of `mesh_hydrograph.py` script for Dead Run channel element 108. Shows the flow vs given time instance, in this case hours after midnight on May 4, 2017.

4.1 ParaView

For other post-processing needs, .xdmf files can be created using a C++ program to act as a medium by which a visualization program, such as ParaView, can be used to create animations of several state variables over time in the mesh or channel shapefiles (**Figure 3**). This was used to create maps and animations of the peak flood extent for the storms of interest within each group's watershed.

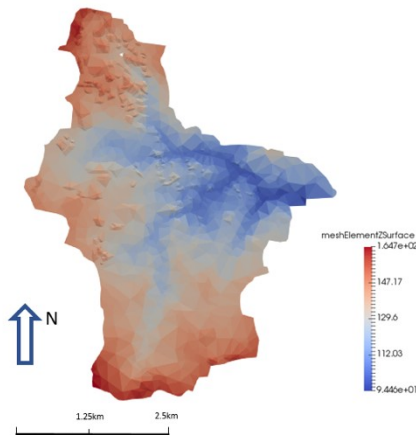


Figure 3. Example plot from ParaView showing the elevation change in the Dead Run catchment with building top elevations included.

References

1. Ogden et al., (2011). Relative importance of impervious area, drainage density, width function, and subsurface storm drainage on flood runoff from an urbanized catchment, *Water Resources Research*, 47, W12503.
2. Niu G. Y., et al. (2011). The community Noah land surface model with multi-parameterization options (Noah-MP): 1. Model description and evaluation with local-scale measurements, *Journal of Geophysical Research*, 116, D12109, doi:10.1029/2010JD015139.
3. Yang Z. L., et al. (2011). The community Noah land surface model with muliparameterization options (Noah-MP): 2. Evaluation over global river basins, *Journal of Geophysical Research*, 116, D12110, doi:10.1029/2010JD01540.
4. Blade et al.,(2012). Integration of 1D and 2D finite volume schemes for computations of water flow in natural channels, *Advances in Water Resources*, 42, pp 17-29.
5. Ogden, F. L., Lai, W., Steinke, R. C. (2016). ADHydro: QUASI-3D HIGH PERFORMANCE HYDROLOGICAL MODEL
6. Ogden, F. L., W. Lai, R. C. Steinke, J. Zhu, C. A. Talbot, and J. L. Wilson (2015). A new general 1-D vadose zone flow solution method, *Water Resour. Res.*, 51, 4282–4300, doi:10.1002/2015WR017126.
7. Talbot, C. A., and Ogden, F. L. (2008). A method for computing infiltration and redistribution in a discretized moisture content domain, *Water Resources Research*, 44(8), W08453, DOI: 10.1029/2008WR006815.
8. Gunduz, O., and Aral, M. M. (2005). River networks and groundwater flow: a simultaneous solution of a coupled system, *Journal of Hydrology*, 301(1-4), pp 216-234
9. Tarboton, D. G.; Sazib, N. TauDEM 5.3 QUICK START GUIDE TO USING THE TAUDEM ARCGIS TOOLBOX QUICK START. 2015.
10. Shewchuk, J. R. Triangle: Engineering a 2D Quality Mesh Generator and Delaunay Triangulator. *Appl.Comput. Geom. Towar. Geom. Eng.* 1996, 1148, 203–222.

Chapter 2

Comparison of Coarse and high-resolution Hydrologic Modeling in Mountainous Areas

Irene Garousi-Nejad¹, Siwei He², Qicheng Tang³

¹ Utah State University, i.garousi@aggiemail.usu.edu

² University of Wyoming, she@uwyo.edu

³ Pennsylvania State University, qut9@psu.edu

Academic Advisors: David Tarboton, *Utah State University*; Noriaki Ohara, *University of Wyoming*; Henry Lin, *Pennsylvania State University*

Summer Institute Theme Advisors: Fred Ogden, University of Wyoming, fogden@uwyo.edu

Abstract: A proper spatial resolution for hydrological modeling is essential due to the spatial heterogeneity of atmospheric conditions, topography, land cover, and soil properties. The National Water Model (NWM) is a hydrologic model that simulates observed and forecast streamflow over the entire continental United States (CONUS). The NWM provides complementary hydrologic guidance at current National Weather Service (NWS) river forecast locations and significantly expands guidance coverage and category for underserved locations. At present, NWM simulates all hydrological processes at a spatial resolution of 1 km except routings at 250 m. Therefore, it's a coarse resolution simulation. ADHydro, on the other hand, is a physical-based hydrological model using unstructured mesh developed for parallel computing environment. Compared with NWM, it represents hydrological processes using point location-scale equations which can be applied for high-resolution simulation. In this study, ADHydro is first run with a spatial resolution of 30 m over the Animas watershed, an alpine mountain area in Colorado, USA. Then, the simulated results of ADHydro and NWM outputs, which can be downloaded from NWM Explorer, are evaluated in terms of streamflow and snow water equivalent over the study area. The results indicate that snowmelt contributes greatly to the stream flow. The reason is that we assume a uniform snow water equivalent as initial condition over the entire study area. We found that ADHydro successfully captured the time lag between snowmelt event and streamflow peak at the outlet. With appropriate calibration and initial conditions, we expect ADHydro could have a good performance over the study area.

1. Motivation

Hydrological modeling in mountainous areas is very important in several ways. For example, mountainous areas are where streams are originated, and snowmelt of the mountainous areas accounts for 75% of annual discharge for the western US⁽¹⁾. However, hydrological modeling in the mountainous area proves to be difficult due to the spatial variability of atmospheric conditions, topography, land cover, solar radiation, precipitation, and soil properties. Therefore, one of the obstacles of current hydrological models in mountainous area is their spatial resolution. Generally, the high-resolution models should have more advantages over the coarse-resolution models in the mountainous areas in that they can represent this spatial variability more accurately. However, models with coarse resolution are more computationally efficient and they're easy to get input data compared

with high-resolution models, which require intensive computation resources and are difficult to get high resolution data.

2. Objectives and Scope

2.1 Objectives

The main objective of this work is to assess the impact of the spatial resolution on hydrologic modeling at mountainous areas, especially for snowmelt. By implementing ADHydro as a high-resolution model, we're able to represent and estimate terrain properties and incident solar radiation more realistically. This allows us to have a more detailed simulation of water and energy balances in complex mountainous area. And with this work, the performance of National Water Model (NWM) will also be quantitatively evaluated over the same mountainous area. Furthermore, we hope this work would be able to provide useful information for the further development on configuration of NWM.

2.2 Case Study

Our case study is one sub-watershed of the Animas River watershed. This sub-watershed is delineated based upon one of the USGS stream stations (Animas River at Durango, 09361500, CO). The watershed extends approximately 82 km from the headwaters in the San Juan Mountains above Silverton Colorado to the Durango city. The drainage area above the outlet is about 1,817 km². The flow rate and volume of streams in this watershed vary greatly seasonally. The seasonal high flow occurs during the spring snowmelt period, which is from late April through early June. There are 14 USGS stream gages located within the study area, as shown in **Figure 1**. However, for now, only 6 of them are active and have available data. Except for the stream gages, there are 6 Snow Telemetry (SNOTEL) gauges located in this watershed, which are operated by National Resources Conservation Service (NRCS). Elevation of the study area ranges from 1985 meters near the Durango city to 4311 meters in San Juan Mountains as illustrated in the **Figure 1**. The average annual precipitation of the study area ranges from 1118 mm in the highest elevations to 330 mm inches in the lowest elevations⁽²⁾. As shown in **Figure 2**, at lower elevations landcover is generally forest land, while at higher elevations where most of USGS gages and SNOTELs are located at, the land coverages are herbicides and barren land.

3. Previous Studies

Haddeland et al. (2002) studied the influence of spatial resolution on simulated streamflow by variable infiltration capacity (VIC) macroscale hydrologic model over a snowmelt dominated watershed and a rainfall dominated watershed⁽³⁾. This study shows that the lower resolution models preserve the general form of the hydrographs at the basin outlets. However, total runoff is lower at coarse spatial resolution than at higher spatial resolution for both snowmelt and rainfall-dominated basins. Singh et al. (2015) studied the effects of fine-scale topography and soil texture on CLM4.0 simulations over the Southwestern U.S. by simulating at 1, 25, and 100 km resolution⁽⁴⁾. The results show changes in the total amount of CLM-modeled water storage, and changes in the spatial and temporal distributions of water in snow and soil reservoirs, as well as changes in surface fluxes and the energy balance. Further, this study demonstrated that although the higher grid-resolution model is not driven by high-resolution forcing, grid resolution changes alone yield significant improvement (reduction in error) between model outputs and observations. Vivoni et al. (2005) studied the effects of triangulated terrain resolution on distributed hydrologic model response by conducting a multiple resolution validation

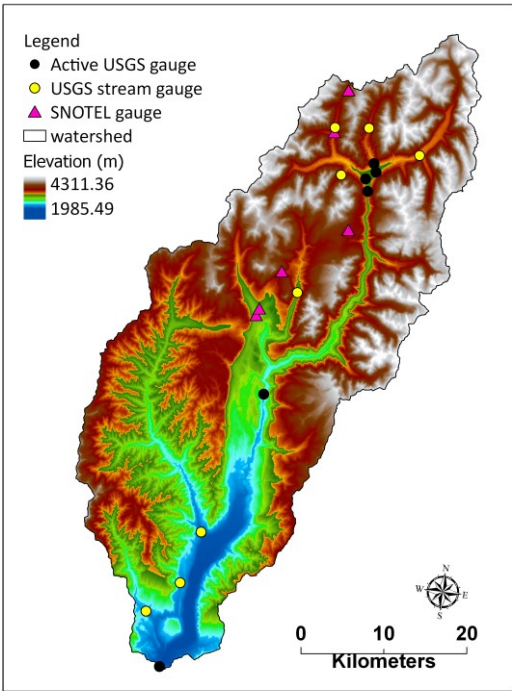


Figure 1. Elevation, USGS, and SNOTEL sites at the study area

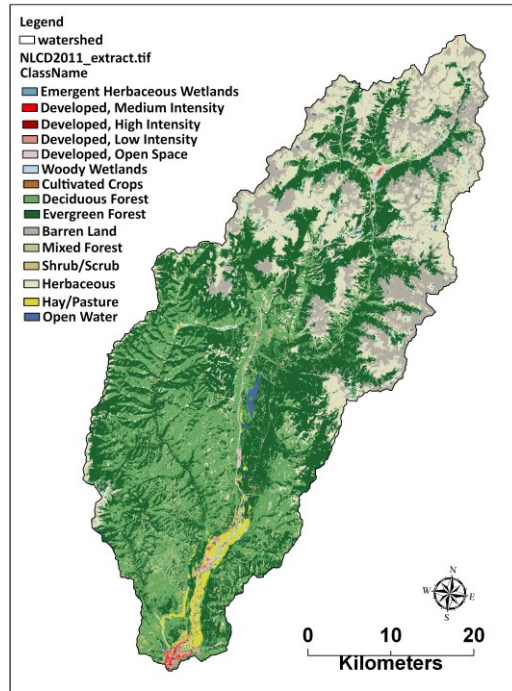


Figure 2. Land Cover (from NLCD) classes over the study area

experiment utilizing the tRIBS model over a wide range of spatial aggregation levels⁽⁵⁾. In their study, the relationship between the hydrologic sensitivity to resolution and the spatial aggregation of terrain attributes is presented as an effective means for selecting the model resolution. Also, this study highlights the important effects of terrain resolution on distributed hydrologic model response. Sulis and Camporese (2011) studied the impact of grid resolution on an integrated and distributed response of a coupled surface–subsurface hydrological model⁽⁶⁾. This study indicates that discharge volumes increase as the resolution is coarsened, and that coarser grids are also wetter overall in terms of water table depth and soil water storage.

4. Methodology

4.1 Model Description

In this study, NWM and ADHydro were used as coarse and high-resolution hydrologic models respectively. The first version of NWM model, namely NWM 1.0, became operational in August 2016 and the newest version, NWM 1.1, was unveiled in May 2017. This model simulates the water cycle with mathematical representations of the different processes and generates real-time water prediction for the CONUS. The configurations of NWM including land surface processes are over 1 kilometer grids and terrain routing over 250 meters grid. Both land surface and terrain routine processes are based on the Weather Research and Forecasting hydrologic model (WRF-Hydro) developed by National Center for Atmospheric Research (NCAR) implementing diffusive wave overland flow routing, saturated subsurface flow, and Muskingum-Cunge channel routing down NHDPlusV2.

ADHydro, developed by CI-WATER watershed modeling team, uses explicit finite volume method to solve conservation laws for flow calculation. Even though ADHydro uses the same land surface model as NWM, it only uses the point-scale processes such as evapotranspiration and snowmelt from Noah-MP⁽⁷⁾. A comprehensive description of ADHydro model is manifested in **Figure 3**. One of the special aspect of ADHydro which we believe can affect the hydrologic modeling in mountainous area is associated with the solar irradiance calculation. ADHydro uses unstructured triangular meshes. Unstructured triangular meshes are more efficient in their use of DEM data than fixed grids when producing solar irradiance information for spatially distributed snowmelt calculations, and they do not suffer from the artifact problems of a gridded DEM⁽⁸⁾. In fact, slope and aspect (from DEM) are identified as large contributors to the spatial variability of the surface energy balance, causing significant differences in snowmelt timing and magnitude. Kumar et al. (2009) indicated that unstructured meshes can provide a high-quality representation of the terrain using many fewer elements while maintaining conformance to the geometrical and physical properties of the basin to some predefined tolerance⁽⁹⁾.

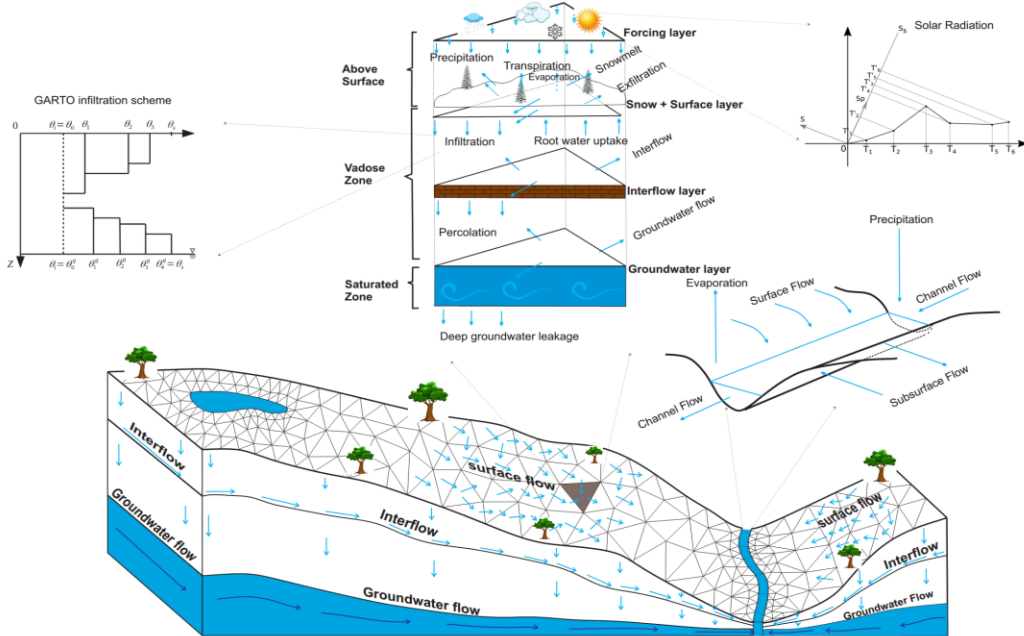


Figure 3. ADHydro model configuration, the ‘GARTO infiltration scheme’ figure is from Lai et al. (2015), the ‘Solar Radiation’ figure is from Moreno et al. (2016)^(10,11)

4.2 Input Data for ADHydro

4.2.1 Atmospheric data

For this study, we used the same forcing data as NWM for ADHydro, not only for the benefit of comparison with NWM, but for its high accuracy as well. NWM uses a combination of different datasets, including Multi Radar Multi Sensor (MRMS), High Resolution Rapid Refresh (HRRR), and Rapid Refresh (RAP), for “Analysis and Assimilation” configuration. MRMS is a Quantitative Precipitation Estimation (QPE) product which integrates about 180 operational radars, i.e. observed precipitation, and generates a seamless 3D radar mosaic across CONtinental United States (CONUS) at very high spatial (~ 1 kilometer) and temporal (~ 2 minutes) resolution. HRRR is a NOAA real-time 3-km resolution, hourly updated, cloud-resolving, convection-allowing atmospheric model, which is initialized by 3 kilometers grids with 3 kilometers radar assimilation at the time resolution of

15 minutes. Compared with HRRR, RAP is assimilated by radar data hourly. To combine the three datasets, a gap-filling method, which is developed by David Kitzmiller (http://github.com/NCAR/wrf_hydro_forcing), is used by NCAR. If MRMS is unavailable at some areas, e.g., mountainous areas, or it is of bad quality, HRRR and RAP are then used. The final forcing includes a set of 1-kilometer precipitation rate ($kg*m^2/s$), surface pressure (Pa), downward shortwave radiation (W/m^2), downward longwave radiation (W/m^2), 10-meter u-wind component (m/s), 10-meter v-wind component (m/s), 2-meter air temperature (K), and 2-meter specific-humidity (kg/kg). **Figure 4** shows the spatial variability of the average precipitation (from NWM forcing) over the study area.

4.2.2 Land Cover and Soil

In this study, NLCD⁽¹²⁾ and SSURGO⁽¹³⁾ database were categorized based on Noah-MP parameter tables (<http://www.ral.ucar.edu/research/land/technology/noahmp/HRLDAS-v3.6/SOILPARM.TBL>) to generate required soil properties (shown in **Figure 5**) for running ADHydro.

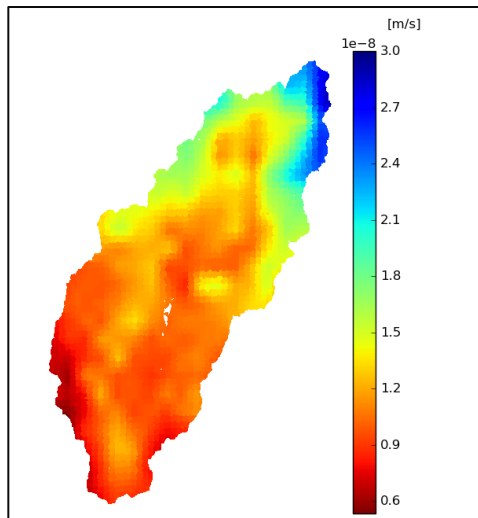


Figure 4. Average precipitation of May 2017

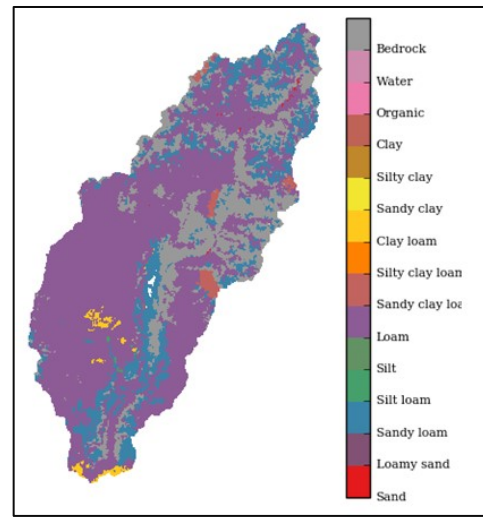


Figure 5. Soil Type over the study area

4.2.3 Mesh

Three steps are taken to generate the mesh for the watershed: *TauDEM preprocessing*, *ArcGIS smoothing* and *Mesh creating*. After getting the DEM and NHD data, TauDEM is then used to delineate the watershed and streams (with a threshold of 800m) based on the D8 method. TauDEM itself, is a suite of DEM tools for the extraction and analysis of hydrologic information from topography⁽¹⁴⁾. By setting the cluster tolerance as 30m for the outputs from TauDEM (catchments, streams and waterbodies), we deleted features under the resolution of 30 m. The difference between the TauDEM outputs and after-smoothing (modified) outputs are shown in **Figure 6 and 7**. Unstructured meshes are generated for the watershed using Delaunay Triangulation as illustrated in **Figure 8**.

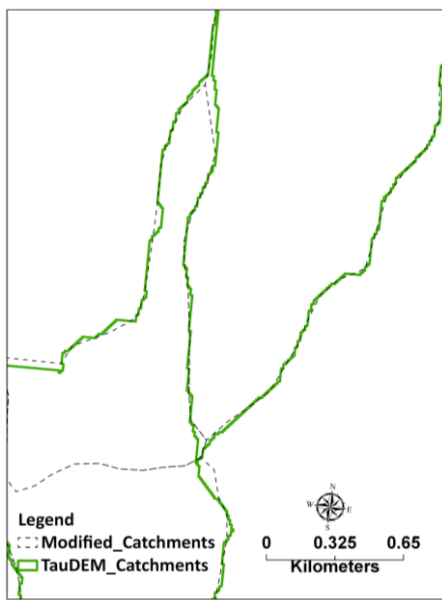


Figure 6. Catchments comparison

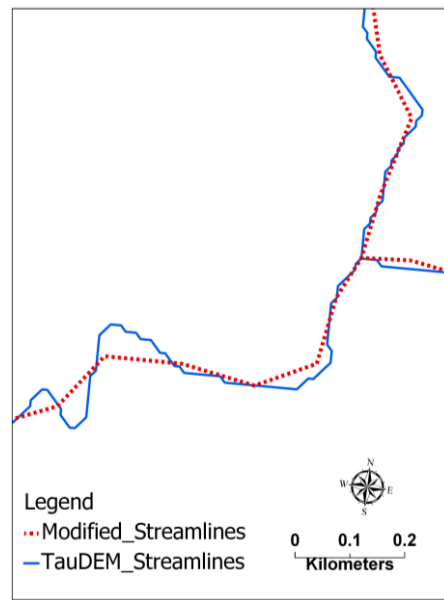


Figure 7. Streamlines comparison

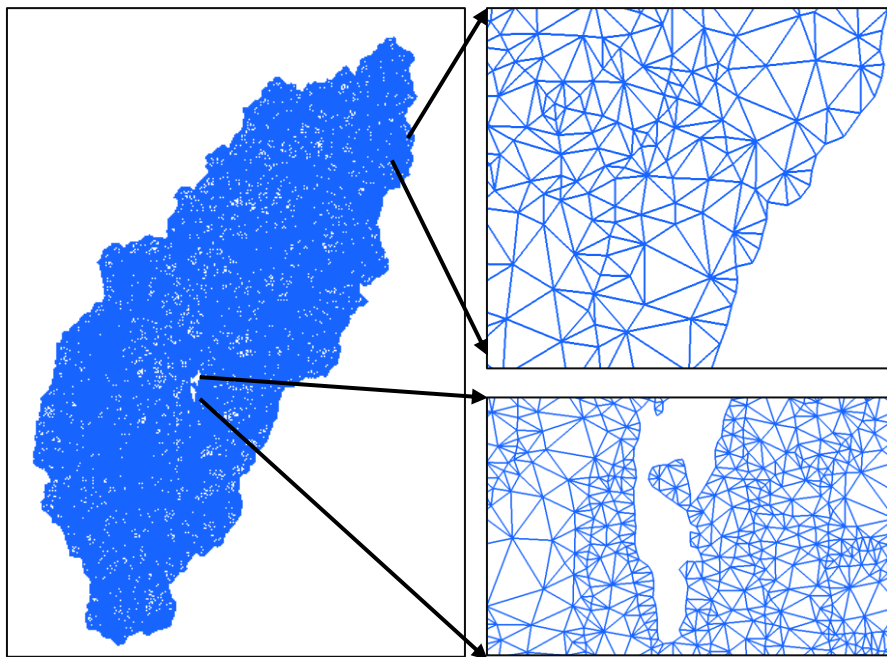


Figure 8. Mesh elements created by using Delanay triangulation method

4.3 Initial states

ADHydro has a bunch of state variables which need to be initialized. In this study, we used the default values defined in ADHydro source code except for snow water equivalent, snow depth, and soil temperatures at different soil layers because the simulation time starts on 05/01/2017, which means

snow water equivalent is not 0 while the default initial condition is no snow. It should be noted that if we had defined a longer period that included winter time or the whole water year, we would not need to change these state variables. However, due to the time limitation (working officially only for four weeks), we prefer to define a short simulation time for the first attempt of evaluating high-resolution modeling in mountainous areas.

5. Results

As shown in **Figure 9**, results from ADHydro are not reasonable at this time. It can be seen that the streamflow has unexpected oscillations. The focus of this section is to find the reasons that may cause these results.

Figure 9(a) and (b) manifest the average air temperature and precipitation, respectively, which are model inputs. We added these time series here to make sure that the forcing data were reasonable. **Figure 9(c)** shows the observed streamflow of the outlet (Animas at Durango gage site) and two simulated streamflow from NWM and ADHydro. Generally, ADHydro (shown as green line) overestimates the streamflow compared to USGS and NWM from May 1st to May 10th. Due to the time limitation, we could only have the outputs of the 10 days by the time of preparing this report. That is why NWM and USGS have the complete time series in **Figure 9(c)** and ADHydro only covers the first 10 days of May 2017. **Figure 9(d)** presents the observed snow water equivalent at the location of one of the SNOTEL gages (Red Mountain, ID=713) and the simulated ADHydro snow water equivalent. It is worth noting that NWM reported zero snow water equivalent at this location for the entire May 2017.

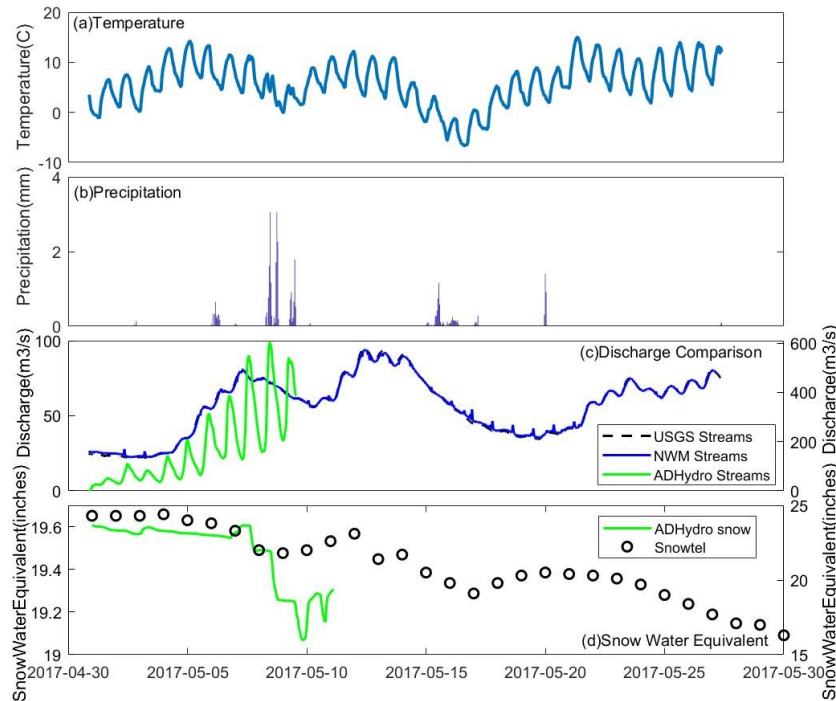


Figure 9. Time Series of different variables

Figure 10 is presented in order to analyze the water balance over the watershed, which shows the time series of the total precipitation, snowmelt, streamflow, evapotranspiration, and

groundwater recharge within the study area. Since there is no considerable precipitation until May 7th, it could be seen that the streamflow is mostly generated from snowmelt. Moreover, streamflow and snowmelt have the same trend. These observations clearly show that snowmelt plays an important role to generate the streamflow. Also, it should be mentioned that the negative values of snowmelt mean that new snow fall happened at that time step. From **Figure 10**, we can see that the effect of groundwater on the water balance is negligible while evapotranspiration plays a more important role in water balance. Water balance analysis gives a good explanation for the unexpected results of ADHydro.

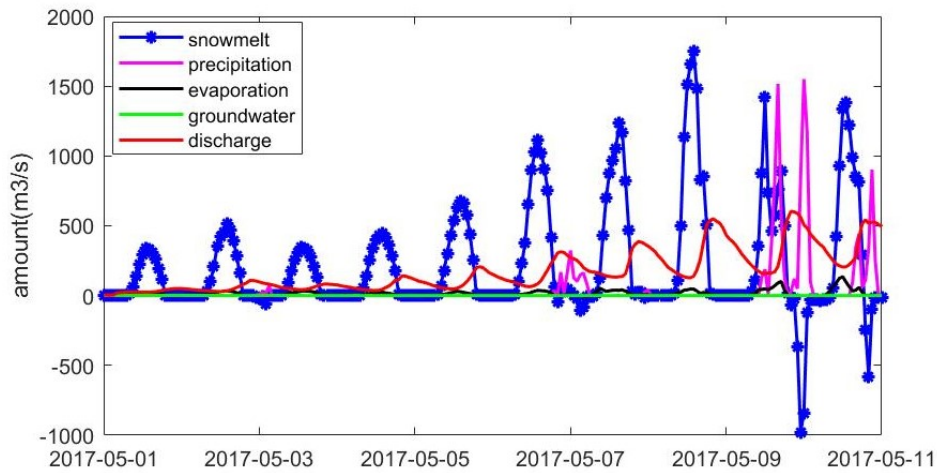


Figure 10. Major components of water balance in ADHydro

The reason that snowmelt contributes greatly to the stream flow is related to the fact that we assume a uniform snow water equivalent as initial condition over the entire study area, which is unreal. Another reason that may cause the unreasonable results from ADHydro is that the model was not calibrated for this study area, and this was the first attempt to run ADHydro over a more complex area. Even though the results of ADHydro are not satisfactory at this time, it successfully captured the time lag between snowmelt event and streamflow peak at the outlet (**Figure 10**). With appropriate calibration and initial conditions, we expect ADHydro could have a better performance over the study area in the future.

6. Conclusion

From running the ADHydro model, we have become more comfortable with running models in an HPC environment. From the beginning, it was expected we would not achieve *perfect* results since this was ADHydro's first attempt in a mountainous area without calibration. However, this was a very joyful and fruitful journey. Not only did we learn a lot from the process on the technical side, but we are now more confident in dealing with setbacks and uncertainties in our work as well. During this summer institute the work ethics and kindness of our group members, the CI participants, and NWC staff have inspired us to be better hydrologists in the future.

References

1. USGS. Snowmelt - the water cycle (2016). <http://water.usgs.gov/edu/>
2. B.U.G.S. Consulting. 2011. Animas River Watershed Based Plan. Prepared for Animas Watershed Partnership. August 2011.
3. Haddeland, I., Matheussen, B. V., & Lettenmaier, D. P. (2002). Influence of spatial resolution on simulated streamflow in a macroscale hydrologic model. *Water Resources Research*, 38(7).
4. Singh, R. S., Reager, J. T., Miller, N. L., & Famiglietti, J. S. (2015). Toward hyper-resolution land-surface modeling: The effects of fine-scale topography and soil texture on CLM4. 0 simulations over the Southwestern US. *Water Resources Research*, 51(4), 2648-2667.
5. Vivoni, E. R., Ivanov, V. Y., Bras, R. L., & Entekhabi, D. (2005). On the effects of triangulated terrain resolution on distributed hydrologic model response. *Hydrological Processes*, 19(11), 2101-2122.
6. Sulis, M., Paniconi, C., & Camporese, M. (2011). Impact of grid resolution on the integrated and distributed response of a coupled surface–subsurface hydrological model for the des Anglais catchment, Quebec. *Hydrological Processes*, 25(12), 1853-1865.
7. Ogden, F.L.; Lai, W.; Steinke, R.C. ADHydro: Quasi-3D high performance hydrological model. Proceedings of the 5th Federal Interagency Hydrologic Modeling Conference and the 10th Federal Interagency Sedimentation Conference, April 19-23, 2015, Reno, Nevada
8. Marsh, C. B., Pomeroy, J. W., & Spiteri, R. J. (2012). Implications of mountain shading on calculating energy for snowmelt using unstructured triangular meshes. *Hydrological Processes*, 26(12), 1767-1778.
9. Kumar, M., Bhatt, G., & Duffy, C. J. (2009). An efficient domain decomposition framework for accurate representation of geodata in distributed hydrologic models. *International Journal of Geographical Information Science*, 23(12), 1569-1596.
10. Lai, W., Ogden, F. L., Steinke, R. C., & Talbot, C. A. (2015). An efficient and guaranteed stable numerical method for continuous modeling of infiltration and redistribution with a shallow dynamic water table. *Water Resources Research*, 51(3), 1514-1528.
11. Moreno, H. A., F. L. Ogden, and L. V. Alvarez. "Irregular-Mesh Terrain Analysis and Incident Solar Radiation for Continuous Hydrologic Modeling in Mountain Watersheds." AGU Fall Meeting Abstracts. 2016.
12. Homer, C.G., Dewitz, J.A., Yang, L., Jin, S., Danielson, P., Xian, G., Coulston, J., Herold, N.D., Wickham, J.D., and Megown, K., 2015, Completion of the 2011 National Land Cover Database for the conterminous United States—Representing a decade of land cover change information. *Photogrammetric Engineering and Remote Sensing*, v. 81, no. 5, p. 345-354
13. Soil Survey Staff, Natural Resources Conservation Service, United States Department of Agriculture. Web Soil Survey. Available online at <https://websoilsurvey.nrcs.usda.gov/>. Accessed [07/22/2017]
14. Tarboton, D. G., Bras, R. L., & Rodriguez-Iturbe, I. (1991). On the extraction of channel networks from digital elevation data. *Hydrological processes*, 5(1), 81-100.

Chapter 3

Hyper-resolution modeling in Urban Landscapes

Lauren Grimley¹, Mariam Khanam², Edward Tiernan³ and Danielle Tijerina⁴

¹ University of Iowa, lauren.grimley@uiowa.edu

² University of Alabama, mkhanam@crimson.ua.edu

³ University of Texas at Austin, etiernan@utexas.edu

⁴ Colorado School of Mines, dtijerina@mines.edu

Academic Advisors: Witold Krajewski, *University of Iowa*; Sagy Cohen, *University of Alabama*; Ben Hodges, *University of Texas at Austin*; Reed Maxwell, *Colorado School of Mines*

Summer Institute Theme Advisor: Fred Ogden, University of Wyoming, fogden@uwyo.edu

Abstract: This study presents the efforts to advance the modeling capabilities of ADHydro and to better understand the importance of mesh resolution when modeling urban areas. ADHydro is a physics-based, distributed, hydrologic model currently under development by researchers at the University of Wyoming in Laramie, WY. In this study, ADHydro was analyzed for its effectiveness at modeling a small and a large rainfall event in an urban watershed called Dead Run near Baltimore, Maryland. A large portion of the work served as alpha-testing for further development of ADHydro. Triangular meshes at 20m and 50m resolutions were created to assess the sensitivity of ADHydro to changes in mesh resolution. Structures were incorporated in both meshes to test the model's ability to handle a complicated urban routing network with structures present. The results were compared to observed United States Geological Survey (USGS) stream gage data and the National Water Model's (NWM) calibrated output for two historical rainfall events. The finest resolution of 20m performed better than the coarser mesh resolutions of 50m and the calibrate NWM of 1km. The inclusion of structures in the model mesh improved the hydrograph accuracy by decreasing the time of concentration. For all the simulation scenarios, ADHydro outperformed NWM with the comparisons of percent bias and root mean squared error metrics.

1. Motivation

The purpose of this study is advance the National Water Center's (NWC) goal to provide real-time, flood forecasts in urban areas, specifically at the street level. Since August 2016, the National Water Model (NWM) has produced a range of hydrologic forecasts over the contiguous United States at a one-kilometer resolution. A long-term goal of the NWC is to increase the high-performance computing (HPC) capacity of the operational NWM. Part of this effort includes testing the use of hyper-resolution models in urban areas for improved flood forecasting. Hyper-resolution hydrologic models enable the user to capture fine-scale features in topography that are hydrologically significant. Modeling with a course resolution, typically greater than 100 m for continental scales⁽¹⁾, does not always yield an accurate depiction of water movement in the catchment, and it is hypothesized that using a finer mesh resolution over a smaller domain can improve model accuracy and predictions.

2. Objectives and Scope

The scope of this work is to test the advantages of unstructured meshes with varying resolutions to capture hydrological processes in an urban watershed using ADHydro. There is a need for models that are capable of accurately modeling various landscapes and fine-scale features while operating in a high-performance computing environment⁽¹⁾. Unstructured meshes provide the user with an opportunity to specify what areas of the model should be more detailed, such as overland flow in streets and around buildings. The goal was not only to test the competence of ADHydro to model urban landscapes but also to investigate the model performance using different meshes.

The objectives of this study are summarized as follows:

- Test the capabilities of ADHydro to model an urban watershed for both a small and large historical rainfall event.
- Compare USGS streamflow records to model streamflow results for meshes of varying resolutions (20 and 50 meter).
- Incorporate structures into both meshes (20 and 50 meter) to better simulate flow at the street level.
- Record mesh statistics and model computational requirements.

2.1 ADHydro

ADHydro is a physics-based, hyper-resolution, hydrological model under development by the CI-WATER modeling team at the University of Wyoming. Additional detail on the physical processes modules and model workflow can be found in the ADHydro Introduction and Workflow document. At this time, ADHydro does not have the capabilities to model subsurface stormwater infrastructure which puts it at a disadvantage when modeling urban areas.

2.2 Site Description

Dead Run is an urbanized watershed about 10 km west of Baltimore, MD near Franklintown. The watershed is a small, fully contained catchment with an area of 14.3 km² ⁽²⁾. As shown in **Figure 1a**, the watershed is located outside of the city limits and is highly urbanized. The watershed land cover is approximately 96% impervious and a USGS streamflow gauge is located at the outlet (see **Figure 1b**).

Baltimore averages 1065 mm (41.94 in) of precipitation per year, with most occurring in the late summer⁽³⁾. The watershed is classified as a humid subtropical climate according to the Köppen-Geiger climate classification⁽⁴⁾ with summers that range from mild to hot temperatures and high humidity. Dead Run watershed has been utilized in various studies related to urban hydrology^(2, 5, 6, 7, 8, 9) and more recently as a test watershed for ADHydro⁽²⁾. Dead Run watershed was modeled in this study because of the data available from previous studies in the area and because it is a compact urban basin suitable for quick model simulations^(2, 6).

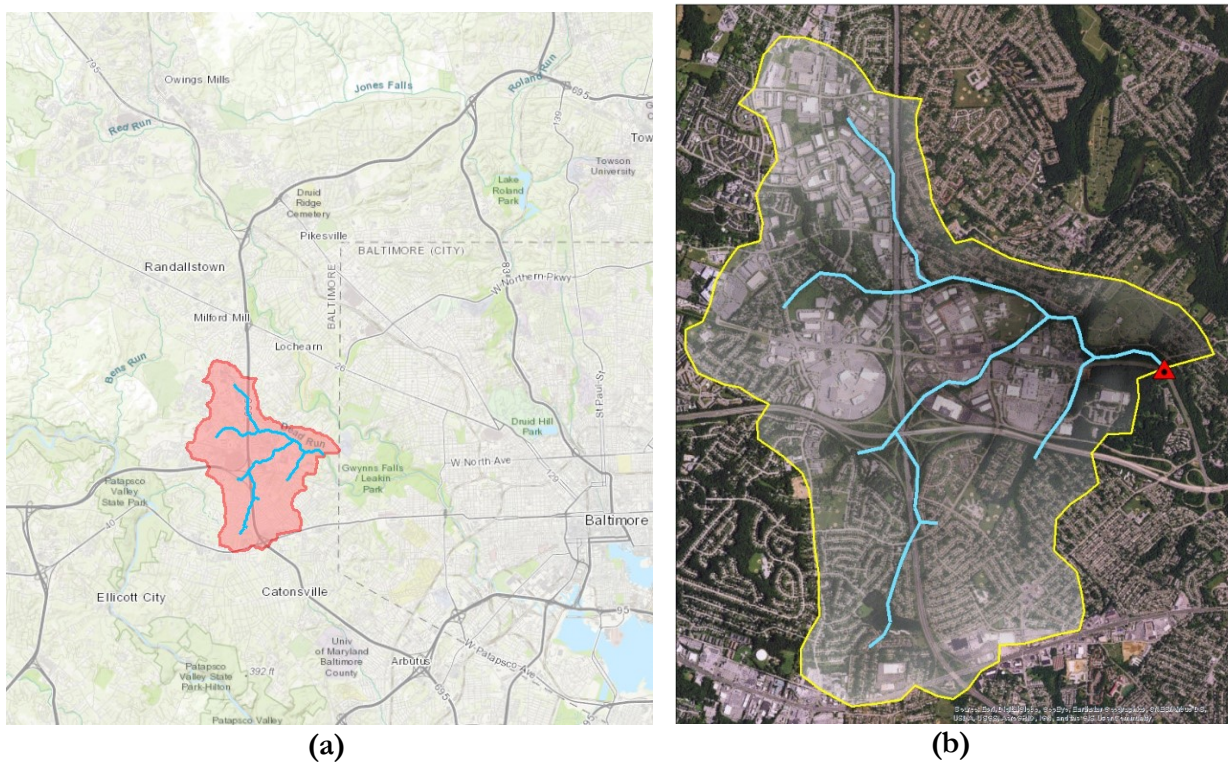


Figure 1. a) Basemap image of greater Baltimore, MD with Dead Run catchment highlighted. b) Land cover of the Dead Run catchment with stream network and USGS stream gage depicted.

3. Methodology

The general workflow is described briefly in the ADHydro Introduction and Workflow document, while the techniques for model development unique to the Dead Run model are described in this report.

3.1 Pre-Processing

3.1.1 Mesh Development

Preparing the geometry of the catchments, reservoirs, and stream network was completed in ArcGIS before the generation of the 2D triangular mesh using Triangle⁽¹⁰⁾. The watershed was delineated with the TauDEM toolbox using a 10m digital elevation model (DEM). The shapefiles of the catchments, waterbodies, and streams generated by TauDEM were smoothed with a vertex cluster tolerance of 20m and 50m to define two distinct meshes. A single reservoir located in the northern area of the watershed was removed from the geometry and no triangle elements were generated for this small portion. The processes of smoothing the geometry and removing vertices affects the complexity of the mesh generated. Determining a method to incorporate structures into the mesh was important to test the capabilities of ADHydro to model fine-scale features. Buildings with an area less than 1,000m² were excluded from the mesh to reduce complexity which directly impacts the model computational needs and run time. **Figure 2** demonstrates the steps of pre-processing the geometry to create the triangular mesh and a comparison of the 20m mesh with and without buildings included.

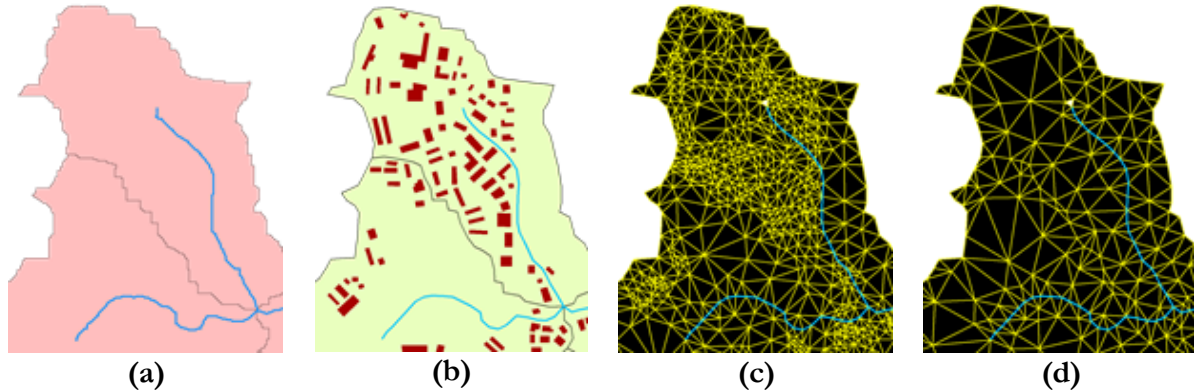


Figure 2. a) Stream network and catchment delineated in TauDEM. b) Catchments and stream network after 20m smoothing with clipped buildings. c) Triangular mesh for 20m buildings compared to the d) 20m mesh without buildings incorporated.

The Triangle program produces mesh statistics that served as a guide to indicate when the mesh geometry needed to be edited to remove small triangles or digital dams. This step is necessary because small triangles require a smaller timestep to be applied to the model, as consistent with the Courant stability condition⁽¹⁰⁾. The final statistics of the 20 and 50m meshes with and without buildings are given in **Table 1**.

Table 1. Triangle generated mesh statistics

| | 20m Simple | 20m Buildings | 50m Simple | 50m Buildings |
|---|------------|---------------|------------|---------------|
| No. of Vertices | 797 | 1,721 | 23 | 1,405 |
| No. of Triangles | 1,380 | 3,219 | 414 | 2,706 |
| Smallest Triangle Area (m²) | 1,430 | 76 | 4,978 | 83 |

The DEM was modified so that an additional 10 meters was added where the building footprints were located. This ensured that the vertex of the triangles that coincided with the edges of the buildings would be raised above the original elevation allowing the water to flow around the hill-like obstructions as shown in **Figure 3**.

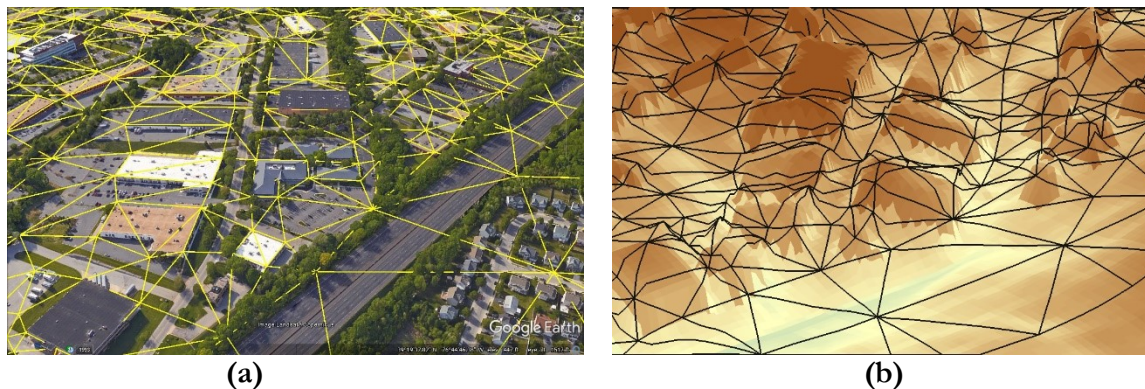


Figure 3. (a) Google earth image of mesh vertices in line with buildings (b) Modified 10m DEM to mimic structures and streets in the mesh

The hydrological parameters were extracted to the triangular elements of the mesh. These hydrological components include the geologic unit, soil type, land use, and elevation. For the Dead Run watershed, the parameters were drawn from STATSGO, SURRGO, NLCD, and NED. These parameters were not calibrated because this was a preliminary assessment of ADHydro's modeling capacity and performance.

3.1.2 Precipitation Forcing

The Dead Run watershed was simulated for two historical rainfall events. Daily precipitation values were gathered from a nearby rain gauge (US1MDBL0039) at Catonsville, MD from the Global Historical Climatology Network (GHCN) database. The smaller event occurred in May of 2017 with a cumulative rainfall of 58.5 mm over a period of 2 days. The NWM precipitation data is produced from Multi-Radar/Multi-Sensor (MRMS) 1km radar by NOAA's National Severe Storms Laboratory (NSSL). This precipitation data was used as an input into ADHydro for the storm of May 2017. The USGS gauge exceeded the flood stage as defined by the NWS during a larger rainfall event in July 2016 when the catchment experienced a cumulative rainfall of 106 mm in 24 hours. NEXRAD Digital Precipitation Rate (DPR/176) data was used as the precipitation forcing in ADHydro for the storm of July 2016 since the NWM forcing was not available. This product uses a dual-polarization quantitative precipitation estimation (QPE) algorithm to provide the instantaneous precipitation rate.

3.2 Model Processing

The steps to run ADHydro and post-process the results are enumerated in the ADHydro Introduction and Workflow document. The simulated streamflow near the drainage outlet was compared to USGS streamflow records (Gauge 01589330) and the NWM output. The computational requirements for the models were documented using a "wall clock multiplier" which is a unitless measure of how much faster the model is running relative to the "wall clock" or real time (*i.e.* seconds of simulation/second). This information is useful when evaluating the accuracy of a model output and its capabilities for producing a real-time forecast.

3.3 Statistical Analysis

The simulated discharge is quantitatively compared to USGS stream gage measurements using percent bias (PBIAS) and root mean squared error (RMSE) objective functions. These metrics show the magnitude of error between the modeled and observed values. Moriasi et al.⁽¹¹⁾ provides a strong overview of objective functions used in statistical analysis of hydrologic data. PBIAS gives the average tendency of a simulated value to be larger or smaller than observed and is given by the equation

$$PBIAS = 100 \left(\frac{\sum (Q_{model} - Q_{obs})}{\sum Q_{obs}} \right) \quad (1)$$

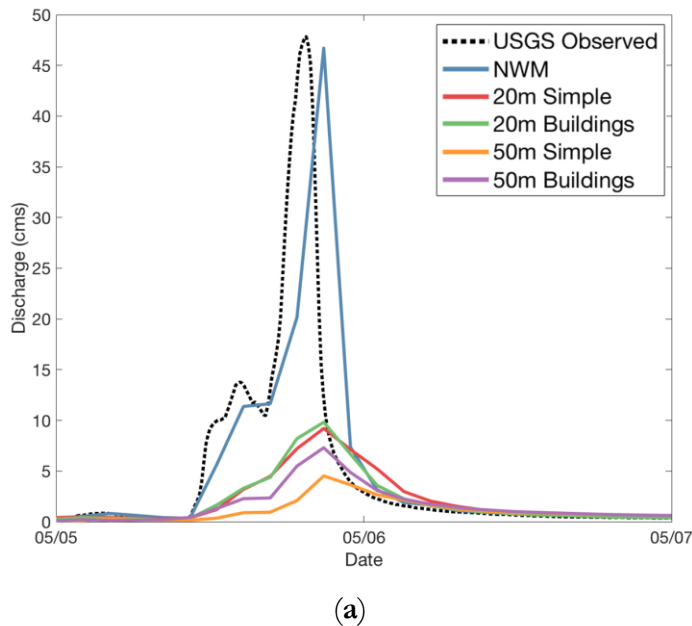
The optimal bias value is zero, positive values show model overestimation, and negative values show model underestimation (Eq. 1). PBIAS is expressed as a percentage. RMSE is an objective function used to compare models using the equation

$$RMSE = \sqrt{\frac{\sum_{t=1}^n (\bar{y}_t - y_t)^2}{n}} \quad (2)$$

An ideal RMSE value is zero, but it is recommended that a value less than half the standard deviation of the observed values is acceptable.

4. Results

The results of this study are intended to advance the modeling capabilities of ADHydro and to better understand the importance of utilizing mesh resolution models in urban areas. The ADHydro and NWM streamflow output compared to the USGS streamflow measurements for the May 2017 and July 2016 rainfall events are shown in **Figure 5a and 5b** respectively. The NWM output is assimilated and calibrated to the nearest USGS gauge hourly. The ADHydro model of Dead Run in this study was not calibrated.



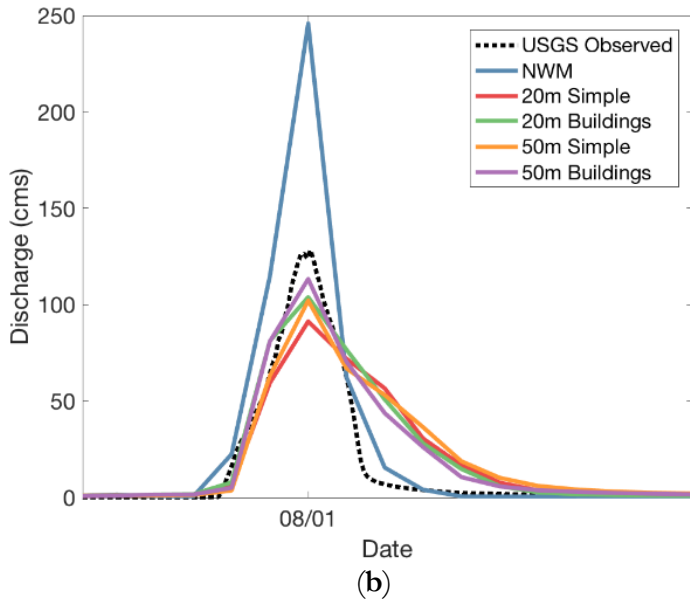


Figure 5. Comparison of ADHydro results and NWM output against USGS observation, a) May 2017, b) July 2016

The model output for the small event varies significantly for the different mesh resolutions. For the smaller rainfall event, all four ADHydro models significantly under predicted the time of concentration and amount of peak flow, as well as missed the initial rainfall pulse in the hydrograph completely. For both events, the NWM over predicted the peak flow. The ADHydro simulations better captured the larger 2016 storm (**Figure 5b**). The hydrographs for the four meshes simulated in ADHydro follow a similar pattern relative to each other without any large variances. The results of a statistical analysis are shown in **Table 2** providing a measurement of the difference in the simulated and observed data.

Table 2. Statistics comparing the different ADHydro meshes and the NWM against the observed USGS streamflow.

| MESH | SMALL STORM (May 2017) | | BIG STORM (July 2016) | |
|--------------------|-----------------------------------|------------------|-----------------------------------|------------------|
| | RMSE (m³/s) | PBias (%) | RMSE (m³/s) | PBias (%) |
| Simple 20 | 14.66 | -58.04 | 13.28 | 42.62 |
| Building 20 | 15.18 | -60.11 | 15.71 | 50.44 |
| Simple 50 | 19.63 | -77.72 | 15.01 | 48.16 |
| Building 50 | 17.08 | -67.63 | 14.84 | 47.62 |
| NWM | 1.022 | -4.044 | 19.16 | 61.6 |

The PBIAS and RMSE are high for the simulations of the larger storm, likely due to all of the simulations overestimating the recession limb. Another aspect of this project was to examine the performance of ADHydro using varying mesh resolutions and level of detail to fine-scale features. Considering the small storm in 2017, the 50m resolution building mesh performed better than the 50m simple mesh with a PBIAS of -68% and -77%, respectively. The converse was true for the 20m resolution of the small storm with PBIAS of -60% for the building mesh and -58% for the simple mesh. The simulations time to peak flow arrived one hour late in the smaller storm but was accurate for the larger storm. For the peak magnitude, the smaller storm simulations underestimated the peak

by 70-90%, but only 10-30% for the larger storm. These last two metrics are important in terms of identifying where and when the peak flooding will occur due to a particular storm event.

Although there is not a significant difference in performance for the varying ADHydro meshes in the two events there are two relevant results. First, the NWM performs much better in the small storm with a percent bias 14 times smaller than any of the ADHydro models, however it considerably over-estimates the large storm. Second, out of all ADHydro simulations, the 20m simple mesh most accurately describes the catchment runoff behavior for both storm events. This supports the hypothesis that a finer resolution model can more accurately capture the overland flow in urban areas.

While considering the statistical accuracy, we also compared the wall clock multiplier for each model run as shown in **Table 3**.

Table 3. *Wall clock multipliers for each mesh and storm, and average wall clock time per mesh*

| Mesh | Wall Clock Multiplier | | |
|---------------------|-----------------------|------------------|---------|
| | Small Storm (May) | Big Storm (July) | Average |
| Simple 20 | 38.8 | 40.3 | 40.3 |
| Simple 50 | 285.1 | 249.3 | 249.3 |
| Buildings 20 | 36.8 | 34.1 | 34.1 |
| Buildings 50 | 39.5 | 36.4 | 36.4 |

This measure describes how quickly the model can provide real-time and forecasted results. The wall clock multiplier is a function of the mesh element size. The smallest element usually determines the computational time step use for the entire model. It is clear that the Simple 50m mesh has the largest wall clock multiplier, meaning that the model ran the fastest. This is very attractive when it comes to performing predictive flood analysis, but it is important to evaluate the accuracy of such a model. Although the 20m simple mesh had a slower run time, it was statistically more accurate.

5. Conclusion

The objective of this project was to create a hyper-resolution model using ADHydro and evaluate its performance with varying mesh resolutions in urban areas. The results support the objective for improving hyper-resolutions models in complex terrains. The finest resolution of 20m performed better than the coarser mesh resolutions of 50m and the calibrate NWM of 1km. Running simulations for rainfall events of two magnitudes reinforced the sensitivity of the hydrological model to initial conditions and precipitation resolution. Often modeling smaller rainfall events requires model calibration to improve antecedent moisture conditions. The smaller the watershed, the more sensitive the watershed is to storm water management practices⁽⁶⁾. ADHydro does not currently have storm drain modeling capabilities, which puts it at a slight disadvantage to other urban models. This was apparent in the poor ADHydro results for the small storm.

Considering the challenges that arose during this project, additional work is suggested to improve modeling urban areas in ADHydro. Smaller structures, such as homes, were not included in the mesh due to project time constraints. It is important that residential areas are able to be modeled without sacrificing real-time computational capabilities. The mass balance discrepancies between the model

simulations is likely caused by the differences in mesh surface area allowing rainfall to runoff or infiltrate. Due to forcing data availability constraints, the spin-up time was cut short for the larger storm. More forcing data could allow for longer spin-up runs to approximate the initial conditions more accurately. Alternatively, the NWM antecedent soil moisture conditions could be used as an input into ADHydro. Improving the groundwater modeling will likely dramatically improve the models performance when baseflow dominates.

For real-time predictions, simple representations of catchments may be more prudent than the accuracy that comes from model detail. This report alludes to a relationship between computational expense and model accuracy, but additional formalized analysis is required for higher-quality predictive flood modeling. Further investigation of various hyper-resolution models and their performance will be a valuable endeavor to improving detailed hydrologic forecasting.

References

1. Wood, E. F., et al. Hyper-resolution global land surface modeling: Meeting a grand challenge for monitoring Earth's terrestrial water. *Water Resour. Res.*, 2011 47, W05301, doi:10.1029/2010WR010090.
2. Ogden, F. L.; Raj Pradhan, N.; Downer, C. W.; Zahner, J. A. Relative importance of impervious area, drainage density, width function, and subsurface storm drainage on flood runoff from an urbanized catchment. *Water Resources. Res.* 2011 DOI: 10.1029/2011WR010550.
3. Maryland State Archives. Maryland at a Glance: Weather. <http://msa.maryland.gov/msa/mdmanual/01glance/html/weather.html>. 2016 (Accessed 7 Jul 2017).
4. Climate-Data.Org. Climate: Maryland. <https://en.climate-data.org/region/1036/> (Accessed 11 Jul 2017).
5. Smith, J. A.; Baeck, M. L.; Meierdiercks, K. L.; Nelson, P. A.; Miller, A. J.; Holland, E. J. Field studies of the storm event hydrologic response in an urbanizing watershed. *Water Resour. Res.* 2005 DOI: 10.1029/2004WR003712.
6. Javier, J. R. N.; Smith, J. A.; Meierdiercks, K. L.; Baeck, M. L.; Miller, A. J. Flash Flood Forecasting for Small Urban Watersheds in the Baltimore Metropolitan Region. *Weather Forecast.* 2007 DOI: 10.1175/2007WAF2006036.1.
7. Wang, J.; Endreny, T. A.; Nowak, D. J. Mechanistic simulation of tree effects in an urban water balance model. *J. Am. Water Resour. Assoc.* 2008 DOI: 10.1111/j.1752-1688.2007.00139.x.
8. Meierdiercks, K. L. Hydrologic Response in Small Urban Watersheds: Analyses from the Baltimore Ecosystem Study. 2009.
9. Smith, B. K.; Smith, J. A.; Baeck, M. L.; Villarini, G.; Wright, D. B. Spectrum of storm event hydrologic response in urban watersheds. *Water Resour. Res.* 2013 DOI: 10.1002/wrcr.20223.
10. Shewchuk, J. R. Triangle: Engineering a 2D Quality Mesh Generator and Delaunay Triangulator. *Appl. Comput. Geom. Towar. Geom. Eng.* 1996, 1148, 203–222.
11. Moriasi, D. N.; Arnold, J. G.; Liew, M. W. Van; Bingner, R. L.; Harmel, R. D.; Veith, T. L.; Arnold, J. G.; Liew, C. W. Van; Moriasi, D. N. Model Evaluation Guidelines for systematic Quantification Of Accuracy In Watershed Simulations. *Trans. ASABE* 2007, 50 (3), 885–900.
12. Ogden, F. L.; Lai, W.; Steinke, R. C. ADHydro: Quasi-3d High Performance Hydrological Model. 2016

Chapter 4

Evaluating the Performance of a Hyper-resolution Model in a Low Gradient Watershed

Tyler Madsen¹, Seungwoo Jason Chang² and Christopher Turnipseed³

¹ Iowa State University, madsen@iastate.edu

² University of Florida, snjason@ufl.edu

³ Louisiana State University, christopherturnipseed@gmail.com

Academic Advisors: Kristie Franz, *Iowa State University*; Wendy Graham, *University of Florida*; Clint Willson, *Louisiana State University*

Summer Institute Theme Advisors: Fred Ogden, *University of Wyoming*, fogden@uwyo.edu

Abstract: This study encompasses the alpha testing of the newly developed hydrologic and hydraulic model, ADHydro. The software was tested in an area of low topographic relief, the Mermentau River Basin of Louisiana. Due to the size of the watershed ($\sim 3600 \text{ km}^2$), simulations were conducted at a 100 meter resolution in the study area. The results indicated that ADHydro underestimated discharge when compared to USGS observations. However, a possible bias in the precipitation forcing data resulted in a large discrepancy between the observed and simulated results. A longer simulation initialization period may improve initial conditions as it would allow model states to further equilibrate. Ultimately, utilizing ADHydro in this experiment was a way of demonstrating the utility of using an uncalibrated, unstructured mesh hyper-resolution model on a large geographic area with a low gradient.

1. Motivation

Flooding is a natural dynamic of river systems that causes significant damage to human infrastructure and poses a risk to human life. In recent decades, the exponential increase in computing power has allowed scientists and engineers to mitigate the issues that arise from floods through higher resolution numerical modeling. A cross disciplinary approach is required when addressing the challenges of numerically modeling an array of physical processes, large geographic areas and long temporal scales. There is a growing demand to model small-scale processes across a variety of different landscapes. Utilizing a model that employs an unstructured, triangular mesh allows for modelers to define key features such as channels and hillslopes at finer scales while coarser grid spacing is used to define features of less importance. This improves the overall computational efficiency of simulations because more emphasis is placed on areas of interest. Thus, this study seeks to assess the application of a hyper resolution hydrologic and hydraulic (H&H) model in novel environments.

2. Objectives and Scope

The purpose of this study is to address the hydrologic and hydraulic model ADHydro's performance in a watershed of low topographic relief. ADHydro, which uses an explicit finite difference volume method for calculating flow, was recently developed at the University of Wyoming, has thus far only

simulated the Colorado River Basin and the Dead Run watershed of Maryland. The watershed for this study was the Mermentau River Basin, upstream of Mermentau, LA, roughly 40 miles west of Lafayette, (**Figure 1.**) which encompasses a 3,600 km² drainage area. North of Mermentau is a confluence of the Bayou des Cantes, Bayou Nezpique, and Bayou Plaquemine Brule which unite to form the Mermentau River. An emphasis is placed on August 2016, where a slow moving inland tropical storm occurred across southern Louisiana, with some regions receiving the cumulative average monthly rainfall within a span of 3 days causing widespread flooding⁽¹⁾. This event caused 13 fatalities and is estimated to have caused 10 billion dollars in damages and considered to be the wettest month in Louisiana history.

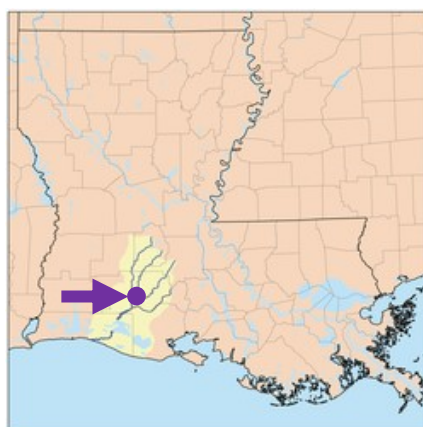


Figure 1. Mermentau River Watershed

3. Literature Review

Process based hydrologic and hydraulic models are mathematical formulations that represent the various physical phenomenon of interest using the laws of conservation of mass, energy, and momentum at appropriate scales. Due to the large spatial and temporal scales of the water cycle, hydrologic and hydraulic field observations and experiments are often cost prohibitive and time consuming. As an alternative, process based models create an inexpensive and robust medium for virtual experiments⁽²⁾. Recent model development has seen incorporation of the dynamic wave approximation to the shallow water equations for overland flow in watershed-scale simulations⁽³⁾. Theoretically, a sufficiently resolute 2-dimensional grid should have the capacity to simulate channel flow, which was initially tested by Shen (2016) on a structured grid⁽⁴⁾. However, computational efficiency problems are quickly encountered when an entire watershed is made more resolute, thus a more feasible approach to simulate 2-dimensional channel flow throughout a watershed is to utilize an unstructured grid with a variable resolution. Until now, ADHydro has not only never been tested on a region as large as the Mermentau River Watershed, but also in a region with a slope percentage this low.

4. Methodology

This study utilized several data bases and software packages to pre-process, simulate, and post-process model output. The initial data mining, which can be seen in **Figure 2**, included retrieving 10m digital elevation map (DEM) from the National Elevation Dataset (NED), land use maps from the National Land Cover Database (NLCD), soil data from the Natural Resources Conservation Service (NRCS), waterbody and precipitation data (~1 km resolution) from the National Centers for Environmental

Information (NCEI), and other climatological data (~ 12.5 km resolution) using the National Water Model Retrospective Analysis.

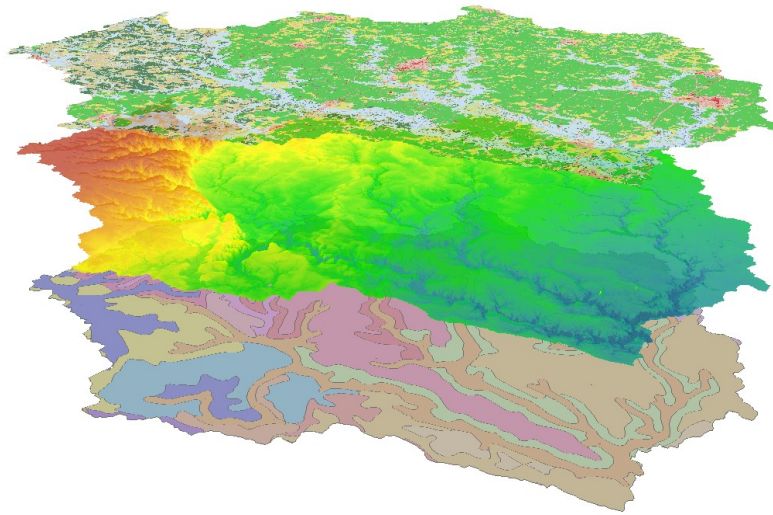


Figure 2. Mermentau Physical parameters (a) Land Use, (b) DEM, (c) Soil Type

The watershed was first delineated with TauDEM, the files were then refined in ArcMAP, and finally two meshes were created with the Triangle script. The mesh has 100m resolution 2-D overland flow and 1-D channel routing, **Figure 3**. The mesh contained 26,000 computational elements and modeled in ADHydro which uses the diffusive wave approximation to solve the 2-D overland flow and 1-D channel routing. Precipitation data was drawn from a NEXRAD from the National Climate Data Center (NCDC), while other weather forcings were drawn from the National Water Model's retrospective analysis. Due to the timing of this event, we were unable to retrieve National Water Model (NWM) precipitation because the NWM wasn't fully operational. Utilizing the Yellowstone High Performance Computer, the simulation time of 24 days required 24 hours of runtime and 18 GB memory. Finally, the post processing was accomplished using Python and ParaView.

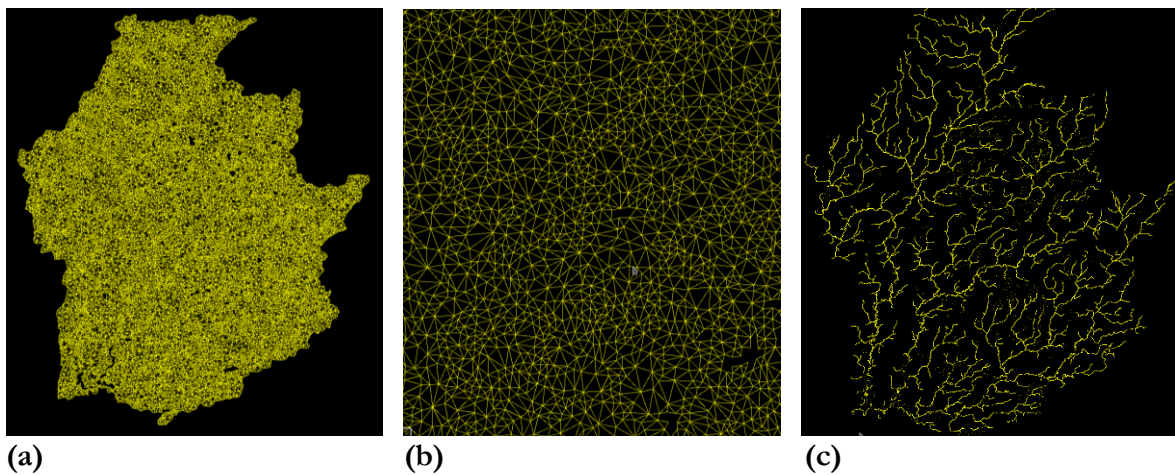


Figure 3. Mermentau Watershed Domain (a) Mesh (b) Mesh Elements (c) Channel routing network

5. Results

Precipitation amounts during the storm produced prolonged flooding leading to inundated areas throughout the watershed extent. Preliminary results indicated the model simulation underestimated observed discharge at the watershed outlet (**Figure 4**). Simulated peak discharge was about 800 cubic meters per second (cms), while observed peak discharge was roughly 1100 cms. The short term hydrologic response from the simulation generated a gentler sloping rising limb on the hydrograph. Thus, causing an underestimation of discharge in comparison with the USGS observed discharge. Furthermore, periods during the rising limb of the hydrograph exhibited sharp fluctuations. The timing of the simulated peak discharge also occurred later than the observed discharge, on the order of a few days. ADHydro simulations were also able to account for instances of negative discharge, but to a lesser degree. A comparison of the USGS observed⁽¹⁾ versus the modeled inundated areas (**Figure 5**). The model output does not accurately show the extent of the inundation. Some areas of the watershed were modeled as inundated when observations indicate otherwise and vice versa. The possible sources for these discrepancies are discussed in the following section.

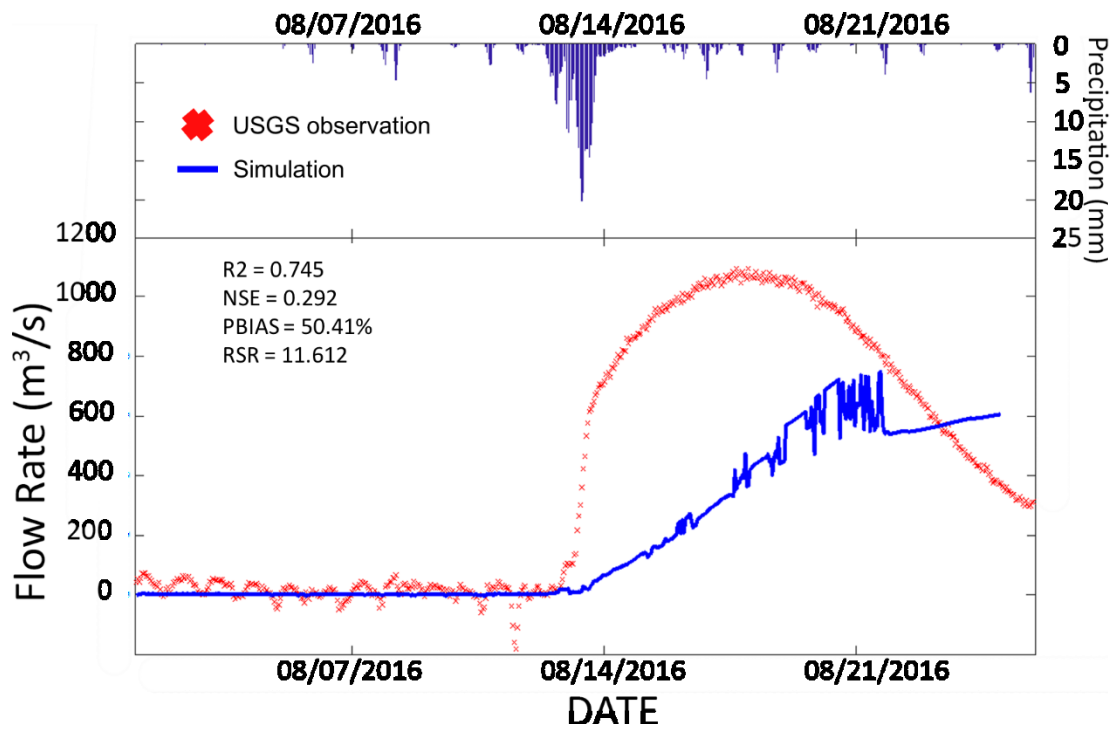


Figure 4. Results (a) NEXRAD Hyetograph (b) Hydrograph

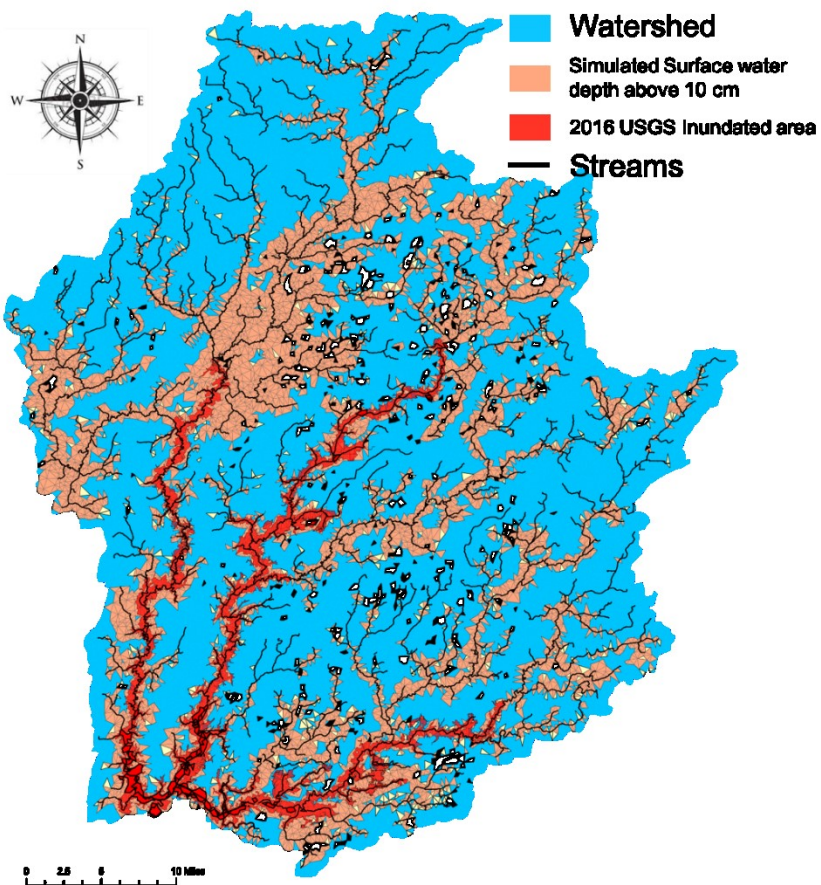


Figure 5. Inundated area

6. Conclusion

A possible source of the discrepancy between the observed hydrograph and simulated hydrograph is the quality of the radar precipitation data. NEXRAD data tends to underestimate precipitation, especially during tropical storms, due to the inability of the radar to distinguish rain droplets with a diameter below a certain threshold⁽⁵⁾. Thus, an under representation of precipitation in an H&H model was reflected in the resulting hydrograph. Based on visual inspection, the timing and magnitude of the precipitation does not correspond well with the output from the simulation further suggesting issues with the precipitation data. In this study, precipitation could be underestimated by approximately 30% based on data provided at three rain gages dispersed throughout the watershed.

The slow response exhibited at the beginning of the event could be a function of poor initial conditions, where model states may be poorly approximated due to an inadequate initialization period. Another potential reason may be the interconnectedness of groundwater and surface water in natural systems. The water table in this region is relatively shallow, which may lead to a higher level of interaction and process complexity between the two systems.

Observed discharge for the days prior to the storm displayed periods of fluctuating discharge and in some instances yielded negative discharge, similar to that of the simulated discharge. This negative discharge was common in regions with low topographic relief such as the study area and caused by a

backwater effect from daily tidal influences at low flows, where the downstream head values exceed upstream head values causing water to pool upstream. ADHydro uses the diffusive wave approximation for routing. Although the routing scheme used isn't fully dynamic, the diffusive wave approximation is still capable of capturing the effects of backwater.

A possible source of the discrepancy between the observed and simulated inundated areas, is in part due to the discrepancy in the hydrographs. However, the inundated areas are also sensitive to the flood threshold used, which was not specified in the observed data. In basins with a lack of topographic relief, effects due to backwater are heavily influenced by the location of precipitation events. One of the limitations directly related to the inundation extent results was the issue of overbank flow not being initiated in the simulation. This had significant implications on the results we obtained because as channel water depths exceeded surface water (ponded) depths, water from overland flow would pool up against channel/land surface boundary, effectively creating a boundary condition similar to a pool. Once channel depths fall below surface water depths, pooled water would be reintroduced to the channel system and routed downstream, as indicated by the large spikes in the hydrograph. Most of the spikes occurred after the storm event when the rain had concluded and channel depths began receding below surface water depths thus causing a rapid release of large amounts of water into the channel, i.e. the spike in the hydrograph.

Future work anticipated for this project still includes redoing the simulation with the overbank flow initiated to visualize ADHydro's ability to simulate inundated areas and how this scheme could be used in a real-time/operational setting. Another part was to finish what we initially sought to do, addressing if channels need to be separately simulated. By comparing 1D channel routing and 2D overland flow routing with a simulation employing only 2D overland routing, we still aim to see if there is any utility in conducting simulations adopting this hydraulic scheme in a high-performance computing environment. Also, it would also be beneficial to utilize the upstream stream gage information for further points of verification. There are two sites nested within the Mermentau River Watershed, each of which are managed by the USGS. A comparison of results from ADHydro and National Water Model would also be beneficial in isolating areas in which these models function best.

The age of big data has begun an incredible period of advancement in the discipline of Hydrology. In a time of ever advancing computational power, the ability to properly manage and forecast a natural disaster that has beset humanity since the dawn of civilization is within our grasp. When this capability is brought to fruition, it will save many lives. However, this opportunity can only be realized through partnership and cooperation of scientists from the many disciplines that encompass Hydrology. The National Water Center's fostering of collaboration is the necessary medium towards this brighter future.

The NWC Summer Institute has created long lasting professional friendships among its participants. As the next generation of Hydrologists, this experience has created lasting interdisciplinary bonds amongst us that will help forward the knowledge and applications of Hydrology. We have learned an incredible amount of skills, ranging from working in an HPC environment and developing Python scripts to interpersonal collaboration. These experiences and connections we have developed will undoubtedly aid throughout our careers.

References

1. Watson, K. M.; Storm, J. B.; Breaker, B. K.; Rose, C. E. Characterization of Peak Streamflows and Flood Inundation of Selected Areas in Louisiana from the August 2016 Flood. 2017, No. Scientific Investigations Report 2017-5005, 1–26.
2. Fatichi, S.; Vivoni, E. R.; Ogden, F. L.; Ivanov, V. Y.; Mirus, B.; Gochis, D.; Downer, C. W.; Camporese, M.; Davison, J. H.; Ebel, B.; Jones, N.; Kim, J.; Mascaro, G.; Niswonger, R.; Restrepo, P.; Rigon, R.; Shen, C.; Sulis, M.; Tarboton, D. An Overview of Current Applications, Challenges, and Future Trends in Distributed Process-Based Models in Hydrology. *J. Hydrol.* 2016, **537**, 45–60.
3. Kim, J.; Warnock, A.; Ivanov, V. Y.; Katopodes, N. D. Coupled Modeling of Hydrologic and Hydrodynamic Processes Including Overland and Channel Flow. *Adv. Water Resour.* 2012, **37**, 104–126.
4. Shen, C.; Riley, W. J.; Smithgall, K. R.; Melack, J. M.; Fang, K. The Fan of Influence of Streams and Channel Feedbacks to Simulated Land Surface Water and Carbon Dynamics. *Water Resour. Res.* 2016, **52** (2), 880–902.
5. Skinner, C.; Bloetscher, F.; Pathak, C. S. Comparison of NEXRAD and Rain Gauge Precipitation Measurements in South Florida. *J. Hydrol. Eng.* 2009, **14** (3), 248.

Chapter 5

Integrity Check of Synthetic Rating Curves for HAND Inundation Mapping

Sayan Dey¹, Oludamilola Eyelade², Lukas Godbout³ and Jeff Zheng³

¹ Purdue University, dey6@purdue.edu

² University of California Santa Barbara, dami.eyelade@geog.ucsb.edu

³ University of Texas at Austin, lukasgodbout@utexas.edu, jeff.yuanhe.zhang@gmail.com

Academic Advisors: Venkatesh Merwade, *Purdue University*; Hugo Loaiciga, *University of California Santa Barbara*; Paola Passalacqua, *University of Texas at Austin*; David Maidment, *University of Texas at Austin*

Summer Institute Theme Advisor: David Maidment, University of Texas at Austin, maidment@utexas.edu

Abstract: Synthetic rating curves (SRCs) need to accurately convert discharge to depth to produce realistic inundation maps using the height above nearest drainage (HAND) method. A generalized framework is created to assess the accuracy of SRCs against validated rating curves. Additionally, potential corrections to the SRCs are proposed to improve performance. The framework allows comparison of SRCs to USGS gage rating curves on the state or national scale, in addition to comparisons to reach-averaged rating curves from calibrated hydrodynamic models such as HEC-RAS. The effect of reach length, slope and channel roughness are investigated, and statistics are calculated for comparison of rating curves. Reach length and slope are found to correlate strongly with divergence between the rating curves, and a scaling analysis is implemented for a moving window approach to calculate slope over a variable minimum length. The SRCs are also recalculated for comparison using separate values of roughness for in-channel and overbank flows rather than a single averaged value. Further, this study develops a continental scale analysis technique which enables automated assessment of SRC performance at all USGS gage stations. Performance metrics for current SRCs are calculated for each USGS gage station in the Continental United States (CONUS) as well as averaged over HUC6 watersheds to facilitate the study of spatial variability in SRC performance across CONUS.

1. Motivation

Flood modelling and mapping on the continental scale requires methods that are efficient and do not require any field measurements. SRCs are used to convert discharge data from the National Water Model to stage height, which is then combined with HAND raster to produce inundation maps. Such maps are critical for emergency response and useful for flood forecasting, mitigation and planning to a wide variety of stakeholders. To ensure these inundation maps produce accurate estimates, it is pertinent to ensure the validity of the rating curves from which they are derived. Generalized integrity checks provide a means of testing these SRCs and ensure that they can be evaluated by any interested organization or individual.

Since rating curves are typically derived from field measurements and calibrated hydrodynamic models, SRCs derived from 10m NED topography data are expected to be less accurate and can lead

to inaccurate inundation maps. To remedy this, we look to facilitate the comparison of SRCs to validated rating curves and suggest correction methodologies to improve performance. Potential indicators of poor rating curve performance are identified, and potential changes to SRC calculation for reaches exhibiting these indicators are explored.

2. Objectives and Scope

This work builds on the efforts of Xing Zheng, a Summer Institute alumnus, who estimated the SRCs for each reach in the National Hydrography Dataset (NHD) across CONUS. Essentially, his SRC comparison is incorporated into our project to further the group's efforts in assessing the Guadalupe and San Antonio River Basins. The primary focus of this study is the development of integrity checks that collectively provide a framework for evaluating HAND SRCs. This is performed by comparing SRCs to those derived from validated hydrologic models and USGS stations. Performance metrics such as Root Mean Square Error (RMSE) and Normalized RMSE (NRMSE) are used to evaluate the performance of SRCs. Comparisons are made between SRCs and validated rating curves by assessing reach length variability, average bed slope and complex channel roughness. These elements are analyzed for possible indicators of performance and potential corrections to the SRCs.

Hydraulic models implemented in HEC-RAS provide a comparison benchmark for results from the integrity checks performed on SRCs for different reaches. HEC-RAS models for comparison with HAND SRCs are obtained with assistance from Dr. Maidment and the San Antonio River Authority. The reaches evaluated are from three rivers in Texas: i) Blanco River, ii) Guadalupe River and iii) San Antonio River. These are presented in **Figure 1**. These river basins are primarily flat with low relief and comprise of regions dominated by urban and agricultural land use.

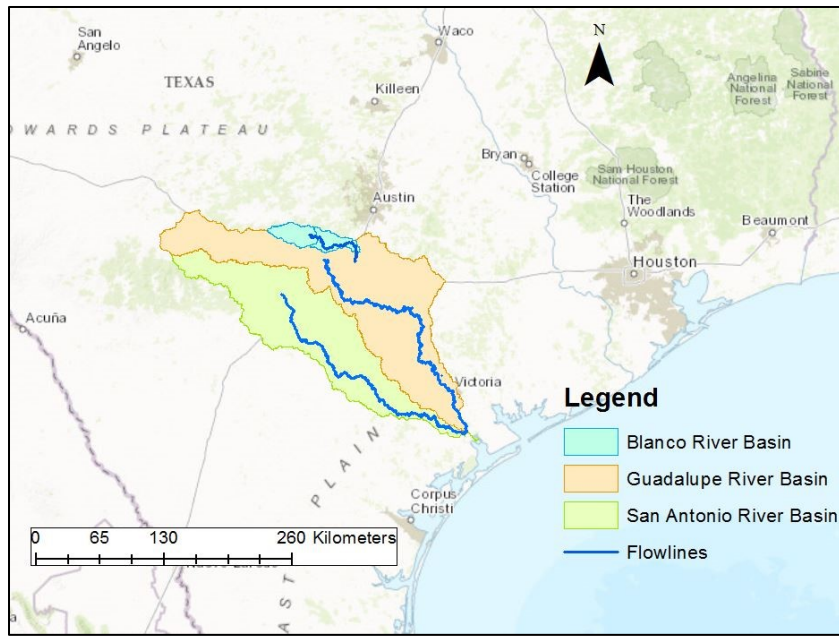


Figure 1. Map of study areas: Blanco, Guadalupe and San Antonio rivers in Texas

3. Previous Studies

Topographic data plays a key role in accuracy of flood modeling. Improvements in the resolution of remotely sensed data have made it possible to analyze and improve inundation modelling and extend

to larger scales⁽¹⁾. The ability of HAND to determine the height differential between a cell and the nearest drainage cell in a raster grid has proven useful for large scale inundation mapping when coupled with a rating curve such as the DEM based SRCs. The combination of HAND and SRCs, offers the possibility of using elevation data to make real time inundation maps across CONUS. In fact, the ability to generate HAND compatible SRCs using attributes derived from a DEM coupled with the assumption of uniform flow has already been demonstrated on a continental scale⁽²⁻³⁾.

Raster based SRCs that relate water level to discharge have been developed by multiple authors and can also be used to calculate several hydraulic geometry parameters for distinct reaches^(4, 5). To be used with a degree of confidence, a SRC must be evaluated for accuracy with validated or observed data. Results are often evaluated with the aid of performance metrics such as RMSE, NRMSE, and percentage errors⁽⁶⁾. A novel approach is the use of the bidirectional reach method which evaluates the results of a rating curve model with randomly sampled parameter sets in each observation⁽⁷⁾. The Manning's roughness coefficient is a particularly important parameter and several studies have modelled the sensitivity of hydraulic models to it^(8, 9). The present study builds on the existing methodology for calculating channel geometry and SRCs from topographic data and further evaluates performance at study sites within the United States.

4. Methodology

4.1. Rating Curve Comparison by Reach Length and Slope

Channel topography plays a significant role in determining the rating curve using uniform depth, because the Manning's equation includes topography related hydraulic variables such as wetted perimeter and slope. While the simplicity of Manning's equation enables its implementation over large scales, it also introduces errors. This is especially true for regions where the reach averaged hydraulic parameters do not represent the reach variability appropriately or where the assumptions of uniform depth are violated. To augment this simplistic method for the effects of terrain variability on SRCs, parameters such as slope and reach length are considered as indicators for determining regions where SRCs can potentially perform poorly.

NRMSE is used to quantify the performance of SRCs. It penalizes the higher errors more and the normalization allows for comparison across reaches. Python scripts are developed for calculating the NRMSE for SRCs relative to the HEC-RAS reach averaged rating curves. The HEC-RAS reach averaged rating curves are generated by taking the median HEC-RAS values and compared with HAND reach averaged discharge and depth values; the assumption being median HEC-RAS values are more representative of reach averages.

The output of the script is a table with information pertaining to RMSE, NRMSE, slope, and length for all COMIDs of interest. The table allows for the analysis of RMSE or NRMSE as a function of varying slope and/or reach length. It is worth noting that the application of RMSE as a performance metric is extremely limiting, statistically. Currently, there is no standardized method for rating curve comparisons, and as such, other possible performance metrics are widely adoptable and should be considered. Furthermore, due to time constraints, this project does not account for other geospatial patterns that may contribute to flaws in SRCs (i.e. flat terrain and urban networks).

4.2. Scaling Analysis of Moving Window

The accuracy of the SRCs depend strongly on the bed slope. Short reaches exhibit more local variability in slope, especially for medium resolution DEMs (resolution $\geq 30\text{ft}$), and due to the impact of slope in Manning's equation, are more likely to exhibit erroneous rating curves. More accurate values for bed slope allow for recalculation of the SRCs for small reaches, resulting in stage heights values that better reflect reality.

The proposed methodology is to introduce a moving window, or minimum distance over which slope is calculated. By taking the average slope over a distance which is greater than the reach itself, the effect of local variability in slope are reduced. The new slope value is calculated by taking a weighted average of the slope of the short reach itself in addition to the slopes of reaches for an equal distance upstream and downstream.

A scaling analysis approach is implemented, where reach-averaged statistics are calculated for a range of moving window lengths. An ideal minimum length or set of lengths can therefore be found for each reach, where that moving window length produces the smallest NRMSE across all reaches for a given river. This approach is generalizable and allows for the calculation of ideal moving window length for SRCs wherever more accurate rating curves are available, such as with calibrated HEC-RAS models and at USGS gage stations.

4.3. Composite Roughness Coefficients

The Manning's roughness coefficient n is another important input in the Manning's equation and computed discharge values can vary significantly due to this parameter. The HAND SRC is currently calculated using a single n value at all reaches and for all stages. A modification is made to the SRC calculation script to decompose the manning's n into two distinct values for in channel and overbank flow. A composite Manning's n value for every stage at each reach is computed using Chow's equation for composite roughness value, shown below.

$$n = \frac{(P_{ch}n_1^{1.5} + P_{ob}n_2^{1.5})^{2/3}}{P_{total}^{2/3}} \quad (1)$$

where n is the composite roughness value; n_1 and n_2 are the initial bank and overbank n values; P_{ch} is the wetted channel perimeter; P_{ob} is the wetted overbank perimeter and P_{total} is the total wetted perimeter.

To implement this, a bank raster is created that classified cells as either within the channel or as over bank. To get cells within stream channels, a buffer of stream segments based on stream order is combined with bank extents interpolated from verified HEC RAS models. The outputs indicate the sensitivity of flow to changes in channel and overbank Manning's n values.

4.4. National Scale Rating Curve Comparisons

This section describes the framework to evaluate the performance of SRCs for HAND inundation mapping. Scripts are developed to download and compare the SRC across CONUS with all available USGS rating curves automatically. The CONUS is divided according to the HUC-2 watershed boundaries – a total of 18 regions.

A script in R filters the gauge list to find gauges with discharge measurements and downloads the USGS basic rating curves using the data retrieval library developed by the USGS. These are downloaded for each HUC-2 unit. The script also downloads the corresponding “Offset” value, which is assumed to be equal to the gauge height at zero flow (GZF). The GZF is subtracted from the stage to estimate the depth-discharge relationship for the USGS gauges. The NHD flowlines dataset and the corresponding SRCs (~2.7 million) are also downloaded using an R script but they are grouped based on HUC-6 units. Python scripts are used to find the nearest flowline for each gauge. A distance filters out the flowline which are far from the corresponding gauge.

In this analysis, the dependent variable is the depth, because the discharge is obtained from the National Water Model (NWM). We compared the depths estimated from SRCs and USGS gauges for different discharge values. The SRCs have discharge calculated for depths at 1ft increments from 0ft. So, the SRCs are further filtered to find those discharges that are in the range of the USGS rating curve. Finally, for these discharges, the depth is estimated from USGS rating curves using logarithmic interpolation⁽¹⁰⁾.

The last step is evaluating the performance of the SRCs by comparing these depths. Six performance metrics are calculated for each gauge site: (i) Mean Absolute Error (MAE), (ii) RMSE, (iii) NRMSE, (iv) Coefficient of Determination (R^2), (v) Maximum Error (ME), (vi) Range and, (vii) Percent Bias (PBias). RMSE allows us to evaluate the absolute performance of SRC, NRMSE and R^2 enables comparison across sites. The Range, PBias and ME gives an indication of the variation in performance with discharge. MAE, RMSE, ME and Range are in feet while the rest are unitless.

5. Results

5.1. Rating Curve Comparison by Reach Length and Slope

Figure 2 represents the performance of SRCs generated for HANR compared to calibrated HEC-RAS models for the San Antonio River Basin. The plot shows that NRMSE is higher for reaches with much smaller slope values as compared to reaches with higher slope values. Medium slope values tend to be more spatially distributed over the given plot and have lower NRMSE when compared to lower slopes.

An interesting observation is that reaches with relatively medium slope values over a given channel network reflect, overall, SRCs that more accurately resemble calibrated HEC-RAS rating curves. It is important to note that this figure supports the overall idea that both slope and reach length are good indicators of rating curve performance. Additionally, it is worth noting that for reaches with shorter lengths there is a poorer performance with the SRCs due to higher variability in slope values. A significant assumption in this analysis is uniform water depth over the reach length. A prospective research topic could be to quantify the uncertainty introduced in SRCs because of the assumption of uniform depth. This research briefly touches upon some of its aspects in the subsequent sections.

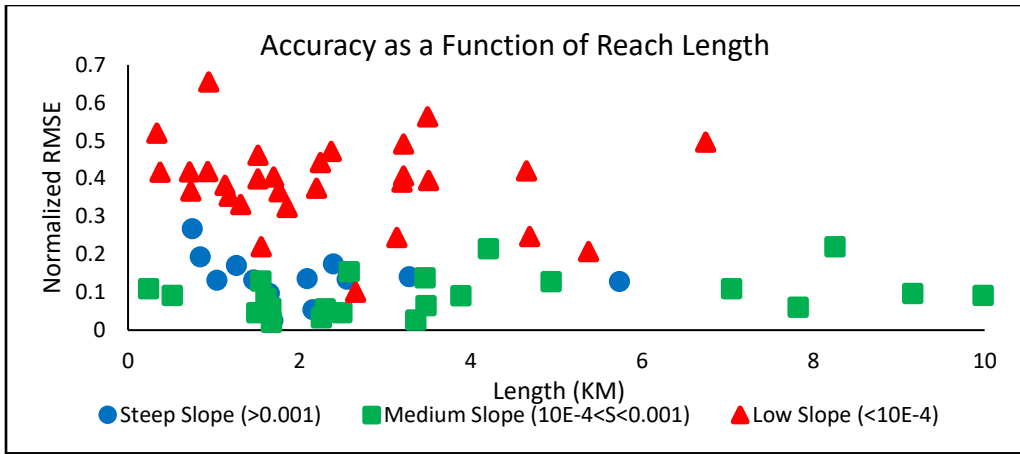


Figure 2. A measure of the departure of H4ND SRCs relative to HEC-RAS reach averaged rating curves as a function of reach length and slope for the San Antonio River Basin

5.2. Scaling Analysis of Moving Window

The scaling analysis for moving window length to recalculate SRCs with updated slope values have been completed for Blanco and Guadalupe rivers in Texas. The plots for reach-averaged NRMSE against moving window length are shown in **Figure 3**. For Blanco river, the average NRMSE decreases from 20.61% to a minimum of 7.41% for a moving window length of 1.25km, while for Guadalupe river the reduction is from 29.00% to 26.43% for a moving window length of 2.25km.

The SRCs for Blanco river are significantly improved by the moving window approach while the rating curves for Guadalupe river undergo only minor improvement. This may be due to the distribution of reach lengths where there are a higher number of shorter reaches in Blanco river, or due to the average slope which is much flatter for the Guadalupe river. The significant improvement in Blanco river suggests that this approach may be able to produce appreciably more accurate rating curves and inundation maps for some areas, but needs further analysis to better quantify the extent of improvement.

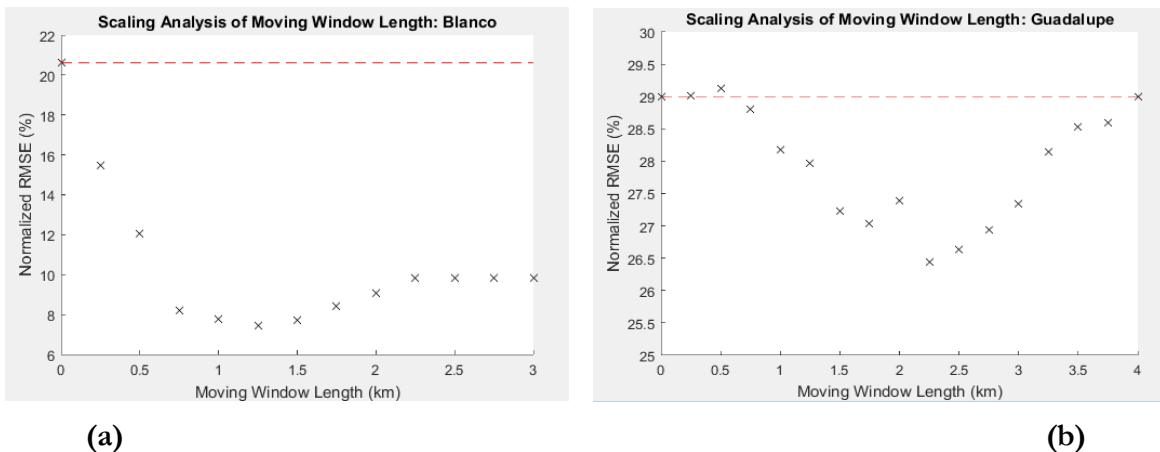


Figure 3. Scaling analysis for comparison of reach-averaged normalized RMSE against moving window length for: (a) Blanco river and (b) Guadalupe river.

5.3. Effects of Separate Roughness Coefficients

Calculating a composite Manning's n for the channel and overbank allows for the evaluation of the response of derived channel geometry to flows that spill over the channel top. Channel and overbank wetted areas are calculated separately and then used to determine the wetted perimeters needed for reach and stage specific composite roughness values. After iterating over several values of manning's n, a channel roughness coefficient of 0.04 and overbank roughness of 0.08 are found to work best.

The results show that in deep or broad channel reaches and those with little overbank area below the drainage height, a stage specific roughness value improves the SRCs. In such reaches, the discharge increases at low water stage (where the flow remains in the channel) when a composite Manning's n is incorporated, while at flood height, the increased roughness over the flood plain reduces overprediction of discharge as can be seen in the top left panel in **Figure 4**.

In areas where the channel is shallow, the results are mixed. Having a large total area below the drainage height in any reach leads to poor performance due to the fact that even at very low water heights, most of the wetted perimeter is calculated as being outside the channel. The root mean square error at most reaches for the roughness adjusted and regular SRCs are within 0.6 meters of each other. The results suggests that incorporation of composite Manning's n can help improve the HAND derived rating curves in areas where the channels are broad or very deep. Better representation of the channel bottom may increase the usefulness of having reach and stage specific roughness values.

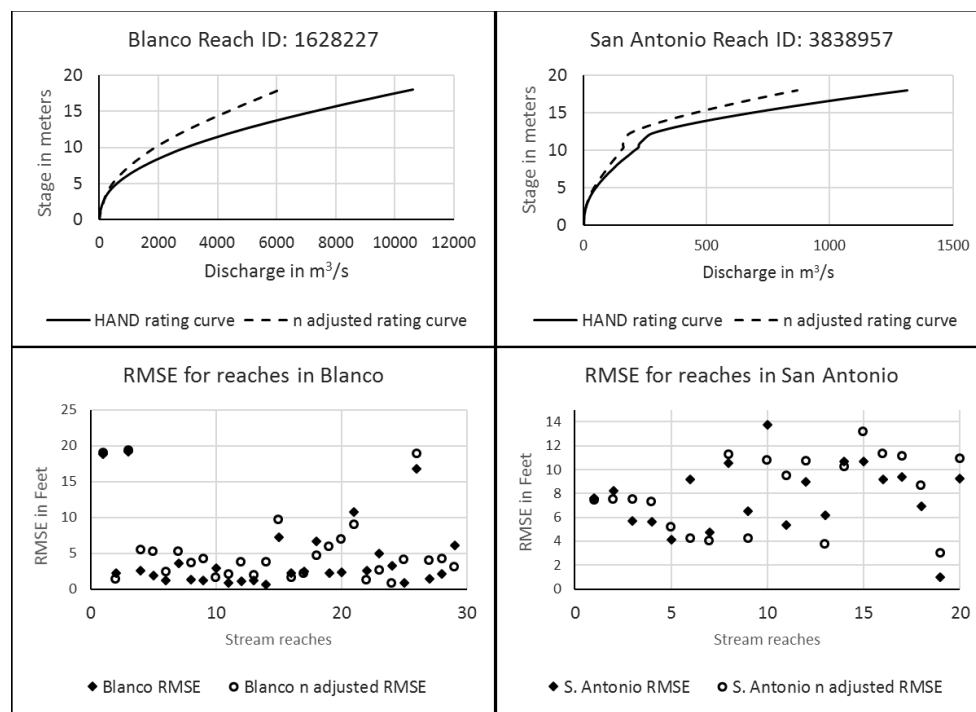


Figure 4. SRCs and root mean square error for reaches on Blanco and San Antonio rivers

5.4. National Scale Rating Curve Comparisons

Before applying the analysis on a national scale, it is important to verify the methodology. This is accomplished by comparing the results of this analysis with Kisters' dataset. Kisters

(nwm.kisters.de/KiWIS/) maintains a database of gauges in Texas for which it calculates the average error in depth estimated by SRC and their own rating curves. The proposed methodology is applied to instantaneous streamflow measurements at these sites for the period spanning 10th December 2016 to 8th July 2017. The average depth error estimated from this analysis is compared to the values estimated by Kisters. **Figure 5**, which shows the frequency distribution of the difference between the values estimated from these two analyses, indicates that there is a reasonable match between the two.

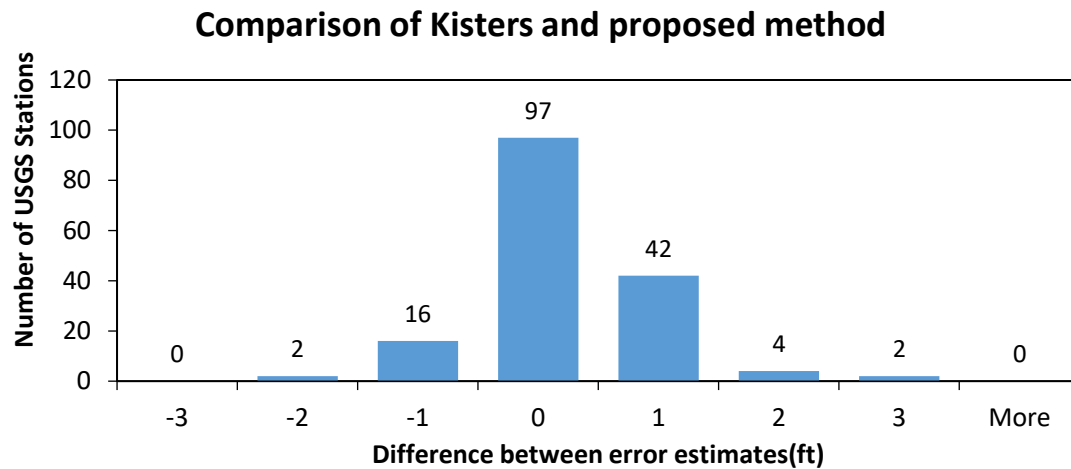


Figure 5. Histogram of difference between error estimates of SRCs and Kisters method

The proposed methodology is applied to the CONUS using the High Performance Computer at University of Wyoming (Mt. Moran). A total of 8712 rating curves are evaluated. **Figure 6** shows all the gauges color-coded by their corresponding RMSE. Additional analyses can be conducted on the performance of SRCs using this framework. **Figure 7** shows the RMSE of the SRCs averaged over HUC6 units. This gives an idea of the spatial variation in the SRC performance. The SRCs seem accurate in the arid New Mexico region while there is relative poorer performance around the Gulf Coast. A frequency analysis of the SRC performance at the USGS gauges using NRMSE indicates that nearly half of the gauge sites have less than 25% error.

The entire framework is automated, and therefore, has the potential to facilitate the investigation of SRC performance as well as the impact of any improvement techniques applied to the SRC on a continental scale. It should be noted that any conclusion made from this analysis should be put in the context that the SRC have been compared using base USGS rating curve with an uncomplicated way of estimating GZF. Also, USGS rating curves are estimated at a cross-section whereas SRC is representative of the whole reach.

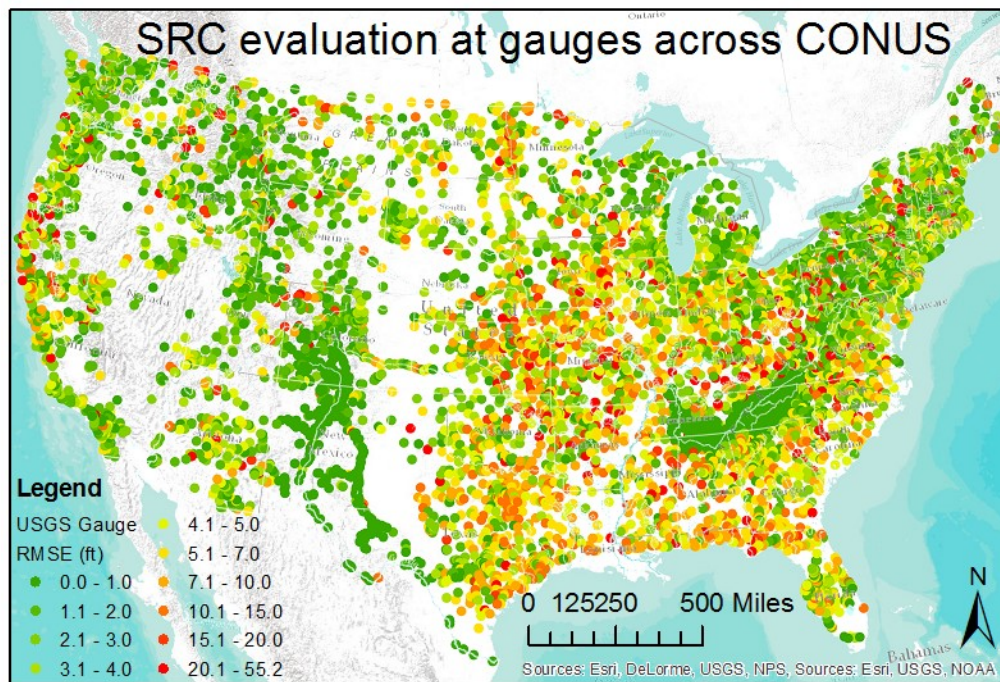


Figure 6. All the USGS gauges across CONUS for which SRCs were evaluated. The color code shows the RMSE at each site.

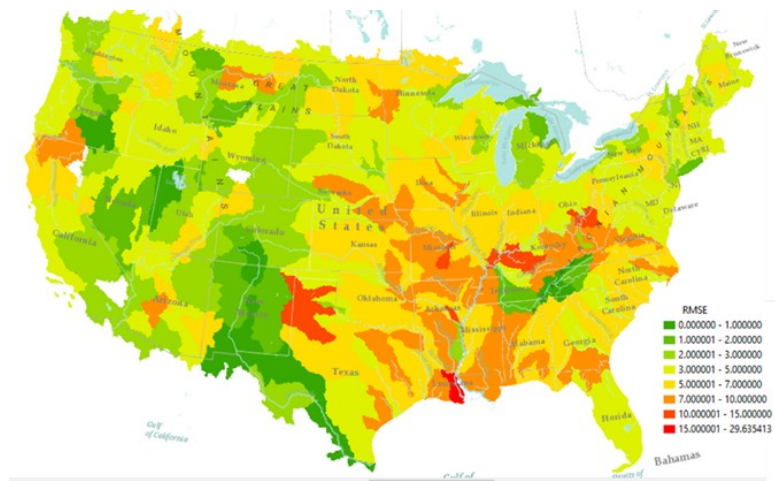


Figure 7. RMSE averaged over the HUC-6 watersheds. Those missing the color code had no gauge information.

6. Conclusion

The HAND methodology coupled with the SRCs, has the potential to provide real time inundation extents for discharges generated by the National Water Model. The SRCs are estimated using terrain data in conjunction with the assumption of uniform flow. This study proposes a framework to analyze and predict the accuracy of SRCs. The terrain derived SRCs are not currently particularly accurate, but their suitability for continental scale inundation mapping warrants further attention and study to improve their accuracy.

True to the idea of intensive, exploratory research in the Summer Institute, this study demonstrates potential improvements to the SRCs that can be implemented across CONUS while at the same time it provides an automated way to evaluate SRCs against USGS rating curves. This framework can be used in future research to not only analyze SRC accuracy, but to find important indicators for poor SRC performance and the necessary corrections for those particular rating curves.

References

1. Nobre, A. D.; Cuartas, L. A.; Hodnett, M.; Rennó, C. D.; Rodrigues, G.; Silveira, A.; Waterloo, M.; Saleska, S. Height Above the Nearest Drainage – a Hydrologically Relevant New Terrain Model. *J. Hydrol.* 2011, 404 (1), 13–29 DOI: 10.1016/j.jhydrol.2011.03.051.
2. Nobre, A. D.; Cuartas, L. A.; Momo, M. R.; Severo, D. L.; Pinheiro, A.; Nobre, C. A. HAND Contour: A New Proxy Predictor of Inundation Extent. *Hydrol. Process.* 2016, 30 (2), 320–333.
3. Zheng, X.; Maidment, D.; Liu, Y.; Tarboton, D. G.; Lin, P. From Forecast Hydrology to Real-Time Inundation Mapping at Continental Scale. In AGU Fall Meeting Abstracts; 2016.
4. Pan, F.; Wang, C.; Xi, X. Constructing River Stage-Discharge Rating Curves Using Remotely Sensed River Cross-Sectional Inundation Areas and River Bathymetry. *J. Hydrol.* 2016, 540, 670–687 DOI: 10.1016/j.jhydrol.2016.06.024.
5. Paris, A.; André Garambois, P.; Calmant, S.; Paiva, R.; Walter, C.; Santos da Silva, J.; Medeiros Moreira, D.; Bonnet, M.-P.; Seyler, F.; Monnier, J. Identifiability of Altimetry-Based Rating Curve Parameters in Function of River Morphological Parameters. In EGU General Assembly Conference Abstracts; 2016; Vol. 18, p 18142.
6. Pavelsky, T. M. Using Width-Based Rating Curves from Spatially Discontinuous Satellite Imagery to Monitor River Discharge. *Hydrol. Process.* 2014, 28 (6), 3035–3040 DOI: 10.1002/hyp.10157.
7. Van Eerdenbrugh, K.; Van Hoey, S.; Verhoest, N. E. Identification of Temporal Consistency in Rating Curve Data: Bidirectional Reach (BReach). *Water Resour. Res.* 2016, 52 (8), 6277–6296.
8. Kalyanapu, A. J.; Burian, S. J.; McPherson, T. N. Effect of Land Use-Based Surface Roughness on Hydrologic Model Output. *J. Spat. Hydrol.* 2010, 9 (2).
9. Ozdemir, H.; Sampson, C.; de Almeida, G. A.; Bates, P. D. Evaluating Scale and Roughness Effects in Urban Flood Modelling Using Terrestrial LIDAR Data. *Hydrol. Earth Syst. Sci.* 2013, 10, 5903–5942.
10. Sauer, V.B., Standards for the Analysis and Processing of Surface-Water Data and Information Using Electronic Methods: U.S. Geological Survey Water-Resources Investigations Report, 2002, 01–4044, 91 p.

Chapter 6

Comparing NWM Inundation Predictions with Hydrodynamic Modeling

Apoorva Shastry¹, Cehong Luo², Fernando Aristizabal³ and Ryan Egbert⁴

¹ The Ohio State University, shastry.7@osu.edu

² University of Alabama, c Luo5@crimson.ua.edu

³ University of Florida, fernandoa@ufl.edu

⁴ Brigham Young University, rjegbert@byu.edu

Academic Advisors: Michael Durand, *Ohio State University*; Sarah Praskiewicz, *University of Alabama*; Jasmeet Judge, *University of Florida*; Jim Nelson, *Brigham Young University*

Summer Institute Theme Advisor: Sarah Praskiewicz, University of Alabama, spraskiewicz@ua.edu

Abstract: The National Water Model (NWM) is a hydrologic model that uses Muskingum-Cunge method to route the streamflow. We use the steady-state version of Simulation Program for River NeTworks (SPRNT), a model that solves the full one-dimensional (1D) Saint-Venant Equations (SVE), to simulate the flood event that occurred in Goldsboro, North Carolina during Hurricane Matthew. The Neuse River experienced record breaking floods and was well documented by the U.S. Geological Survey. The streamflow data from the National Water Model retrospective analysis is used as input data for the SPRNT simulation. The river stages from SPRNT are utilized to produce flood inundation maps using Height Above Nearest Drainage (HAND) that uses the local relative heights to find out the local draining potentials and provide an accurate spatial representation of inundations. Thus produced flood inundation maps were validated by comparing against remote sensing data from Sentinel-1 with auxiliary data. The study found that the flood inundation accuracy for NWM and SPRNT were 74.68% and 78.37%, respectively. The difference in the accuracies, sensitivity/recall, precision, and specificity were found to be statistically significant and supported rejecting the null hypothesis that the NWM is better at predicting inundation for the limited study area and the assumptions made. We also built an interactive Tethys App to display and compare the inundation maps created.

1. Motivation

Floods are one of the most damaging natural hazards. In the U.S. alone, the 30-year flood loss yearly average is \$7.96 Billion in damages and 82 fatalities per year⁽¹⁾. With growing population exposure and climate change, the number of people that are exposed to flood risks, and the frequency and magnitude of floods can be expected to increase⁽²⁾. There is a need for better flood forecasting, and flood inundation models play an important role with these problems.

The National Water Model (NWM) simulates the water cycle, and produces streamflow forecasts, runoff, among other variables, for 2.7 million reaches across the entire continental United States. NWM is a hydrologic model that applies the Muskingum-Cunge channel routing techniques to the

National Hydrography Dataset (NHD) stream reaches. The Muskingum-Cunge method is solely based on the continuity equation. To obtain better estimates of streamflow and stage in rivers, especially for applications such as flood inundation mapping, the momentum equation also needs to be considered.

SPRNT is a fully dynamic model for large scale river networks created by a collaborative effort between a computer scientist and a hydroscientist⁽³⁾. SPRNT solves the full nonlinear Saint-Venant equations for 1D unsteady flow and stage height in river channel networks with non-uniform bathymetry⁽⁴⁾, using the NHD flowline framework to define the river network. Given the computational efficiency of SPRNT⁽⁴⁾, and the fact that SPRNT and NWM use the same framework of stream reaches, it would be an ideal set-up to run SPRNT along with the NWM to get streamflow and stage forecasts. The river stages from SPRNT can be converted to flood inundation maps using the HAND method^(5, 6).

The presented work is a case study to assess the applicability of using SPRNT along with the NWM to produce better flow and stage forecasts, and convert them to flood inundation predictions using HAND. The unsteady state SPRNT solution does not converge due to the uncertainty in the data for cross-section and bed slopes. The difference between the real world and theoretical solution to SVE, and the limitation of Pressimann Scheme solving transition flow between supercritical and subcritical flow also causes instability in the unsteady state SPRNT. For this reason, we used steady state SPRNT in the current work.

Hurricane Matthew brought in heavy rainfall to North Carolina between October 7th and October 9th of 2016 and caused major flooding in the region. The calamity resulted in 28 fatalities and estimated damages of \$1.5 billion⁽⁷⁾. We use the steady state SPRNT to simulate the peak flow and stages in the Goldsboro region of North Carolina.

2. Objectives and Scope

The goal of this study is to compare the performance of NWM against a steady-state hydraulic model (SPRNT) in predicting river stages that can be converted into flood inundation maps using HAND. The accuracy of the flood inundation maps can be evaluated by comparing them to Synthetic Aperture Radar (SAR) data gathered by the European Space Agency's (ESA) SENTINEL-1 satellite constellation. We use the Goldsboro region in North Carolina as our case study to simulate the peak inundation for Hurricane Matthew. The specific objectives of the case study are as outlined below:

- i. Build a steady-state model of Goldsboro region during the flood peak of Hurricane Matthew.
- ii. Use HAND to convert river stages from SPRNT and NWM into flood inundation maps.
- iii. Validate the flood inundation maps obtained from SPRNT and NWM stages using remote sensing data. Compare using binary comparison statistics and hypothesis testing.
- iv. Build a Tethys app to communicate the results.

3. Previous Studies

Muskingum-Cunge method is based on flow and channel characteristics, but does not account for non-uniform flows⁽⁸⁾. Hence, the Muskingum-Cunge does not capture the dynamics of backwater effects and unsteady flows, and solution to the dynamic wave equation is needed. 1D St. Venant equations, which constitute a continuity equation and a momentum equation, are used to model river networks, but most existing models are not capable of handling continental scale networks⁽⁹⁾. SPRNT, a hydrodynamic model that solves the full 1D St. Venant equations, can handle river networks at

continental scales 330 times faster than real time⁽⁴⁾. In the present study, we build a model of the Goldsboro region using the steady-state version of SPRNT. HAND, a normalized terrain model⁽⁵⁾, has been used to accurately predict the inundation extent of the channel carrying the flood wave⁽⁶⁾.

4. Methodology

The study area was the region of Goldsboro, NC. **Figure 1** shows the map of the study area, along with the stream-network. The study area consisted of five HUC12 watersheds: Buck Swamp-Little River, Headwaters Stoney Creek, Outlet Stoney Creek, Quaker Neck Lake-Neuse River, Seymour Johnson Air Force Base-Neuse River. The main stems of the Neuse River, Little River and Stoney Creek were modeled using SPRNT. SPRNT needed NHD flowlines, runoff data, and river geometry for the model to be set up. A streamflow upstream boundary condition and a stage downstream boundary condition were also needed. A SPRNT preprocessor took all the above input and produced a netlist (.spt) file that describes the channel network, channel geometry, forcing terms, junction contribution ratios and boundary conditions. For a steady state simulation, the runoff data is not required.

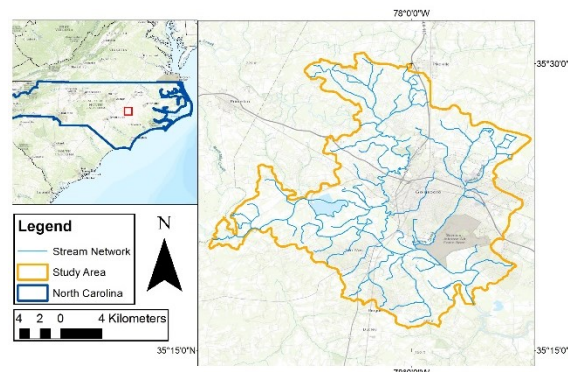


Figure 1. Study Area Map of Goldsboro, NC along the Neuse River

The river geometry was defined using SPRNT's intrinsic definition which takes in the wetted area (A), wetted perimeter (P), stage (Y) and top width (W) data and derives the channel bathymetry. This data can be obtained from HAND rating curves⁽¹⁰⁾. SPRNT needs a minimum of five monotonously increasing points of data for A, P and Y to successfully derive a channel bathymetry. The A-P-Y-W data from NHDPlus does not always conform to this rule of monotonous increase. It is because the channel property calculation is bounded by the NHDPlus catchment boundary, and all the variables related to inundated area end up having constant values, except for stage. We tried to resolve the non-monotonous A-P-Y-W problem by removing the data points when one of the variables stopped increasing. We used Piecewise Cubic Hermite Interpolating Polynomial to produce five points for A-P-Y-W from the existing data where there weren't enough monotonously increasing data points. These interpolated points can lead to unreasonable cross-sections. To resolve this problem we used the data from the upstream node to define the unreasonable cross-sections. It should also be noted that some unreasonable A-P-Y-W data exist for the stream segments that conform to the monotonous increase; those were replaced with cross-sections from the upstream node as well.

NWM retrospective analysis data for the Neuse River at Goldsboro was used as input for our models. The peak October 12th, 2016 flow data was used for the upstream boundary condition, and the corresponding stage as the downstream boundary condition. The steady state simulation was executed and the river stage data from the simulation was used to generate flood inundation maps. The stages in each HUC 12 were tested for outliers and were removed, using three times interquartile range as the threshold. To produce SPRNT flood inundation maps using HAND, we aggregated the stages from all the streams in each HUC12, and used the mean stage as input for the HAND inundation map.

The HAND tool was used to generate inundation maps for both the NWM and SPRNT. A HAND raster was created for the five HUC12s using a Digital Elevation Model in ArcMap. Values from NWM and SPRNT were used as the inputs for the HAND inundation maps. The NWM flow values were converted to stage values using HAND rating curves. A Python script designed by Xing Zheng at UT Austin was used to create HAND inundation maps that had individual depth values for each HUC12. In the script, the COMID of each catchment is linked to specific depth values, catchments, and the corresponding HAND raster grids. The output was a HAND inundation map based on the aggregated mean stage for each HUC12. The HAND inundation map for SPRNT results was obtained by using average stage from SPRNT for each HUC12.

To validate the flood inundation maps from SPRNT and NWM, a remote sensing approach was leveraged utilizing the European Space Agency's (ESA) SENTINEL-1 C-Band (5.405 GHZ) Synthetic Aperture Radar data that was collected on October 12th, 2016. This particular dataset was selected because of its spatial and temporal alignment with the peak stage for the Goldsboro, NC area⁽⁷⁾. The imagery was collected in the Interferometric Wide (IW) Swath acquisition mode which supports VV and VH dual polarization for land targets and processed to the level-1 Ground Range Detected (GRD) at a high resolution (Copernicus).

The SAR data was treated to additional preprocessing prior to classification which included reprojection to WGS84 UTM Zone 17 and speckle filtering to reduce noise. The SAR VV and VH polarizations were filtered using a single product, refined Lee filter with the help of the Sentinel Applications Platform (SNAP). Due to the forested and urban nature of the study area, SAR alone was found to not be a valid predictor for inundated areas due to the canopies' and buildings' interference with the radar backscatter and reflectance. In order to correct for this, the HAND data for the given study region was utilized as an auxiliary predictor to improve the classification performance of the SAR data.

Training data needed to be designated in order to classify the selected study area into water and non-water categories. The USGS report for Hurricane Matthew documents a series of High Water Marks (HWM). This dataset along with the National Hydrography Dataset (NHD) Plus was used to derive eighty training points that are spatially distributed in the study area⁽¹²⁾. **Figure 2** illustrates the spatial distribution of the training points within the study area as well as the USGS HWM and the predictors represented in false color. In order to classify the entire study area, Quadratic Discriminant Analysis (QDA) was selected from the MASS package within R programming language⁽¹³⁾. The trained model parameters were generalized to the entire study area with parallel computing^(14, 15).

In order to test the hypothesis of our study, we used a pixel based, binary evaluation that compares areas modeled as flooded by SPRNT and NWM to the reference classified remote sensing data. The fundamental statistics for binary comparison of True Positive (TP), False Positive (FP), True Negative (TN), and False Negative (FN) were computed as well as the secondary statistics including accuracy,

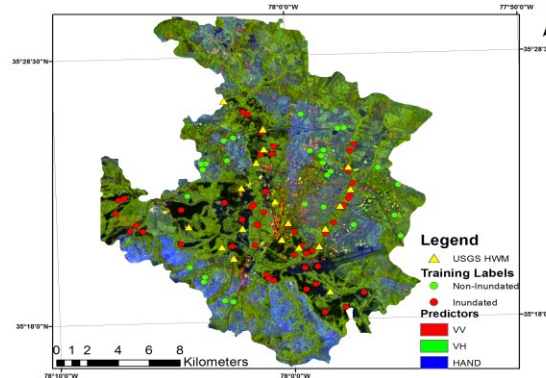


Figure 2. Data points and high water marks used to classify the three band raster consisting of SAR VV, SAR VH, and HAND. The three bands are represented as a false color image.

sensitivity, specificity, and precision. The secondary statistics were designated as test statistics for hypothesis testing.

To communicate our results we developed a Tethys web application called SPRNT Viewer that displays and compares the different inundation maps geospatially using Tethys framework software in an interactive environment⁽¹⁶⁾. The workflow was similar to the West Virginia HAND Flood Map app⁽¹⁷⁾. The app is comprised of four web pages including SPRNT-NWM Comparison, Validation, HAND, and Hurricane Matthew. The SPRNT NWM Comparison page has the SPRNT HAND Map, the NWM Hand Map, and the Validation Map displayed on a Bing aerial basemap. The user can zoom and scroll on the map to view different sections of the inundated areas. On the left pane the user can toggle on and off the different maps using checkboxes. The Validation tab presents the work that went into building the Validation Map. It displays the training labels, USGS High Water Marks, Predictors Raster, and Classified Reference Raster. The HAND page shows the different HAND inundation maps generated for the five HUC12s. The Hurricane Matthew tab has information about the inundation event and includes an aerial video clip of the inundation event.

5. Results

We simulated Hurricane Matthew in the Goldsboro region using steady state SPRNT, and obtained flows and stages in each stream segment in the network. SPRNT stage was compared to that from NWM at each COMID and is shown in **Figure 3**. In general, NWM derived stages are higher.

Figures 4 and 5 show the inundation extent of Hurricane Matthew at Goldsboro, NC on October 12th. **Figure 4** shows the inundated extent from the results of NWM, and **Figure 5** shows the flooding extent from the results of SPRNT. We aggregated the stream segments in HUC12 units for both NWM and SPRNT to get a mean value of stage, as only the main stem was modeled using SPRNT. Based on the figures, the flood extent appears similar between the NWM and SPRNT. In fact, **Figure 4** shows more inundation extent because of the higher stage value from NWM.

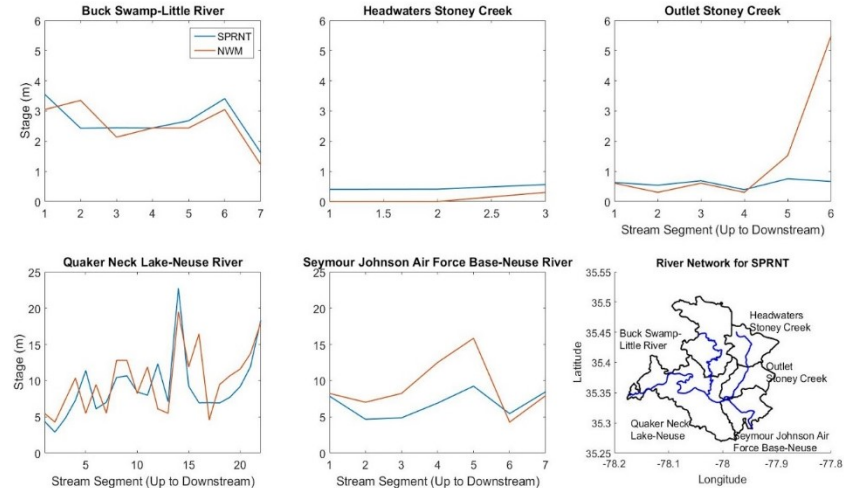


Figure 3. Comparison of Stage between NWM and SPRNT results.

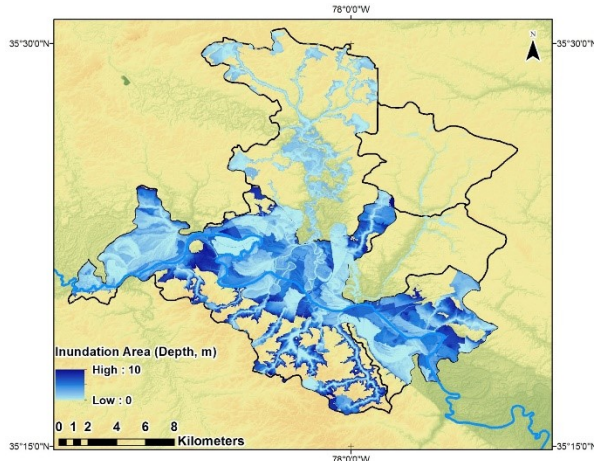


Figure 4. Inundation Map Produced by Using Aggregated Stage Values of Mainstream from NWM.

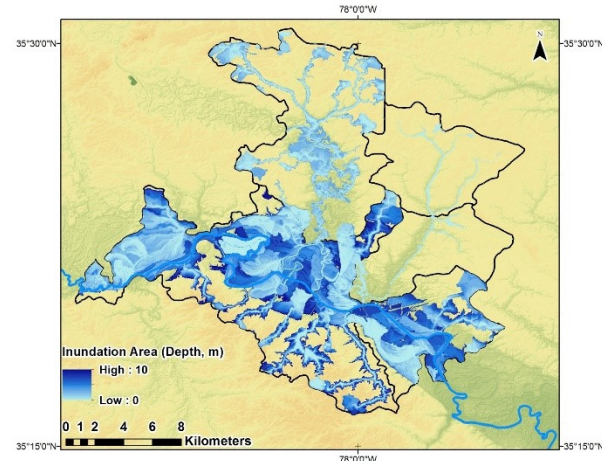


Figure 5. Inundation Map Produced by Using Aggregated Stage Values of Mainstream from SPRNT.

Figure 6 shows the direct comparison of the inundation area of SPRNT and NWM. It is clear that the inundation extent from NWM is larger than that of SPRNT model and it is noted that most additional inundated areas from NWM are situated along or near the mainstream of Neuse River while most additional inundated areas from SPRNT are located along the tributaries: Buck-Swamp Little River and Headwaters Stoney Creek. This indicates that steady state SPRNT possibly captures backwater effects.

The results of the QDA classification of SAR data along with auxiliary information is presented below in **Figure 7**. The image captures the flooded extent accurately given its agreement with all the USGS HWM as seen below. By adding the HAND data as an auxiliary predictor, the under canopy inundated areas were properly captured while limiting the FPs for forested lands in non-inundated areas. Further research is required to show how HAND auxiliary data can better improve SAR or multi-spectral satellite water detection.

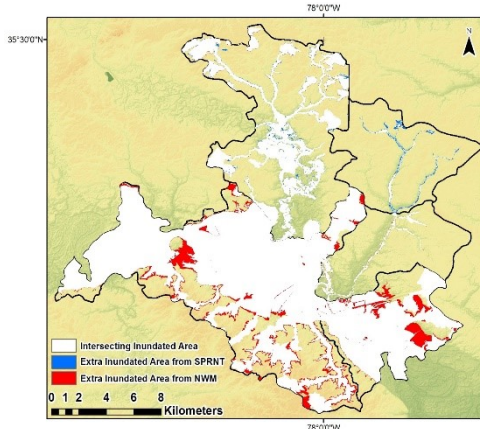


Figure 6. The Comparison of Inundation Area from Results of SPRNT and NWM.

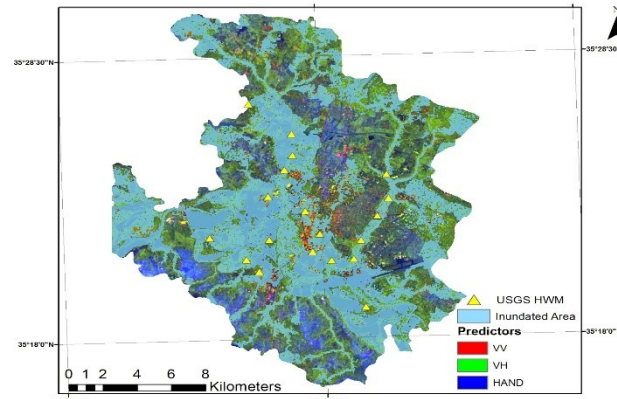


Figure 7. QDA Classified Inundation Map for Goldsboro, NC Region Using SAR and HAND as Predictors.

The results of the pixel based inundation comparison are presented for both the NWM and SPRNT model as a confusion matrix in **Table 1**. The confusion matrices present a binary comparison of flood inundation maps from the models against the classified image that list the number of TP, FP, FN, TN

as well as their relevant percentages in the entire image. It is important to note that the prevalence of inundated areas in the reference raster is 44.02%.

Table 1. Confusion Matrix Demonstrating the Performance of the NWM and SPRNT Compared to Reference Classified Map. Pixels are shown in Millions ($\times 10^6$) and Percentages are out of the Total Number of Pixels in Study Area (3.1690×10^6).

| | | Classified Reference Image | | | | | |
|-------|----------------------|----------------------------|-------|-----------|-------|--------|--------|
| | | Non-Inundated | | Inundated | | Total | |
| | | Pixels | % | Pixels | % | Pixels | % |
| NWM | Non-Inundated | 1.3310 | 42.00 | 0.3592 | 11.34 | 1.6902 | 53.33 |
| | Inundated | 0.4430 | 13.98 | 1.0358 | 32.68 | 1.4788 | 46.67 |
| | Total | 1.7740 | 55.98 | 1.3950 | 44.02 | 3.1690 | 100.00 |
| SPRNT | Non-Inundated | 1.4371 | 45.35 | 0.3485 | 11.00 | 1.7855 | 56.34 |
| | Inundated | 0.3369 | 10.63 | 1.0465 | 33.02 | 1.3834 | 43.44 |
| | Total | 1.7740 | 55.98 | 1.3950 | 44.02 | 3.1690 | 100.00 |

In order to test the hypothesis that SPRNT performs better than NWM, the following test statistics were selected: accuracy, sensitivity/recall, specificity, and precision. **Figure 8** declares null and alternative hypothesis selection for the test statistics (TS). Also, declares the level of significance and the rejection region given the normal distribution assumption. The results for these statistics as well as the results of the hypothesis test for each statistic are presented in **Table 2**.

$$H_0: TS_{NWM} \geq TS_{SPRNT}$$

$$H_a: TS_{NWM} < TS_{SPRNT}$$

$$\alpha = 0.05$$

$$RR: Z < -1.6449$$

Figure 8. Null and Alternative Hypothesis Selection for the Test Statistics.

Table 2. Results of Hypothesis Test

| Test Statistics (TS) | NWM | | SPRNT | | P-Value | Reject H ₀ ? |
|---------------------------|--------|-----------------|--------|-----------------|---------|-------------------------|
| | Value | 95% CI | Value | 95% CI | | |
| Accuracy | 0.7468 | (0.7464,0.7472) | 0.7837 | (0.7833,0.7841) | ~0.0000 | Yes |
| Sensitivity/Recall | 0.7425 | (0.7419,0.7431) | 0.7502 | (0.7496,0.7508) | ~0.0000 | Yes |
| Specificity | 0.7503 | (0.7497,0.7508) | 0.8101 | (0.8096,0.8106) | ~0.0000 | Yes |
| Precision | 0.7004 | (0.6998,0.7011) | 0.7565 | (0.7559,0.7571) | ~0.0000 | Yes |

Due to the high number of pixels, the standard error of all the TS is fairly low. The confidence intervals do not overlap for either of the TS and none of the P-values fall above the level of significance selected. The null hypothesis for all the TS were rejected. We concluded that SPRNT derived flood inundation maps were more accurate.

These results were built into a web application, the SPRNT Viewer app, using the Tethys framework. The app allows users to view the created inundation maps, see **Figure 9**. The SPRNT app is available at <http://tethys-staging.byu.edu/apps/sprnt>.

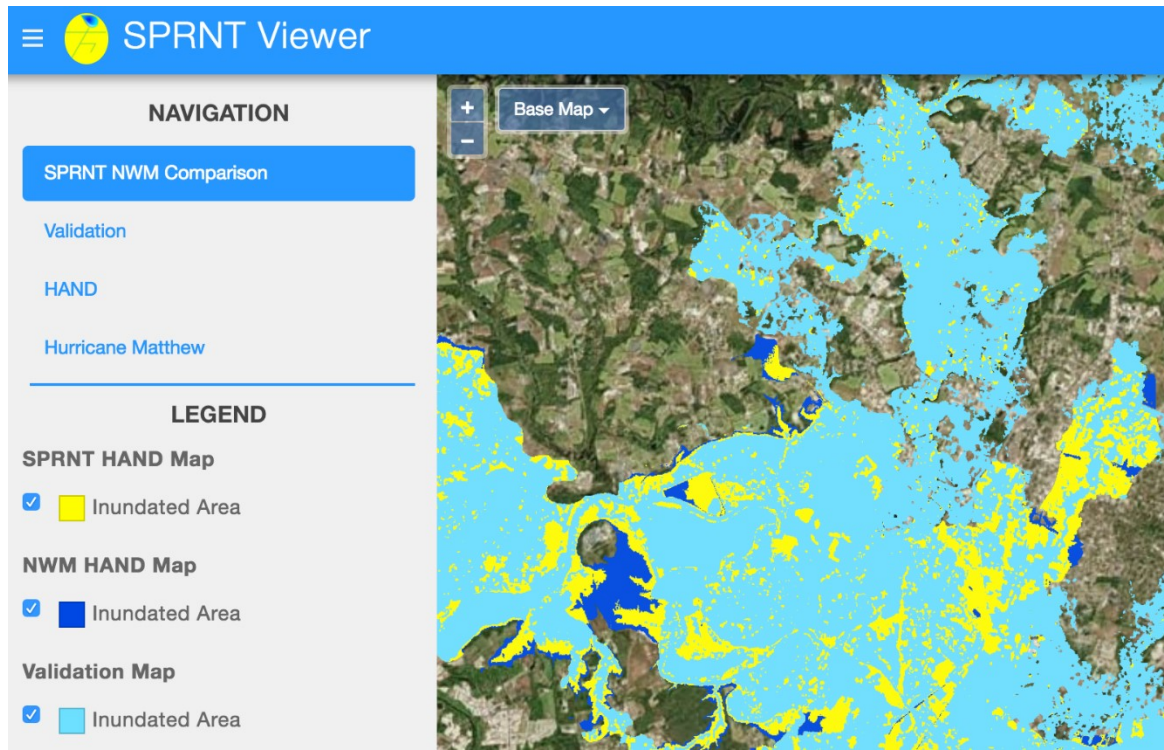


Figure 9. The Interface of the Tethys Web Application for SPRNT

6. Conclusion

SPRNT needs more detailed geometric data than what the NWM uses for flow routing. The data can be obtained from the HAND rating curves, but are not always reliable. Cross-sections for streams need to be checked for any unreasonable values; adjacent streams should not have drastic changes in cross-sections.

With the available data we have, setting up SPRNT to run along with the NWM is not a trivial exercise. For the given TS's that were used in this study, SPRNT outperformed the NWM with statistically significant results ($P = \sim 0.0000$ for all TS). However, our study area is limited and a more expansive study area should be modeled to draw a final conclusion on the applicability of SPRNT for forecasting floods with backwater effects. It suggests that stable unsteady state SPRNT simulations might capture backwater effects. The flood inundation map produced from steady state SPRNT results is an improvement from that of NWM results. However, it is interesting to see that aggregating the NWM results to just the main stem of the river produces similar results.

Acknowledgements: Fred Ogden, Alison Appling, Donald Johnson, Fernando Salas, Sagy Cohen, Ehab Meselhe, Mike Johnson, James Coll, Nathan Swain, Xing Zheng, David Maidment, Ed Clark, Jim Nelson, Cheng-Wei Yu

References

1. National Weather Service-Hydrologic Information Center <http://www.nws.noaa.gov/hic/>.
2. IPCC. *IPCC 2014*; 2014.
3. Liu, F.; Hodges, B. R. Dynamic River Network Simulation at Large Scale. Design Automation Conference, 2012.
4. Liu, F.; Hodges, B. R. Applying microprocessor analysis methods to river network modelling. *Environ. Model. Softw.* 2014, *52*, 234–252.
5. Nobre, A. D.; Cuartas, L. A.; Hodnett, M.; Rennó, C. D.; Rodrigues, G.; Silveira, A.; Waterloo, M.; Saleska, S. Height Above the Nearest Drainage - a hydrologically relevant new terrain model. *J. Hydrol.* 2011, *404* (1–2), 13–29.
6. Nobre, A. D.; Cuartas, L. A.; Momo, M. R.; Severo, D. L.; Pinheiro, A.; Nobre, C. A. HAND contour: A new proxy predictor of inundation extent. *Hydrol. Process.* 2016, *30* (2), 320–333.
7. Musser, J. W.; Watson, K. M.; Gotvald, A. M. *Characterization of Peak Streamflows and Flood Inundation at Selected Areas in North Carolina Following Hurricane Matthew*; 2017.
8. Ponce, V. M. *Engineering Hydrology, Principles and Practices*; Prentice Hall: Englewood Cliffs, NJ, 1989.
9. Hodges, B. R. Challenges in continental river dynamics. *Environ. Model. Softw.* 2013, *50*, 16–20.
10. Maidment, D. R. Conceptual Framework for the National Flood Interoperability Experiment. *J. Am. Water Resour. Assoc.* 2017, *53* (2), 245–257.
11. SAR Basics with the Sentinel-1 Toolbox in SNAP Tutorial. Available online: <http://step.esa.int/main/doc/tutorials/> (accessed on 22 May 2017).
12. Horizon Systems Corporation, National Hydrography Dataset Plus: Documentation <http://www.horizon-systems.com/nhdplus/documentation.php>.
13. Venables, W. N.; Ripley, B. D. *Issues of Accuracy and Scale* 2002, No. March, 868.
14. Tierney, L.; Rossini, A. J.; Li, N.; Sevcikova, H. snow: Simple Network of Workstations. 2016.
15. Hijmans, R. J.; van Etten, J. R package version. 2010, p r948.
16. Swain, N. R.; Latu, K.; Christensen, S. D.; Jones, N. L.; Nelson, E. J.; Ames, D. P.; Williams, G. P. A review of open source software solutions for developing water resources web applications. *Environ. Model. Softw.* 2015, *67*, 108–117.
17. Kesler, C. HAND Flood Mapping and National Water Model access through Tethys Platform, 2017.

Chapter 7

Framework for Statistical Analysis and Visualization of the National Water Model Streamflow Product

Aaron Heldmyer¹, Neelam Tahneen Jahan² and Kerim Dickson³

¹ University of Colorado Boulder, aahel1976@colorado.edu

² University of Texas at El Paso, tneelam@miners.utep.edu

³ Carnegie Mellon University, kedickso@andrew.cmu.edu

Academic Advisors: Ben Livneh, *University of Colorado Boulder*; Ali Mirchi, *University of Texas at El Paso*; David Dzombak, *Carnegie Mellon University*

Summer Institute Theme Advisor: Jim Nelson, Brigham Young University, jimn@byu.edu

Abstract: The National Water Model (NWM) is a powerful hydrologic model that simulates observed and forecast streamflow for 2.7 million reaches across the continental United States (CONUS). However, the large scale of the NWM presents a unique challenge in that the quantity of data produced stands as an obstacle to quick and timely analysis. Therefore, it is prudent that a framework for efficient statistical analysis of NWM data, as well as a comparison to observed data, be developed. This work presents a framework developed to statistically analyze and visualize NWM data against observed U.S. Geologic Survey (USGS) stream gage data. The framework includes both a method for data extraction and statistical analysis between modelled and observed data, and an application for visualization of the data. The extraction and analysis framework converts hourly retrospective data (stored as NetCDF) into daily, and stores these into a SQL database. This database is then incorporated into a Tethys application (called RetroStats), which allows the user to visualize and compare retrospective data to USGS National Water Information System (NWIS) streamflow data, as well as compute several statistics. This framework has implications for NWM diagnostics, and for hydrologic modelers interested in using NWM data.

1. Motivation

The National Water Model (NWM) is a powerful preparation and response tool for addressing water-related events, such as flood inundation and high flow conditions. However, inherent uncertainties in the model's configuration can result in predictions that differ from observed data. To improve the model's accuracy in forecast predictions, updated versions of the NWM are produced periodically that address these uncertainties. This framework provides a basis for analyzing each subsequent iteration of the NWM and ensures that areas of inaccuracy are quickly identified, allowing greater priority to be assigned to refine the model for areas which may be most affected by inaccurate predictions from the

NWM. To aid in identifying specific streams or regions that may be producing more inaccurate predictions, a visualization of the data and the statistical analyses performed is also important. By producing a scalable and accessible framework, rather than a single set of results, this analysis can be replicated for every subsequent iteration of the NWM, providing a consistent method for checking the effectiveness of each new version against observed data provided through United States Geologic Survey (USGS) stream gages.

2. Objectives and Scope

The purpose of this work is to provide validation procedures for each iteration of the National Water Model. By running statistical analyses comparing modelled data in each new version of the NWM with observed data from the USGS stream gage network, key information regarding the effectiveness of the updated model can be obtained rapidly, aiding in the development of subsequent versions. The objectives associated with this process are to extract and compare data from the NWM's retrospective dataset and their associated streamgages using Python scripts, and concurrently produce a visual interface, utilizing the Tethys platform, to allow an interactive demonstration of the results of the analyses on the extracted data.

To achieve a diversity of reach characteristics across CONUS, as well as a manageable yet robust sample size, 5% (344) of the USGS gage station network was selected to demonstrate the framework. To provide basic initial functionality, several statistical analyses were selected for the initial framework, including: Nash-Sutcliffe Efficiency (NSE), Log Nash-Sutcliffe Efficiency (LNSE), Kling-Gupta Efficiency (KGE), Correlation, Bias, Percent Bias, Root Mean Squared Error (RMSE) and Mean Absolute Error (MAE).

3. Methodology

3.1 Selection of Stream Gages and Reaches

To select which USGS stream gages to utilize, and consequently the correlating NWM stream reaches of interest, ArcGIS software was used in conjunction with a Python script to randomly select 5% (344 total) of stream gages across CONUS for examination. This sample size yields approximately one gage for each HUC6. Selection of gages using this methodology ensures that there would be no selection bias within the test dataset. Since each gage is connected to a stream reach identified in the model, this method of selection also provides the set of NWM reaches for examination. The ArcGIS tables also contain data on the latitude and longitude of the reach and associated gage, which is passed on to the Tethys application for mapping of each location.

3.2 Data Extraction

The two sets of data utilized for this framework are the NWM retrospective data for the stream reaches, compiled from the 1.0 version of the model, and the USGS stream gage data accessed through the National Water Information System (NWIS) online API and the 'ulmo' Python library.

The NWM retrospective data is locally stored in a series of NetCDF files. Each file contains modeled flow data for every stream for a specific hour within the year. As a result, each year contains over 8,750 files, with each file containing approximately 2.7 million cells of data. Attempting to extract data for a specific stream over the entire span of the retrospective data, 23 years, requires accessing over 200,000 files. This would require intensive processing by a computer, resulting in a large time lag between requesting data and retrieving it in a format suitable for examination.

To reduce the time lag between a user request for data and completion of formatting, the data was preprocessed and repackaged into a database. A Python script was created to extract the flow data for each reach of interest over the 23 years of retrospective data. Once the hourly data for each reach was extracted, it was converted to a daily time format and stored as a CSV file as an intermediate step.

These CSV files were imported into a SQL database for use in the application. A database provides superior data retrieval times and minimizes storage space, as well as allows for the efficient querying and retrieval of desired information. The database is comprised of three tables called ‘StreamInfo’, ‘StreamFlow’, and ‘StreamStat’, which store stream metadata, flow data, and preprocessed statistics, respectively. These tables can be cross-referenced within the application to retrieve data in a straightforward and efficient manner.

The NWIS stream gage data are not preprocessed, but rather retrieved within the application. Due to the regular updates of gage data, preprocessing would limit data availability to the point where the data was initially processed. As a result, comparisons will be available for dates extending beyond the time of application completion. The data is extracted through a Python function which accesses the gage data associated with the stream selected using the ‘ulmo’ Python package. The extracted gage data is provided in cubic meters per second (cms), and is converted post-extraction into the same units as the retrospective data, cubic feet per second (cfs).

3.3 Statistical Analyses

To analyze the data, two hydrographs are plotted and overlaid for visual inspection between the model and observed data in the application interface. A suite of statistical analyses are conducted, with results organized in a table immediately below the plot.

The statistical analyses conducted on the dataset were NSE, LNSE, KGE, correlation, bias, percent bias, RMSE and MAE. The NSE, LNSE and KGE metrics provide calibration information for the NWM, with NSE favoring performance in high flow conditions, LNSE favoring low flow conditions, and KGE providing further information for model comparison and diagnostics for NSE. Correlation, bias, percent bias, RMSE, and MAE are included to provide context to the values obtained through the NSE, LNSE and KGE analyses. This enables improved diagnostic capacity for specific errors within the model that may cause low values of NSE, LNSE and KGE.

These analyses were performed by importing functions from the Statistical Parameter Optimization Tool for Python (SPOTPY)⁽¹⁾ into the application. This tool computes a wide range of statistics using defined mathematical functions, allowing the modelled and observed data to be compared as desired.

In addition to the in-application statistical computation for single reaches, the statistics for all reaches were also computed beforehand and included in the database as the ‘StreamStat’ table. These data were then used for the CONUS-wide inter-gage statistical comparison, viewable through selectable layers on the main map page.

3.4 Tethys Platform

The Tethys platform includes a suite of Free and Open-Source Software (FOSS) that can be used to develop and host water resources and environmental web applications. Tethys platform 2.0.1 was utilized to build the RetroStats application, which combines the extracted data and the statistical analysis functions, providing a visual representation of the results. A basemap of CONUS was imported from OpenStreetMap.org to serve as the background. The latitudes and longitudes of the USGS gage stations corresponding to NWM reaches were then retrieved from the database to populate the basemap, showing the location of each gage. These points are the mid-points of their respective reaches. A JavaScript file was used to show a pop-up window on the map upon the selection of a point with gaging station and NWM COMID metadata from the StreamInfo table of the database. On the left side of the application user interface, an HTML-based navigation bar allows users to go to the ‘About’ page to learn more about the application and the statistical metrics that have been featured in it. Also on the left side, an application navigation item was added using the Tethys ‘Select Input’ gizmo which enables a drop-down menu allowing users to choose from the list of statistical metrics. Metrics for each point were pre-calculated and stored in the SQL database using a Python script. Upon selection of a metric, the result is called from the StreamStat table of the database through a function and gets passed on to a JavaScript file which enables a color-coded layer of the gaging points on the map; each layer divides statistical results into a series of six ranges and color-codes for inspection of all statistical results at a glance.

On the second page of the application, two hydrographs are generated on initialization using the Tethys ‘TimeSeries’ gizmo and ‘HighCharts’, a JavaScript charting library. The hydrograph for modelled data was created by calling NWM flow data from the StreamFlow table in the database whereas the hydrograph for observed data was created by requesting data from the USGS NWIS web service using a Python script. A table below the hydrograph is created by the Tethys ‘TableView’ gizmo and represents the statistical comparison of the two hydrographs for that gage and reach. On the left side of the application user interface, the ‘DatePicker’ gizmo was used to allow the user to select a date range to assess the model’s performance for a desired time period.

4. Results

4.1 Retrospective Dataset Extraction

Using the methodology described previously, the NWM retrospective data was extracted and converted into a database to provide daily mean flow data for the selected reaches. This resulted in a considerable reduction in file size from approximately 500 GB for the retrospective dataset to 130 MB for the database, which increased computational efficiency.

4.2 Tethys Application (*RetroStats*)

The application produced for the Tethys platform provides a visual interface for selection of gages and streams of interest. **Figure 1** shows the basemap displayed when the application is opened, consisting of the CONUS basemap and points indicating each stream gage and associated reach. Clicking a point opens a window containing a brief summary of the site: the USGS gage site name, the USGS gage identification number (site number) and the unique identification number for the reach (COMID) (shown in **Figure 1**). This window also contains the option to continue to another page to view statistical information on the gage data as compared to the modelled data.

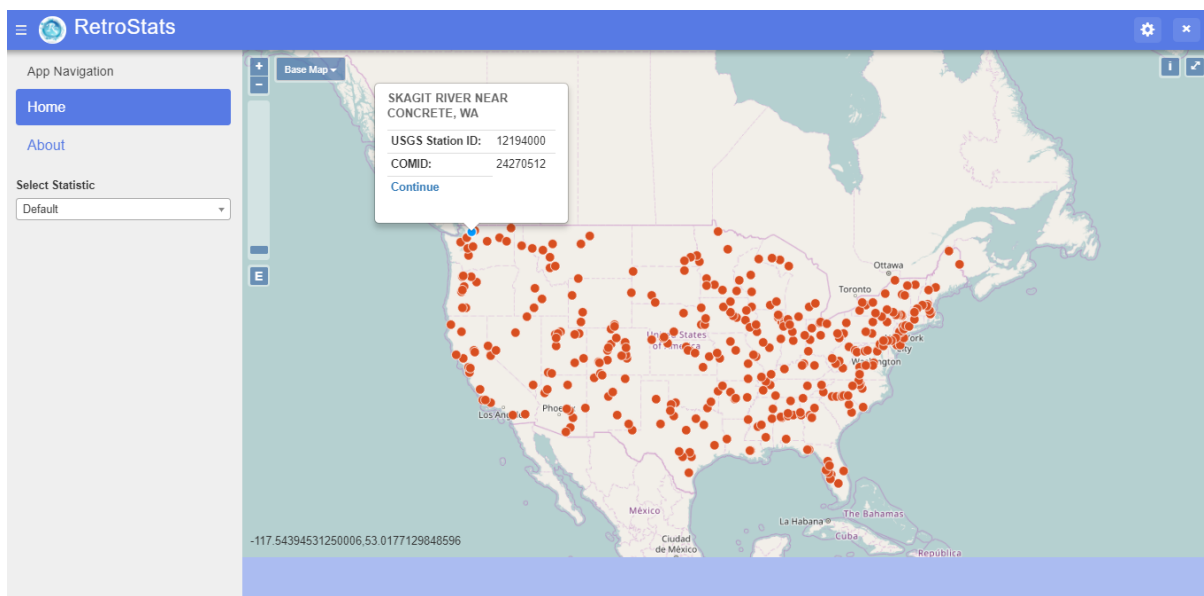


Figure 1. *RetroStats* CONUS basemap with plotted gages and site-identifying information

On the left side of the application, a drop-down menu allows national scale analysis of statistical results, with a legend for each statistic available to indicate the range of values for the colors shown. Each statistic is available as a viewable layer with the exception of LNSE. The LNSE is not included since gaps present in the retrospective data result in the function failing to yield useful results. **Figure 2** provides an example of this interface for the NSE statistic.

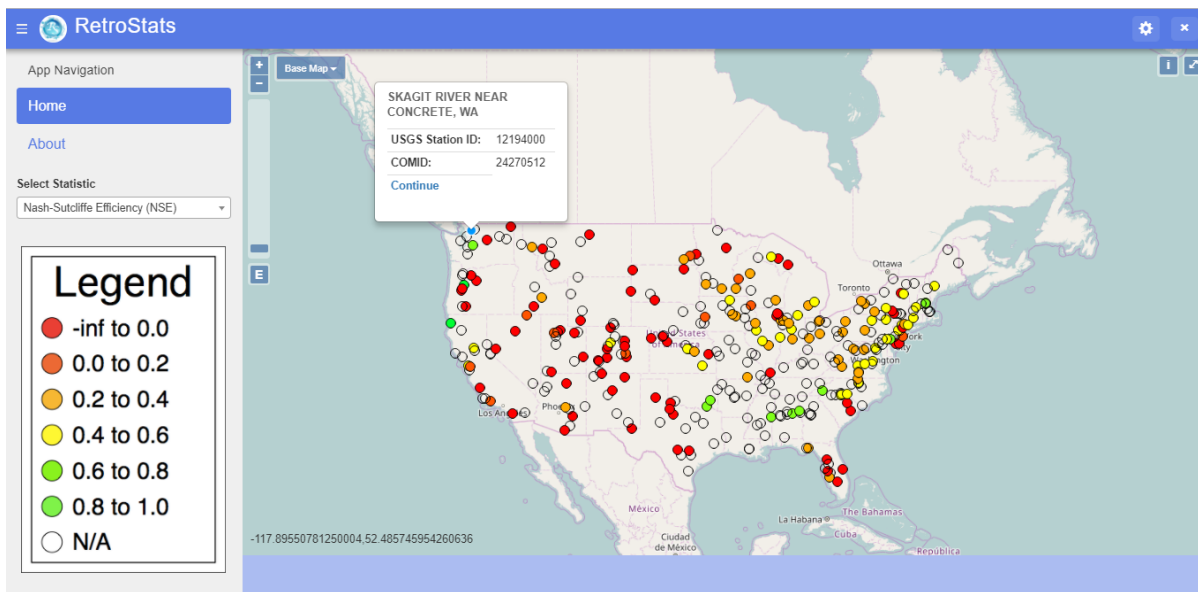


Figure 2. RetroStats CONUS basemap showing NSE values for each gage station

4.3 Statistical Visualization

Clicking the option to continue for a single gage on the main page of the Tethys application provides a new page of data. The data is initially visualized as a hydrograph, showing the observed data from the NWM retrospective data, in blue, overlaid with the data from the selected USGS stream gage, in red. The statistical analyses are also represented as a table below the hydrograph on this page of the Tethys application, showing the name of the analysis performed and the value obtained. An example of this hydrograph is shown in **Figure 3**. A date range can also be selected for the data to provide more focused hydrographs and statistical results, seen on the left of **Figure 3**. Allowing date ranges to be selected for analysis gives the potential for analysis of seasonal cycles and other factors of interest.

To provide context to the values within the table, the link “Learn more about the statistics” provides information to the users about each statistic listed, including the optimal values and explanations regarding intermediate values, where applicable.

5. Conclusion

This framework is an important proof-of-concept that provides the opportunity to verify the NWM results against observed data for each iteration of the model. It allows for modification of both application and datasets as the NWM evolves, so it can be an effective tool for every future version of the model. Statistical analyses of the data can be used to focus efforts in areas where the model is shown to be underperforming, particularly in locales with critical infrastructure or large populations that need to be well-informed of potential water events. Overall, this tool carries implications for evaluation and refinement of the National Water Model.

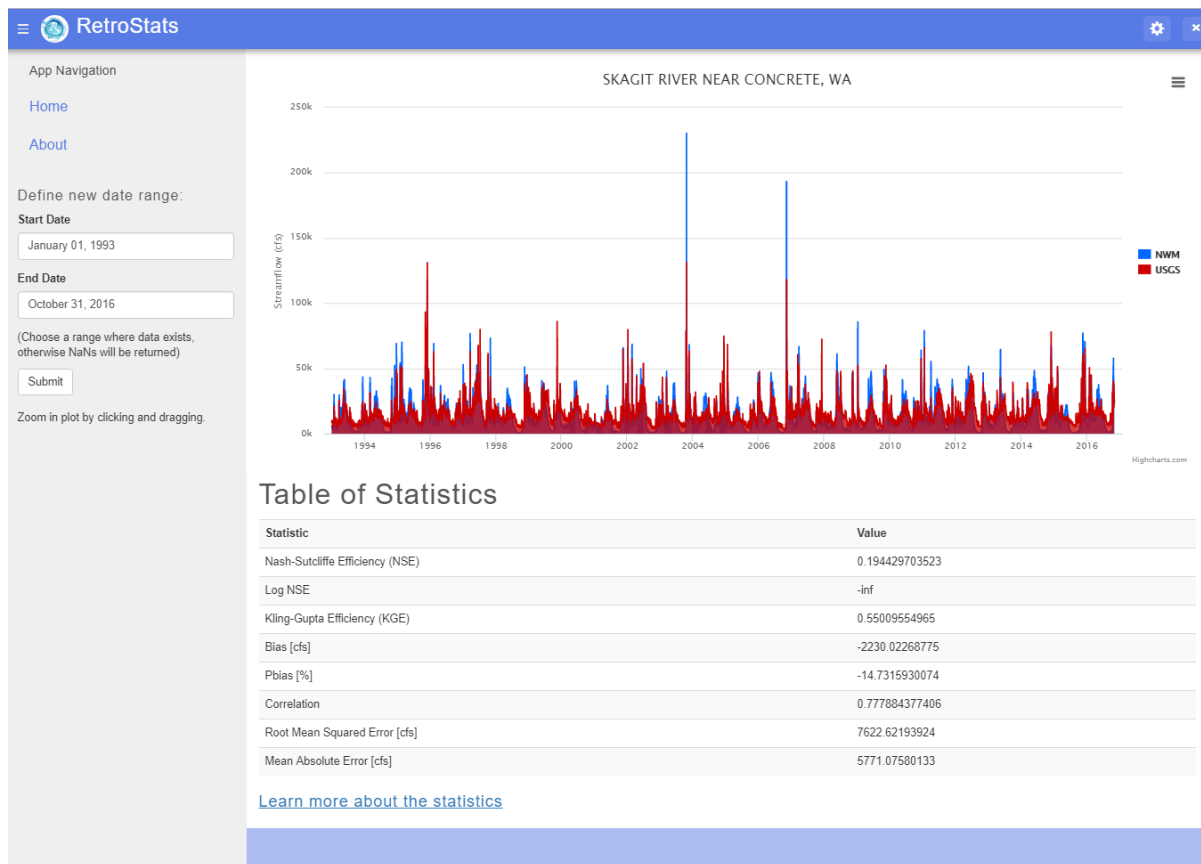


Figure 3. Sample comparative hydrograph and associated statistics for a single gage station

6. Further Work

This work provides a framework to extract data from the NWM's version 1.0 retrospective dataset and compare it with observed data from the USGS stream gage network. Additional statistical analyses can be added to the framework in the future. The gage network available for statistical examination in comparison to the NWM data can also be expanded to cover all gages within CONUS (approximately 7000). The provided framework is especially useful for testing future versions of the NWM, as the data extraction process and statistical analyses can be run in the same manner with newer data when it is available. This will allow each updated model to be regionally evaluated and result in more efficient analysis of the model, and implementation of improvements.

References

1. Houska, T.; Kraft, P.; Chamorro-Chavez, A.; Breuer, L. "SPOTting Model Parameters Using a Ready-Made Python Package". *PLoS ONE* 2015, 10(12): e0145180. <https://doi.org/10.1371/journal.pone.0145180>
2. Nash, J.E.; Sutcliffe, J.V. "River flow forecasting through conceptual models part I — A discussion of principles" *Journal of Hydrology* 1970, 10(3), 282-290, ISSN 0022-1694,

- [http://dx.doi.org/10.1016/0022-1694\(70\)90255-6.](http://dx.doi.org/10.1016/0022-1694(70)90255-6)
[\(http://www.sciencedirect.com/science/article/pii/0022169470902556\)](http://www.sciencedirect.com/science/article/pii/0022169470902556)
- 3. Krause, P.; Boyle, D. P.; Base F. "Comparison of different efficiency criteria for hydrological model assessment" *Advances in Geosciences* 2005, 5, 89–97, <https://doi.org/10.5194/adgeo-5-89-2005>
 - 4. Swain, N. "Tethys Platform Documentation", Release 2.0.1, 12 December 2016.
<http://docs.tethysplatform.org/en/stable/index.html>. Accessed July, 2017.

Chapter 8

Using the National Water Model Forecasts to Plan for and Manage Ecological Flow and Low-Flow during Drought

Carly Hansen¹, Spencer McDonald², April Nabors³, and Javad Shafiei Shiva⁴

¹ University of Utah, carly.hansen@utah.edu

² Brigham Young University, spencer.mcdonald@byu.edu

³ University of Alabama-Birmingham, annabors@uab.edu

⁴ Syracuse University, jshafiei@syr.edu

Academic Advisors: Steven Burian, *University of Utah*; Jim Nelson, *Brigham Young University*; Robert Peters, *University of Alabama at Birmingham*; David Chandler, *Syracuse University*

Summer Institute Theme Advisor: Jim Nelson, Brigham Young University, jimn@byu.edu

Abstract: Streamflow must be monitored carefully during periods of drought and during conditions of low flow in order to meet consumptive, industry, and ecological needs. This report aims to 1) compare low flows in the National Water Model (NWM) streamflow product during drought conditions using NWM retrospective data and historical stream gage observations for several locations in varying climates and lengths of drought, 2) utilize long-range forecasts for visualizing and warning of potential low flows and 3) communicate the results in a meaningful way. The comparison between modeled and observed data shows a variation in performance which depends on the season and location. In the comparison of non-drought versus drought periods for the study locations in California, the NWM consistently performs better during non-drought conditions than during drought conditions. Additionally, an application for users interested in monitoring and maintaining minimum streamflows, called Low Flow Warning System, was created on the Tethys application development platform for visualizing low flows in the long-range (30-day) forecast. Methodology and results of the retrospective model evaluation, as well as an overview of the Low Flow Warning System application are detailed in an Esri Story Map.

1. Motivation

Water managers concerned with allocation, and water resource professionals from industries such as fisheries, hydropower, drinking water utilities, transportation/shipping) must maintain minimum streamflows in order to meet consumer and business needs. Some of these needs are influenced by water or energy demands, some by economic factors, and others by environmental or ecologic requirements. While real-time data are widely used for tracking low flows when they occur, forecasted streamflow data (such as the long-range forecasts provided by the National Water Model (NWM)) would be beneficial to these users in order to plan for and manage resources during potential times of low flow. Understanding the accuracy and performance of the NWM streamflow products under the specific conditions of low flow and periods of drought is integral to ensuring continued use and expanding application of the streamflow forecasts to more of these users.

2. Objectives and Scope

The primary goals of this research are to 1) evaluate the low flows from the National Water Model (NWM) streamflow product during drought and non-drought conditions using NWM retrospective data and historical stream gage observations for a number of locations in varying types of drought conditions and 2) utilize long-range forecasts for visualizing and warning of potential low flows and 3) communicate the results in a meaningful way.

The evaluation of the NWM includes several measures of the “goodness of fit” (GOF) between the time-series produced by the retrospective NWM run and an observed historical record from corresponding United States Geological Survey (USGS) stream gages. The evaluation also provides a look at how well the modeled streamflow represents low flow conditions (defined in the following section) compared to USGS observed records. This evaluation is limited to four locations with corresponding NWM reaches/USGS gages; however, the process could be easily scaled up to a national scale to evaluate the matching stream reaches/gage records nationwide.

An interactive application that puts NWM forecasts in the context of low flows was developed for two of the locations and their surrounding watersheds. The demonstrative application provides an example of how the long-range forecasts could be used to benefit a variety of water users and managers. Additionally, a public Esri Story map describes the project and methodology, summarizes the findings from the retrospective analysis, and provides an overview of the application, called Low Flow Warning System.

3. Previous Studies

3.1. Definitions of Low Flow and Drought

There are many different methods of defining low flow and drought⁽¹⁾. For the purposes of this project, low flow was defined using four statistical thresholds: 5th percentile (very low), 25th (low) percentile, 7Q10 (very low), 7Q2 (low). These definitions of low flow are based on historical streamflow data, and all of them are calculated on a monthly basis (e.g. the 25th percentile in June reflects only mean daily streamflow values from the retrospective dataset during the month of June.)

These four methods are commonly used by organizations such as the USGS and EPA to represent how current streamflow data compares to historical flows. For a more detailed explanation of how these thresholds are computed, please refer to the USGS Scientific Investigations Report⁽²⁾.

3.2. Examples of Low Flow Monitoring and Visualizations

A number of visualization tools have been developed with a focus on low flows and droughts, especially in areas that have experienced sustained or recent periods of drought, such as California. For example, the California USGS Water Science Center has created an interactive map showing the current streamflows compared to historical streamflows at the active gages throughout California⁽³⁾. This provides a near-real-time view of streamflow (as a rate and as a percentile) which can be used to alert water resource professionals of current issues; however, this visualization does not include ungauged streams or the ability to forecast streamflow conditions. Other regional and nationwide tools are available through National Integrated Drought Information System (NIDIS), including static maps for forecasted drought coverage and forecasted streamflows, which are also expressed as a percentile

of historical streamflow⁽⁴⁾. These streamflow forecasts are limited in availability (published from January to June) and extent (for a limited number of reaches throughout the western United States). The forecasts provided by NIDIS are calculated using statistical methods (rather than physically-based like the NWM). While these products have been recognized for their growing use, effective communication of the forecasted low flow information remains a challenge⁽⁵⁾.

4. Methodology

4.1. Data

Historical modeled streamflow data were obtained from a 23-year retrospective run (from January 1, 1993 to October 31, 2016) of version 1.0 of the NWM. It should be noted that this version of the model does not include some of the adjustments to parameters that were made during the calibration process of version 1.1 (and subsequent models). Long-term retrospective data are not currently available for the newer versions of the model. Historical data of observations of streamflow were obtained from USGS gage locations from the National Water Information (NWIS) database for the same time period.

4.2. Selecting Case Study Locations

Four locations for model evaluation and forecast demonstration were chosen from regions which have experienced varying degrees of longer, sustained periods of drought (Northern and Southern California) or shorter, seasonal droughts (Alabama). These locations are shown in **Figure 1**. The recent drought in California, lasting roughly from 2012 to 2015, was one of the most severe events on record (and according to some measures, is the most severe drought during the last 1200 years)⁽⁶⁾. In Alabama, the most severe seasonal drought in 100 years occurred in 2007⁽⁷⁾, and another seasonal drought affected much of the state again in 2016. The individual case study locations were selected based on: availability of an observed historical record, stream order (stream order greater than three was used to eliminate smaller streams that are likely ungaged and to simplify visualizations of forecasts), and the amount of disturbance of the gage locations.

One of the most common methods for measuring disturbance is the hydrologic disturbance index (HDI)⁽⁸⁾. This method quantifies the cumulative impact of anthropogenic disturbance surrounding each stream gage. HDI is a composite of number of disturbances, including major dam density in the upstream of the gage, change in the dam storage, the number of channels and man-made paths along the upstream stems of each gage, distance of each gage from National Pollutant Discharge Elimination Site (NPDES) locations, freshwater withdrawn from the basin (surface water or groundwater), and landscape fragmentation. For each of these disturbances, a score between 0-8 is assigned, where 0 means no disturbances and 8 means completely disturbed. The cumulative score is then calculated for a given location. The USGS has conducted a study on 6786 of its gages and provided HDI values, which range between 2 and 42. For this study, locations were chosen with the HDI of less than or equal to 10, which corresponds to the low - moderately disturbed range⁽⁹⁾.



Figure 1. Map of Case Study Locations

4.3. Pre-processing and Evaluation Workflow

Figure 2 summarizes the workflow used to obtain and process data from their respective sources, and evaluate the performance of the NWM data against USGS observations.

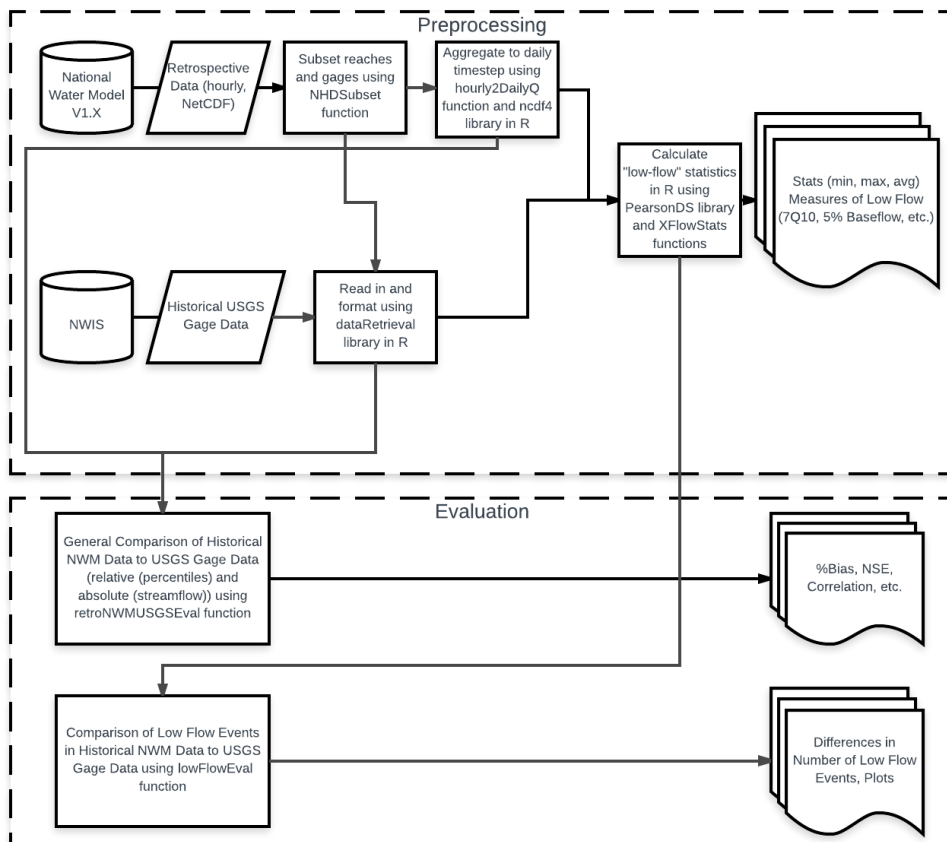


Figure 2. Flowchart of Preprocessing and Evaluation.

First, retrospective modeled data were aggregated from an hourly to a daily mean streamflow (neglecting any missing values). Historical observed streamflow data were then obtained for sites in the study area that met the criteria described in 4.1.1. (corresponding with NHD stream reach, HDI, and stream order) using the USGS dataRetrieval package in R. These historical time series (both modeled and observed) were then used to calculate low flow thresholds (including 7Q10, 7Q2, 5th percentile and 25th percentile) on a monthly basis.

For the evaluation of the NWM streamflow product, a number of measures of “goodness of fit” were calculated using the hydroGOF package in R, using both the actual streamflow rates and the relative streamflow (streamflow as a percentile of the corresponding historic record). The following measures are reported for comparison of the relative streamflow: Mean Absolute Error (MAE) and Root Mean Square Error (RMSE), which measure the average magnitude of the errors in the modeled data (but do not provide information about the direction of error). For the absolute streamflow, the Percent Bias (PBIAS) is reported, which does provide information about whether the model errors are over- or underestimation of streamflow compared to the observed record. In addition to these goodness of fit measures, the number of low flow events (defined as days with streamflow below the low flow threshold) are compared between the modeled and observed historical records.

These measures were calculated for the entire historical period (1993-2016), on a seasonal basis, and during drought and non-drought periods. The long-term drought period for California is defined as January 2012-December 2015, and the non-drought comparison period is defined as January 2003-December 2006 (which has relatively low percentages of the state under any category of drought classification). The short-term drought period for Alabama is defined as January-December 2007, while the non-drought period is defined as January-December 2013.

5. Results

5.1. Evaluation of the NWM Retrospective Data

5.1.1. Goodness of Fit

Over the 23-year period of retrospective and historical data, model performance varies depending on location and season. For example, the East Santa Ynez location, consistently performs the worst compared to other sites. At this location, there is extreme overestimation in streamflow during fall and winter seasons, with PBIAS between 185-450%, and generally larger MAE and RMSE than other locations in all seasons. While the location in Alabama has lower biases, the errors in relative streamflow are generally in the same range as the errors in other locations. For all locations, the errors (MAE and RMSE) for relative streamflow during the summer are generally higher than other seasons.

The model performance was also evaluated for each of the locations during drought and non-drought periods. During drought conditions in California, the PBIAS greatly increase compared to non-drought conditions. The RMSE and MAE increase for two of the locations, and shows minimal changes for the East Santa Ynez location. For the shorter-term drought comparison in Alabama, there were minimal differences in model performance (PBIAS, MAE, and RMSE) between drought and non-drought conditions.

5.1.2. Low Flow Event Frequency

The frequency of low flow events (using the 7Q10 threshold) are shown for each of the case study areas in **Figure 4**. Although the events detected by the NWM and USGS show significant differences in seasonal low flow events, they do appear to correspond well during large periods of drought.

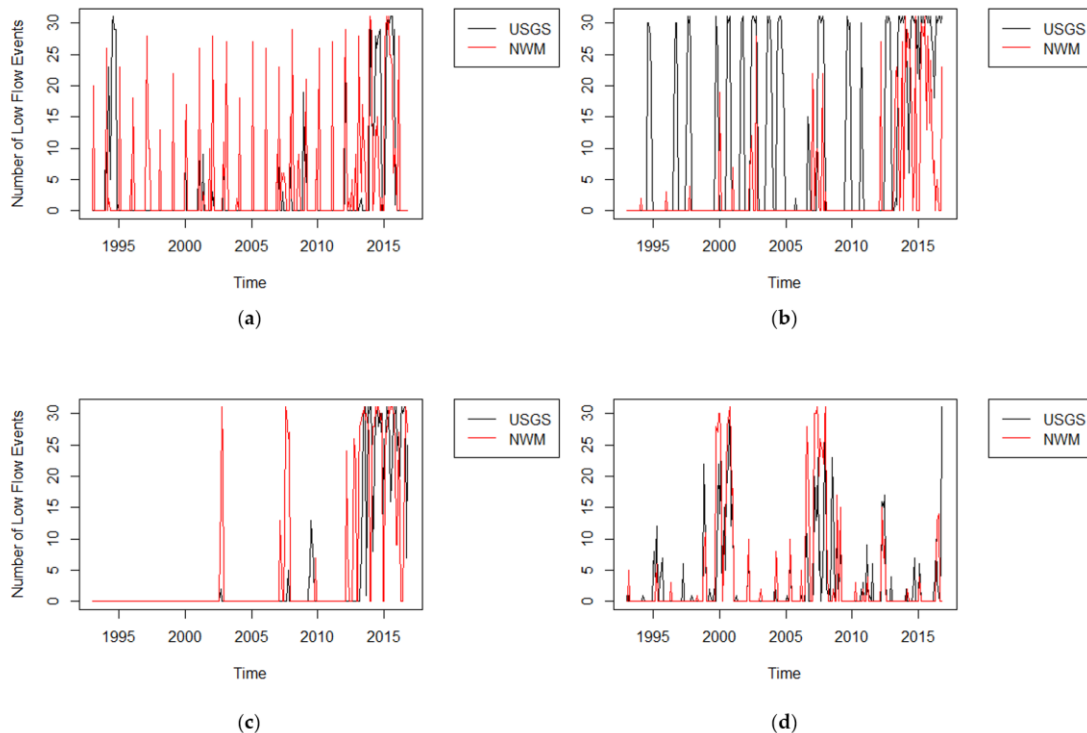


Figure 1. Modeled and Observed Low Flow (7Q10) Events for (a) Deer Creek, CA; COMID: 08020924, (b) East Santa Ynez, CA; COMID: 17611425, (c) West Santa Ynez, CA; COMID: 17609017, and (d) Sipsey Fork, AL; COMID: 18578829.

5.2. Visualization of Model Evaluation Results and Low Flow Forecasts

5.2.1. Esri Story Map

One of the objectives for the project was to effectively communicate the methodology develop an Esri Story Map which describes the project, highlights its importance, provides an overview of methodology, and summarizes results of the NWM streamflow product evaluation at each of the four study locations. Lastly, it directs the reader to the Low Flow Warning System application. **Figure 5** shows an example of the content in the Story Map, with background information about the study location.

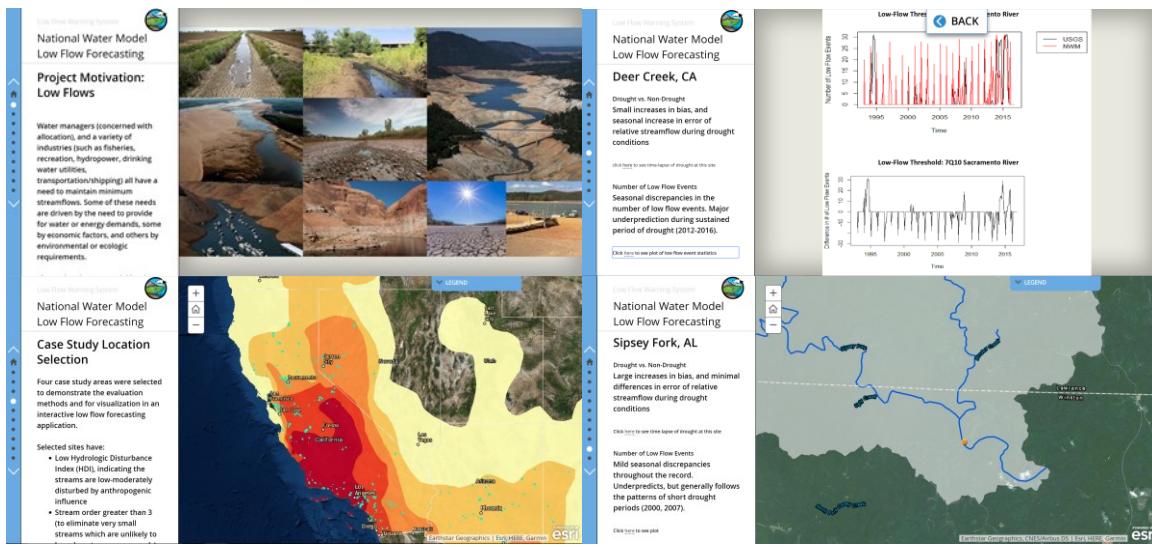


Figure 5. Content in Esri Story Map including Project Motivation, Case Study Descriptions, and Summary of Results.

5.2.2 Tethys Application

The purpose of Low Flow Warning System application is to demonstrate how visualizations of long-range National Water Model (NWM) forecasts and retrospective data can be used to help alert water users/managers of potential low flow conditions. The app provides a number of services, including: allowing a user to put forecasted flows in the context of ecological or hydrologic streamflow needs and visualization of low flow conditions throughout a stream network or watershed.

For demonstration purposes, there are three watersheds available to choose from in the “Select Watershed” drop-down menu. In the future, a user will be able to upload a boundary shapefile of their own watershed. The uploaded watershed shapefile will be used to subset the NHD streams within the watershed boundary and with a stream order greater than three.

After selecting a watershed, the user can then select one of the four statistical low flow thresholds (5%, 25%, 7Q2, and 7Q10) to display on the map. The map display (shown in **Figure 6**) updates the color of the stream based on whether the forecasted streamflow drops below the selected threshold value (for example, red corresponds to a forecasted low flow while blue corresponds to a forecasted flow that stays above threshold during the forecast period).

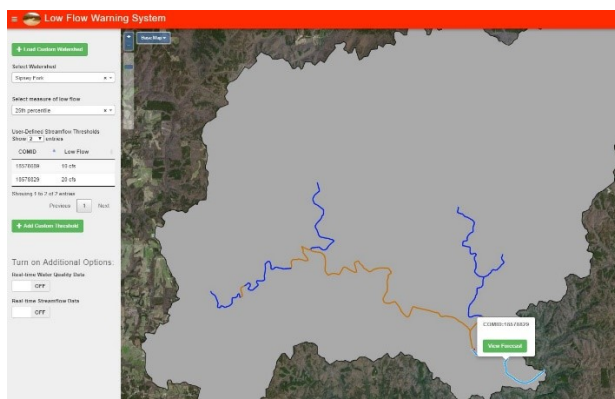


Figure 6. Interface of the Low Flow Warning System Application and Visualization of Reaches with Forecasted Low Flows.

The app also allows the user to specify a custom threshold for any stream in the selected watershed based on legal or desired streamflow requirements, ecological/habitat needs, etc. In addition to the automatic map visualization that occurs when a statistical method is selected, the app provides a way to select a stream and view a plot comparing the 30-day NWM forecast with the statistical threshold, as shown in **Figure 7**.

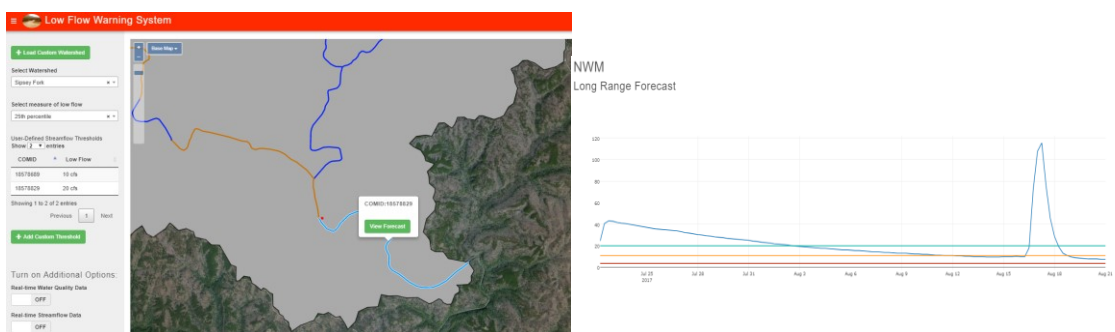


Figure 7. Visualization of NWM Long Range Forecast.

Suggestions for future iterations of the Low Flow Warning System include the following capabilities and upgrades: 1) Custom watershed boundary uploading and NHD stream subsetting, 2) visualization of real-time streamflow and water quality data at all gage locations in the United States, 3) a more robust data management system to store and compute large datasets, and 4) water quality forecasting capabilities based on a statistical model linking streamflow to water quality parameters.

6. Conclusion

Performance of the NWM retrospective analysis varied greatly by location and across seasons. In the comparisons of drought conditions versus non-drought conditions, some locations indicated little sensitivity to drought conditions, while others showed large differences in bias and error. A broader exploration with reaches in diverse locations would be necessary to understand factors that may contribute to this sensitivity.

It should also be noted that the record of low flow events varied depending on the definition of low flow threshold (only 7Q10 was shown in this report). Definitions of low flow need to be considered carefully, and a particular threshold may be more appropriate for some streams or applications than

others. There are also a number of environmental perspectives that could extend this work, including linking information about the unique habitat and ecological needs of a stream network to determine thresholds.

One of the biggest challenges to this work that prevented a larger-scale evaluation was the processing of the historical retrospective data, which is necessary for calculating relative streamflow values (percentiles). In the future, once the retrospective data has been processed and formatted properly, all of the reaches and corresponding gages could be compared with ease, following the general workflow and using the tools that were created for the demonstrative cases in this study.

Finally, the evaluation of the retrospective NWM data used in this study may provide a useful baseline for comparison of updated iterations of the model. We recommend comparing the retrospective records of these updated model iterations (following the pattern set forth in this study) to explore how well the newer model features, calibration, and assimilation have improved with respect to low flow and drought conditions.

Supplementary Materials: The R Package NWMLowFlows (which contains documentation and functions used to accomplish the evaluation workflow) is available on GitHub at <https://github.com/cahhansen/NWMLowFlows>. The Esri Story Map can be accessed at <http://arcg.is/008aW8>. The code for the Low Flow Warning System application, including everything necessary for installation can be accessed at https://github.com/spence97/Low_Flows/tree/master/tethysapp.

References

1. Smakhtin, V. U., Low flow hydrology: a review. *Journal of hydrology* **2001**, *240* (3), 147-186.
2. Risley, J.; Stonewall, A.; Haluska, T., Estimating flow-duration and low-flow frequency statistics for unregulated streams in Oregon: US Geological Survey Scientific Investigations Report 2008-5126. *United States Geological Survey* **2008**, 22.
3. Drought Impacts. <https://ca.water.usgs.gov/data/drought/drought-impact.html> (accessed July 20, 2017).
4. Wood, E. F.; Schubert, S. D.; Wood, A. W.; Peters-Lidard, C. D.; Mo, K. C.; Mariotti, A.; Pulwarty, R. S., Prospects for advancing drought understanding, monitoring, and prediction. *Journal of Hydrometeorology* **2015**, *16* (4), 1636-1657.
5. Li, H.; Luo, L.; Wood, E. F., Seasonal hydrologic predictions of low-flow conditions over eastern USA during the 2007 drought. *Atmospheric Science Letters* **2008**, *9* (2), 61-66.
6. Griffin, D.; Anchukaitis, K. J., How unusual is the 2012–2014 California drought? *Geophysical Research Letters* **2014**, *41* (24), 9017-9023.
7. Luo, L.; Wood, E. F., Monitoring and predicting the 2007 US drought. *Geophysical Research Letters* **2007**, *34* (22).
8. McManamay, R. A.; Bevelhimer, M. S.; Kao, S. C., Updating the US hydrologic classification: an approach to clustering and stratifying ecohydrologic data. *Ecohydrology* **2014**, *7* (3), 903-926.
9. Falcone, J. A.; Carlisle, D. M.; Weber, L. C., Quantifying human disturbance in watersheds: variable selection and performance of a GIS-based disturbance index for predicting the biological condition of perennial streams. *Ecological Indicators* **2010**, *10* (2), 264-273.

Chapter 9

Using Public Input to Create a Better Online Flood Mapping Framework

Bradley Carlberg¹, Kathleen Eubanks² and Courtney Jackson³

¹ Iowa State University, bcarl@iastate.edu

² Louisiana State University, keuban4@lsu.edu

³ Penn State University, cobj5074@psu.edu

Academic Advisors: ¹Kristie Franz, *Iowa State University*; ¹ William Gallus, *Iowa State University*; ² Clinton Willson, *Louisiana State University*; ² Robert Twilley, *Louisiana State University*; ³ Guido Cervone, *Pennsylvania State University*

Summer Institute Theme Advisor: Sagy Cohen, University of Alabama, sagy.cohen@ua.edu

Abstract: One topic of consistent relevance in flooding research is how best to provide information and communicate risk to the general public. Additionally, communicators face challenges on how to fully convey the dangers flooding poses in a manner that the public comprehends and will apply to reactions to flooding. Many of the inundation and hazard maps currently in use are highly technical, making it difficult for the average person, without formal education in flooding, to glean valuable information and insight from the intended tools. Working with the public, a set of surveys were administered to gain insight into public understanding of floods and flooding risk. Using the feedback from each survey, a conceptual framework was produced for a set of inundation maps, including more relatable terms and educational components within a user-friendly web interface. Goals for the website, shaped by survey feedback, included simple and readable map layers, a clear and detailed legend, the ability to show or hide components of the map, and the option to learn more about flood terminology from the site or via links to outside resources. The public indicated that the final map interface was more concise and simplified than the current inundation map platforms.

1. Motivation:

Flooding is the most common and omnipresent natural hazard in the United States and has occurred with increased frequency in recent decades. As floodwaters recede, they leave massive emotional and physical damages in their wake. There is a push for producing timely, accurate flood forecasts and inundation maps to properly prepare citizens with the information needed, ultimately reducing casualties. However, these critical results are meaningless if not properly presented and communicated to the public in understandable context.

2. Objectives and Scope:

Merging social science practices with physical science techniques provides an invaluable depth to research, giving scientists the opportunity to make their work relatable and usable by the general public. The goal of this project is to provide an updated inundation map framework that serves as a source of information, a learning tool, and a bridge between technical flood communication and

general understanding. Through the application of Geographic Information Systems (GIS), streamflow forecasting, and flood mapping, social science ideas can be utilized to influence the work produced in these three areas of study. The approach taken in this project is a conceptual one; implementing features that the general public has recognized as important so that future work done in this field may take these results into consideration. The main project objectives include: 1) create better visualization of flooding and risk in an understandable and relatable context to the public; 2) provide map features which highlight flood forecast uncertainty and enhance public flood knowledge; and 3) produce a map framework that can be referenced in future inundation map creation.

The focus of this project centers around the concept of simplifying flood inundation maps (FIM) in order to enhance comprehension of flooding and risk. In an attempt to achieve this, feedback from the public is used to give insight into what features they find useful or hindering to their overall perception of FIMs. Deliverables completed for the project are 1) Public evaluation of flood concepts and inundation map usability; 2) Creation of probabilistic flood depth using the Height Above Nearest Drainage (HAND) method of analysis; and 3) Web map interface implementing the feedback provided by the public for map enhancement.

3. Previous Studies

Conveying flood risk and other pertinent information is becoming increasingly important as more people settle into flood-prone areas, and as the threat of floods increase in many regions due to extreme weather events associated with climate change⁽¹⁾. Studies by Haer, et al. (2016) concluded that conveying flood risk through people-centered flood risk communication is more effective than top-down communication. Appealing to a specific location with unique approaches and information seems to be more beneficial⁽¹⁾. People who live within natural hazard prone areas often fail to act to reduce their risk of injury, death, or property damage^(2, 3). A person's response to a natural hazard such as flooding is typically based on the outcomes of threat and coping appraisals. Threat appraisal, or risk perception, has three subcomponents; perceived probability of a threat such as a flood affecting them personally, perceived severity of consequences, and fear. Coping appraisal takes place after the threat appraisal has been completed. Coping appraisal also has three subcomponents; a person's belief that protective responses will be effective, a person's believed ability to perform the protective response, and the assumed costs (monetary and time) it will take⁽⁴⁾.

4. Methodology:

4.1 Study Locations

4.1.1. 2016 Baton Rouge Flood

During the period of August 9-16, 2016, a slow-moving area of low pressure and high atmospheric moisture moved across southern Mississippi and Louisiana, dumping record-breaking rains upon the area. Rainfall records were set in numerous stream basins in the surrounding area⁽⁵⁾. The historic heavy rainfall also resulted in record-breaking peak streamflow readings at ten United States Geological Survey (USGS) stream gage sites and top five stream flows at seven more sites. As a result, major flooding occurred in southern parts of Louisiana such as Baton Rouge and Lafayette. The flooding caused at least 13 deaths and \$10 million of damage to around 140,000 homes⁽⁶⁾.

4.1.2. 2015 Dallas Flood

During the span of late April to early May 2015, intense rainfall occurred throughout Texas leading to substantial, widespread flooding across the state⁽⁷⁾. Widespread flooding occurred across all major rivers in Texas during the span of May 23rd to June 3rd, commonly referred to as the Memorial Day Weekend Flood. The Office of the Texas State Climatologist determined that 18 of the 19 cities recorded total monthly precipitation amounts exceeding the monthly average precipitation for May⁽⁸⁾. The Trinity River at Elm Fork crested at 41.98 feet on May 29th, 2015, causing minor flood damage to thousands of buildings, residences, and infrastructure. Statewide, the flooding amounted to approximately \$3 billion in damages⁽⁹⁾, with \$61 million of damages in Dallas County alone⁽¹⁰⁾.

4.2 Forecasted Water Depth

Two probabilistic flood inundation forecast layers were initially visualized to convey risk and uncertainty; a highest probability forecast and a worst case scenario forecast. These forecasts were to be created from an ensemble of National Water Model (NWM) forecasts, however, no flooding events occurred during the 7-week span of the National Water Center Innovators Program in either study area. Therefore, the NWM retrospective discharge was used as an alternative method to produce probabilistic inundation forecasts for the purposes of this study. The Advanced Hydrological Prediction System (AHPS) and United States Geological Survey (USGS) were used to select dates and times of the two forecasts. A worst case scenario forecast was chosen from the highest crest that occurred during the 23-year period (1994-2016) that NWM retrospective data is available at the Amite River near Denham Springs, LA and the Elm Fork Trinity River at Spur 348, Irving, TX gages. The next highest crest that occurred during the same period was selected as the highest probable forecast.

The dates and times of probabilistic forecasts were used to create flood inundation layers using the HAND method from corresponding NWM retrospective data. Results from the HAND analysis were then converted into flood depth. Flood depths were separated into four relatable risk levels; ankle to knee (0.4 - 1.5 ft), knee to waist (1.5 - 3.3 ft), waist to head (3.3 - 5.5 ft), and overhead (>5.5 ft). For consistency, the levels were displayed using the same color scheme as the National Weather Service to portray increasing levels of risk (yellow, orange, red, and purple). Although there is some danger with flooding depths below the ankle, action does not necessarily need to be taken until water rises above the ankle (>0.4 ft) category. Each forecast flood layer was displayed individually so users can easily compare the forecast to the recent flood extents from the events described in section 3.1. It should be noted that these probabilistic forecast flood inundation layers are for a single date and time rather than an entire event.

4.3 Public Evaluation

In order to gain better insight into the public understanding of flooding and flood risk, an evaluation was created. The goals of this evaluation were to 1) Gain insight into public perception of flood risk; 2) Identify features that the public consider to be useful or not useful in an inundation map; and 3) Gain better understanding of public knowledge about flood inundation maps. The evaluation was divided into three survey rounds. Round One was used to examine the public's knowledge of flood concepts as well as gather opinions on a current inundation map format. The Round Two survey updated the public on the interface development and gathered additional feedback on map features that had been implemented. Results from the first two surveys were used to enhance the conceptual

framework of the web map interface. Round Three was the final survey distributed to the public, which displayed the final (at that time) version of the web map. The purpose of the third survey was to have participants identify the web map interface functionality and usability. Involving the public throughout the development of the interface allowed them to see firsthand how their suggestions were being integrated, aiding them in visualizing the functionality of their ideas. All three survey links were shared with the public for voluntary participation through the following social media outlets: Facebook, Twitter, Reddit, and Imgur.

5. Results and Discussion:

5.1 HAND Model Results

The highest probability (**Figure 1a**) and worst case scenario (**Figure 1b**) HAND-derived probabilistic forecast flood depth layers are shown overlaid onto the entire inundation extent of the 2016 Baton Rouge flood. For both probabilistic forecasts, a majority of the flooded areas have depths between ankle to knee and knee to waist categories (0.4-3.3 ft.) with areas in and around streams reaching depths of the waist to head category (3.3-5.5 ft.). Despite being from the same event, the worst case scenario forecast extent does not match the observed flood extent. A few explanations may be able to account for this difference: 1) the forecast is a snapshot of a particular date and time, whereas the observed extent covers the highest extent that occurred in the area over the course of the event; 2) flood depths less than ankle deep (<0.4 ft.) were not included in the forecast layer; 3) NWM is a model and may not portray the true observations; 4) there is inherent uncertainty in the conversion from NWM streamflow to stage depth and HAND calculations; and 5) the observed flood extent was derived from a point-to-point basis, which may not be accurate.

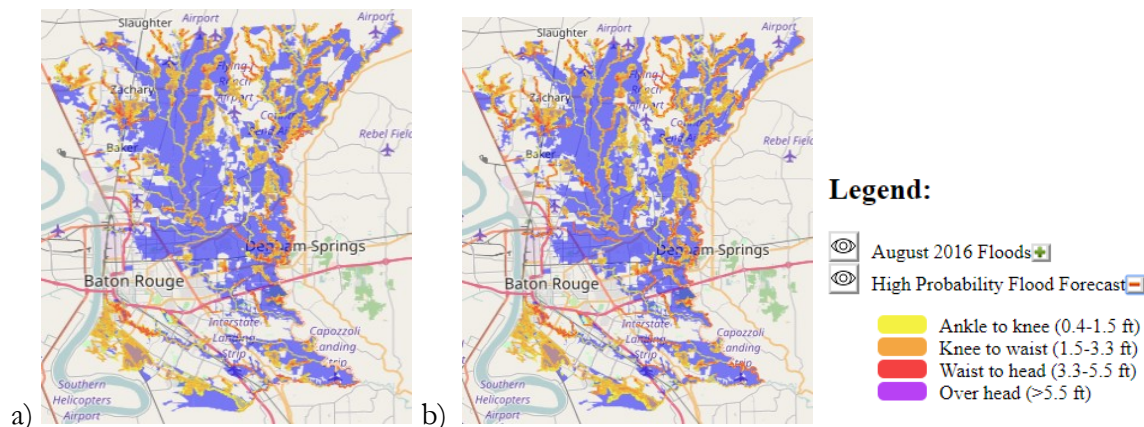


Figure 1. Baton Rouge flood inundation maps showing probabilistic forecast flood extent and depths for the (a) highest probable scenario and (b) worst case scenario. The August 2016 flood aerial extent is shown in blue as a comparison.

5.2 Public Evaluation

5.2.1. First Round Survey

For this survey there were 160 voluntary participants; 44 of which were determined to be repeats. Repeated responses were removed from the survey record, resulting in 116 actual participants. The first section of the survey was to gauge the public's understanding of basic flood concepts. Questions tested the participant's knowledge of basic flood concepts, such as 'flood stage' and 'inundation maps',

and were asked to define concepts if they indicated an understanding. Please see the supplementary materials section for a link to survey questions. The predominant pattern that arose from these questions was that the majority of people were not entirely familiar with these terms; most selected either 'No' or 'I have a general idea'. Out of the 116 participants, less than a quarter (Stage-23%, FIM-19%) indicated knowledge of basic flood concepts. Thirty-eight participants provided a definition, however, less than half (Stage-39%, FIM-47%) correctly defined the terms. **Figure 2** shows the responses to the question, 'What does it mean if a flood event is a '100-year Flood?'. A majority of the participants (61.2%) selected incorrectly that a 100-year flood would occur only once every 100 years, 18% indicated that they did not know the definition of a 100-year flood, and the remaining 21% selected the correct response of a "1% chance that a flood of that magnitude will happen in any given year". Although a limited number of terms were tested, it appears that the general public understanding of flooding concepts and risk is limited.

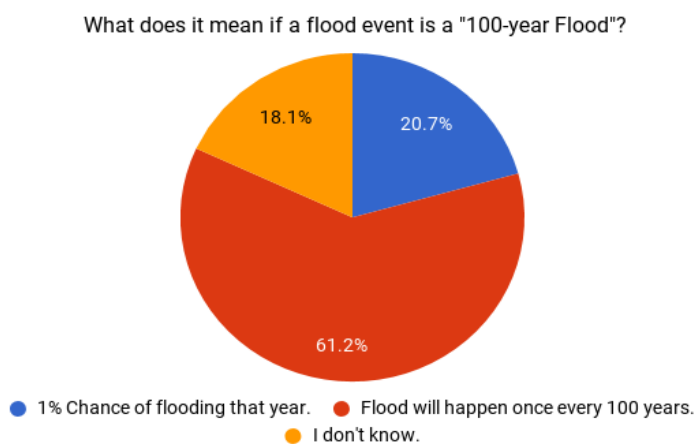


Figure 2. Participant response frequency determining public knowledge of a 100-year flood event.

The second section of the survey gathered public opinions of a current FIM by determining the usability of the map and what features they find helpful or hindering for an inundation map. NOAA's AHPS produces inundation maps for a selective list of inundation mapping locations. The Tuscaloosa, AL site along the Black Warrior River (<https://water.weather.gov/ahps2/inundation/index.php?gage=toda1>) was used for an example of current FIMs. **Figure 3** lists the negative responses of the sample AHPS map. There were 22 participants (26% overall) which stated there was a disconnect between the legend and map; they added that once they found the legend, it was too complicated for them to interpret. In addition to the complicated nature, 20 participants (17% overall) noted that the site was very scientific and formal, using technical jargon and showing too much information for the average person to process. This deluge of information made it difficult for them to comprehend and actually use, as the content was unfamiliar to the participants.

Given the features seen on the AHPS site, participants were then asked what would they exclude from the map. The technical, scientific nature of the site was determined to be something that needed modification to cater to the uninformed public. Suggestions ranged from putting things into layman's terms to removing all ancillary data in order to simplify the map layout. The final follow up question asked the participants what features they would like to see implemented into a map based upon a list of features we generated (**Figure 4**). Features that would allow a user to relate to the information that

they were seeing (i.e. a layer showing the extent of a recent flood or images showing water depths at known landmarks) were most popular amongst the participants. The ability for the map user to control the information that they saw was also expressed as another important feature.

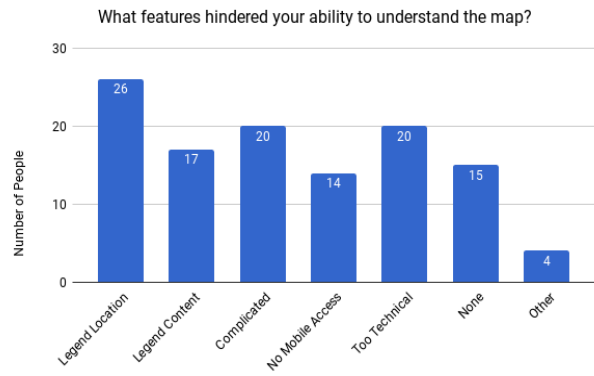


Figure 3. Hindering features of AHPS site indicated in Round One survey by participants.

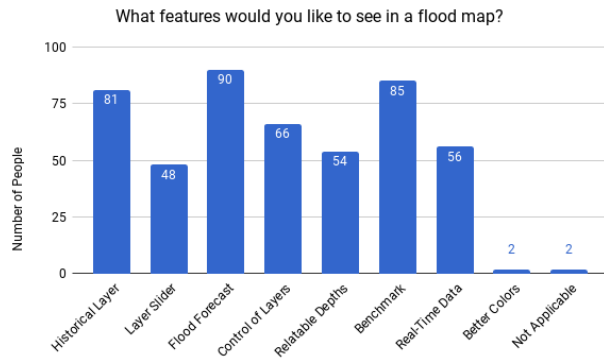


Figure 4. Features that should be included in a FIM as indicated by the public.

5.2.2 Second Round Survey

Feedback collected from the first survey was taken into consideration during the development of the web map. Once an initial draft of the web map was constructed, a second survey was administered through social media outreach as a follow-up. The purpose of this survey was to keep the public up-to-date on the web map progress as well as gain further feedback on other features that could be included through the development process. There were 69 voluntary participants; however, similar to the Round One survey, repeated participant responses occurred; after the repeat responses were removed, the final total of the participants was 54. Survey participants were first asked to indicate if they had done the previous survey to track consistency and commentary provided across the surveys from returning participants. Remaining questions in the survey asked for opinions of features implemented in map at the time of the evaluation (**Figure 5**). User control over features, as well as features that helped relate flooding content to the participant, were features found to be of most value. Disliked features were primarily the layer slider and relatable flood depths. Non-numeric, relatable flood depths were previously indicated as important, however this was the most disliked feature for the second evaluation. Participants stated that the non-numeric depths were subjective as it did not specify the height of the person the depths were scaled to; users suggested having both numeric and non-numeric depths in the legend to avoid further confusion. Throughout the survey participants expressed confusion over different map features, primarily stating that they were unsure how to use them or what their purpose was for the map. Because of this, 31% of participants indicated that they found the map to be confusing and/or complicated.

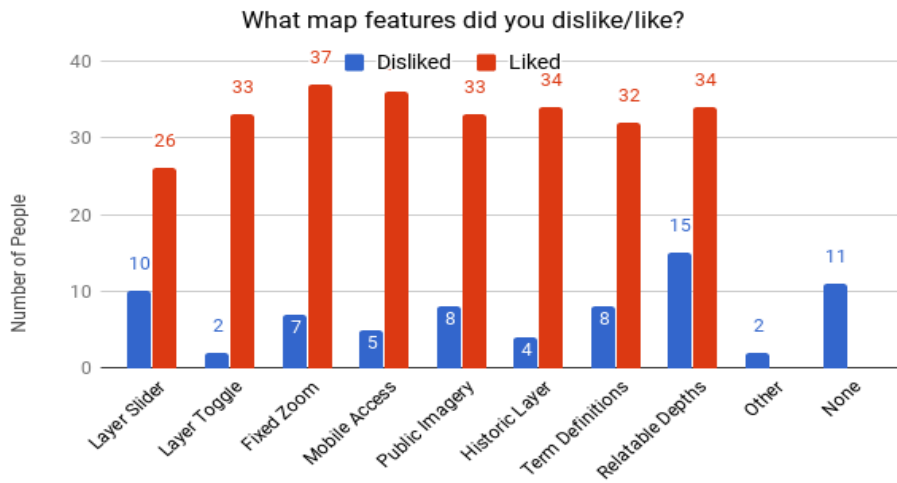


Figure 5. Map features participants indicated as liked/disliked in Round Two survey.

5.2.3. Third Round Survey

For the final survey, there were 49 participants total. The survey's purpose was to have the public explore the final (at the time) map interface and comment upon the usability and functionality of the features. Survey participants were first asked to indicate if they had done any of the previous surveys to track consistency and commentary provided across the surveys from returning participants. Of the 49 participants, 31% indicated that they had taken all surveys prior. To test the user's ability to extract information from the map, the survey participants were asked to observe a defined extent and determine the risk of that area based on the depth categories. In an area that would be defined as having a knee to waist (1.5 – 3.3 ft) depth, 34 participants selected a 'Moderate Risk' while 13 participants selected 'High Risk'. Participants were then asked to list features that they liked/disliked from the map. The simple layout and understandable content of the map were both 20% of the favorite features of the map; features that were specifically identified as useful were the legend/layout (14%) and color ramp of layers (18%). A significant proportion of participants (27%) indicated that they had no disliked features. However, the major complaint from users (22% of the participants) was the slow loading speed of the site. The final question of the survey asked participants if they would be likely to use a map with this kind of framework in the future and approximately 80% of the participants selected 'Yes' (**Figure 6**). Overall, participants responses were positive about the map framework and any improvements suggested could be attained through continued work on the project.

If more inundation maps followed this basic design framework for map features, would you be more likely to use a resource like this during an

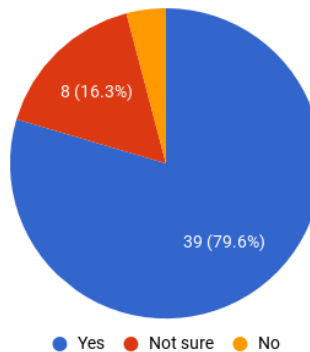


Figure 6. Participant response to use of map with similar framework in future events.

5.2.4. Evaluation Uncertainty

Because surveys were administered through social media outreach, participants were most likely those of close relation to each group member. The overall evaluation results could potentially be biased as the participants may not have been entirely honest in their opinions about map features and map development. Had the individual surveys been administered through another media form, more blind participation would have been able to occur. Another cause for uncertainty is the repeated participant responses. Initial statistics calculated for Round One and Two surveys were incorrect due to these repeated responses and had to be manually corrected.

5.3 Final Web Map Interface:

After incorporating public input, the web map interface was finalized (**Figure 7**). Some of the main features on the map include selectable layers showing a recent historic flood inundation extent, two forecast inundation maps showing extent and depth, and clickable points that show photos taken at that location with descriptions of depth at the time of the image. There are also sections in the legend that users can open to click on terms to get term definitions and a set of links such as the National Weather Service and USGS websites for users to find more information. Participants expressed interest in a local forecast, so a weather widget was added beneath the map which displays current weather and can be clicked to see the forecast.

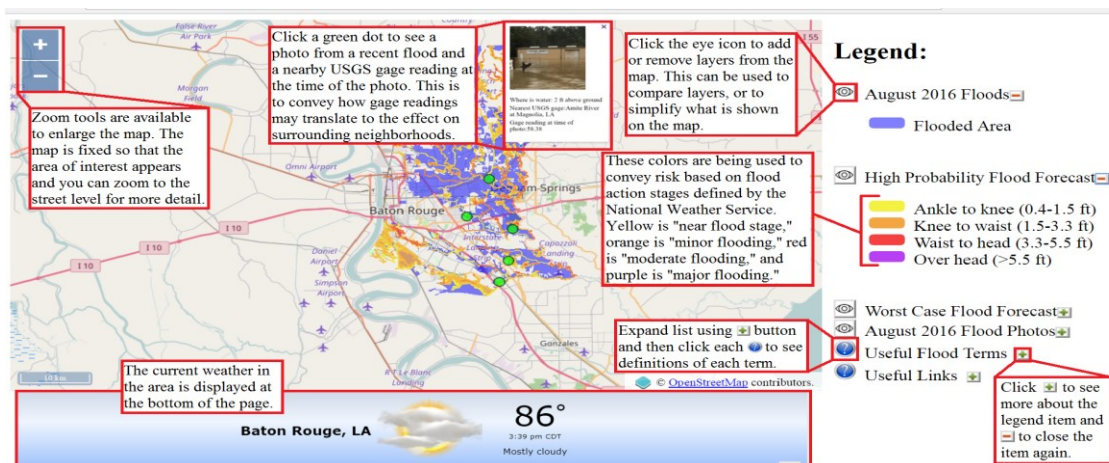


Figure 7. Finalized web interface for Baton Rouge complete with features recommended through the public feedback. Text on the figure explains how to use each map feature. Web map for Dallas (not shown) follows this same framework.

6. Conclusions and Future Work:

With increasing frequency of hazards such as flooding, it becomes critical that the communication of flooding and its risk be understandable to the public. Current flood inundation maps are too technical and complex in nature, making it hard for the average person to retain any sort of information from them. An evaluation with three rounds of surveys were administered to the public over the course of the project to gain insight into their opinions on project development. Through working with the public, a conceptual framework was able to be created for future FIMs implementing features they identified as useful/helpful.

Given the limited time frame for the project, we were unable to execute all features or methodologies. Future probabilistic inundation forecast layers would, and should, use NWM current and predicted discharge over the course of the event to create more accurate FIMs. Throughout the evaluation the public repeatedly expressed interest in features such as emergency routes or real-time social media data input. These features were unable to be executed because they require situation specific data input, which were unavailable during the project. More time for enhancing the functionality of features would help further the success of the framework as well as the overall usability of the tool for the public. Due to the large nature of the data layers, the rendering of each layer took time to load rather than being instantaneous. Hosting the web map through a different hosting server would help correct this issue, allowing a faster, more streamlined experience for the user.

Evaluation participants expressed interest in features like location identifier and control over individual depth layers, however these were unable to add to the web map during the project span. Additional features need public consideration before implementing. This will ensure that any features included in the final map help enhance and compliment any information the FIM tries to convey to the user. As public perception and understanding of flooding varies greatly from the scientific community, it is imperative that their level of understanding be taken into consideration. To create a truly successful tool that is not only simple, but conveys the correct information and message, public input should be used in the design of future mapping frameworks. This will help bridge the gap

between science and the public, allowing for a greater universal comprehension of flooding and its risk.

Supplementary Materials: The final website of Baton Rouge can be found at <https://bradleycarlberg.github.io/oofda/mapcreation.html> and Dallas can be found at https://bradleycarlberg.github.io/oofda/Dallas_mapcreation.html. The codes are house in a GitHub repository found at <https://github.com/bradleycarlberg/oofda>. Survey questions can be found at <https://goo.gl/forms/f3A86FbasmGZMakk1> for Round 1, <https://goo.gl/forms/iI7IPKks5Q8jcfDv2> for Round 2, and <https://goo.gl/forms/txVN8IE3ZMTKaGmF3> for Round 3.

References:

1. Haer, T., W.J.W. Botzen, and J.C.J.H. Aerts. "The Effectiveness of Flood Risk Communication Strategies and the Influence of Social Networks: Insights from an Agent-based Model." *Environmental Science & Policy*. Elsevier BV, 01 Jan. 1970. Web. 19 July 2017.
2. Kunreuther, H. (1978). Even Noah built an ark. The Wharton Magazine (Summer), pp. 28–35.
3. Peek, L. A. and Mileti, D. S. (2002). The history and future of disaster research, In: R. B. Bechtel & A. Churchman (Eds.), *Handbook of Environmental Psychology* (pp. 511– 524). New York: John Wiley & Sons.
4. Grothman, T. and Ruesswig, F. (2006). People at risk of flooding: Why some residents take precautionary action while others do not. *Natural Hazards*, 38, pp 101-120.
5. National Oceanic and Atmospheric Administration (NOAA), 2016, accessed July 19, 2017, at <https://www.climate.gov/news-features/event-tracker/august-2016-extreme-rain-and-floods-along-gulf-coast>.
6. Watson, K.M., Storm, J.B., Breaker, B.K., and Rose, C.E., 2017, Characterization of peak streamflows and flood inundation of selected areas in Louisiana from the August 2016 flood: U.S. Geological Survey Scientific Investigations Report 2017-5005, 26 p., <https://doi.org/10.3133/sir20175005>.
7. East, J. W. (2016). US Geological Survey response to flooding in Texas, May–June 2015 (No. 2016-3027). US Geological Survey.
8. Texas A&M University (2015). Climatic bulletins—May 2015: Texas A&M University. Office of the State Climatologist. Accessed 5 July 2017. <http://climatexas.tamu.edu/climatic-bulletins/may-2015/>.
9. Baddour, D. (2015). Texas flood damage could top \$3 billion for 2015. Houston Chronicle. Accessed, 5 July 2017. Repko, M. (2015). Dallas County damage more than \$61M after extreme rainfall, floods. Dallas News. Accessed, 5 July 2017. <https://www.dallasnews.com/news/news/2015/06/08/dallas-county-damage-more-than-61m-after-extreme-rainfall-floods>

Chapter 10

FloodImpact: A Web Application to Identify Flood Extent and Community Vulnerabilities for Real-time Weather Forecasts

Suzanne Goldstein¹, Chiamaka Oyekwe-Madumelu², Jason Regina³ and Arpan Man Sainju⁴

¹ San Francisco State University, sgoldst1@mail.sfsu.edu

² University of Texas at Dallas, cxo121730@utdallas.edu

³ University of Wyoming, jregina@uwyo.edu

⁴ University of Alabama, asainju@crimson.ua.edu

Academic Advisors: Leonard Sklar, *San Francisco State University*; Bryan Chastain, *University of Texas at Dallas*; Fred Ogden, *University of Wyoming*; Zhe Jiang, *University of Alabama*

Summer Institute Theme Advisor: David Maidment, Univ. of Texas at Austin, maidment@utexas.edu

Abstract: Water resource managers, emergency responders, and the general public do not currently have widespread access to flood forecast information linked with projections of potential community impacts. We developed a web-based application, called FloodImpact, that combines real-time estimates of inundation depth and extent with local level data on community impacts. The application displays on-the-fly estimates of potential population affected, number of address points, emergency services facilities, and other community assets threatened by flood. The application uses several commonly available open-source tools, publicly available datasets, and the Tethys web-development platform to automate inundation prediction and community impact estimates. The workflow has potential for deployment in underserved and “hydro-blind” regions.

1. Motivation

The National Water Model simulates current and forecasted streamflow for the entire Continental United States (CONUS), with current research focused on hyper-resolution flood forecasting. Such flood forecast information could be extremely useful to emergency responders, water resources managers and the general public, particularly when paired with localized information on the people and infrastructure that may be in harm’s way. Currently, there are a few web-based applications that provide flood forecast information to the general public, however to our knowledge none link inundation forecasts to community impact data on a real-time basis for the entire CONUS. Such information would be especially helpful for hydrologically-blind regions – areas that suffer from a lack of real-time hydrometric measurements and flow forecasts. Officials and the general public in hydro-blind areas may be forced to plan for and react to extreme flood events with insufficient advanced warning and scarce real-time intelligence. Especially in regions where flash-flooding is common, lack of advanced warning has led to significant property damage and loss of life. The FloodImpact project was developed to address these gaps in flood information services.

2. Objectives and Scope

The goal of our project was to create a web-based application with a user-friendly interface that would provide real-time information about flooding extent and community impacts in any local area of the U.S., with a focus on information of greatest immediate interest and use to both the general public and emergency responders. While a number of products already exist to communicate flood risk and support emergency planning, many of these are limited to selected geographic areas and/or are not dynamic enough to respond to real-time weather forecast information. Further, those that do have real-time functionality often contain information that is aimed more at scientific than general public audiences and can therefore be difficult for the public to navigate.

We set out to build the workflow for a web application that would demonstrate how all the necessary data retrieval, modeling and visualization processes could be connected to provide localized information on forecasted flooding and associated social and economic impacts. On the back-end, our objectives were to:

- Automate the exchange and analysis of datasets across the different technology platforms necessary for the entire workflow.
- Design a modular system that could allow for modifications to individual components, e.g., changing the flood modeling method or the web application platform.
- Use data sources and methods that could allow for the application to be scaled to work for any location in the United States.
- Incorporate hyper-resolution flood modeling and social and economic data in order to display impact at a locally actionable scale.

On the front-end, we wanted to create a clean and simple user interface that would:

- Display flood information relative to a user's location.
- Map forecasted flood inundation area and water depth based on real-time precipitation forecasts.
- Identify locations of vulnerable populations and critical infrastructure at risk of inundation.
- Provide summary statistics data on potential social and economic impacts of the flood event.

As the Summer Institute proceeded, we maintained our overall objectives, but we had to scale back our implementation methods in several areas. Most notably, limited computing capacity led us to lower the resolution at which we ran our chosen flood inundation model, and to supply the application with social impact data for a limited geographic area corresponding to our prototype case study area. In addition, we did not upload and build the user interface for all available social and economic datasets. Rather, given time constraints, we decided to focus on demonstrating effective functionality and visualization for a few of the most important data.

3. Previous Studies

To guide the project design, we conducted a limited review of the research literature on flood modeling, visualization and mapping, and social vulnerability to flooding. We also searched for existing

web-based and mobile applications designed to communicate flood inundation information. Several tools exist that convey flood forecast information based on precipitation or discharge forecasts. However, relatively few products provide on-the-fly estimates of potential social or economic impacts due to a forecasted flood. Dewetra and the Flood Inundation Mapper both offer data assimilation capabilities similar to those planned for FloodImpact. Dewetra is a web-based platform, developed by the International Centre on Environmental Monitoring (CIMA), that can combine real-time and forecasted flood and wildfire risk information using a geographic information system (GIS) interface. The Flood Inundation Mapper produced by the United States Geological Survey (USGS) displays inundation maps from a library and for some locations provides pre-calculated social and economic impact data. When designing FloodImpact, we wanted to go beyond presenting estimations of discharge and flood extent. We wanted to provide an application that highlighted the potential effects of impending inundation in terms of people and services affected.

4. Methodology

The web-application has four primary components: the inundation forecast scheme, social and economic data retrieval, data processing necessary to estimate potential community impacts, and visualization using the Tethys-based user interface. A schematic of the application workflow is shown in **Figure 1**.

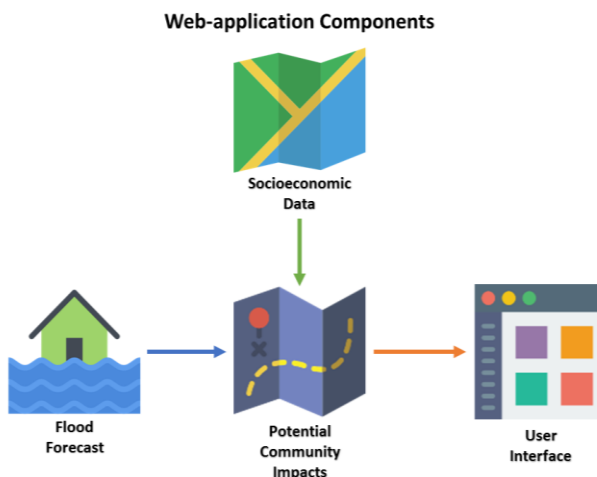


Figure 1: Web-application Workflow Graphics used courtesy Madebyoliver and Nikita Golubev from flaticon.com

4.1. Inundation Forecasting

To produce inundation maps, we used the day-1, 24-hour quantitative precipitation forecast (QPF) from the National Weather Service as input to the Gridded Surface Subsurface Hydrologic Analysis (GSSHA)⁽¹⁾, a hydrological model developed by the Army Corps of Engineers. To automate the process, we created a batch script which runs every 24 hours using Vixie-cron, to retrieve the most recent QPF via FTP and initiated the modeling. Several tools from the Geospatial Data Abstraction Library (GDAL) were used to convert the QPF to GSSHA input and to convert the GSSHA output to vector and raster representations of flood extent and depth. These output files are served to the application interface using Dropbox, a file-sharing service. If flood depths exceeded 0.15 m (6 inches), the batch script would also send a text message to predefined users with instructions to refer to the

FloodImpact application. The batch script uses the Textbelt short message service (SMS) application programming interface (API) to send text messages.

Modeling at high resolution (less than 100 m) can have a high computational cost unsuited to on-the-fly impact estimation. We initially planned to use a “canned-model” approach to develop a database of flood inundation scenarios keyed to forecasted rainfall. However, time did not allow us to build such a database. We decided to work with a relatively simple model of a specific basin that would run quickly enough to produce a timely forecast. Modeling the entire Blanco River basin using GSSHA limited resolution to 150 m, but reduced computational time. Ideally, the inundation forecasting component of FloodImpact would include several basins running at much higher resolution.

4.2 Social and Economic Impact

4.2.1 Data Identification:

A core purpose of FloodImpact is to show the location and number of people and places that are vulnerable to harm from a flood event. The literature on vulnerability to flooding and other natural disasters, identifies at least three different types of vulnerability – physical, social and economic. For the first prototype of our application, we focused primarily on social vulnerability, along with a few indicators of physical vulnerability, drawing on federal government databases to provide potential for nationwide coverage. The literature on social vulnerability identifies a large number of factors, such as age, income, family structure, race, disability, access to transportation, etc.⁽²⁾. Data indicators for all of these factors, separately or in composite indices, could be incorporated into the application with sufficient development time and resources. We began with the most fundamental – age and income. We also incorporated data on housing units, emergency services facilities and transportation infrastructure that could be inundated. **Table 1** shows the complete list of datasets included in the FloodImpact prototype.

Table 1: Data Indicators for Social, Economic and Physical Vulnerability

| Category | Data Indicator | Source* |
|--------------------|----------------------------|---|
| Population | Total population | 2010 U.S. Census, U.S. Census Bureau |
| | Under 18 years old | 2010 U.S. Census, U.S. Census Bureau |
| | 65 years old and over | 2010 U.S. Census, U.S. Census Bureau |
| Property | Income below poverty level | American Community Survey, U.S. Census Bureau |
| | Housing units | 2010 U.S. Census, U.S. Census Bureau |
| Emergency Services | Address points | Texas Div. of Emergency Mgmt. |
| | Police and fire stations | National Structures Dataset, USGS |
| Schools | Medical centers | National Structures Dataset, USGS |
| | Schools | National Structures Dataset, USGS |
| Transportation | Roads | Texas Division of Emergency Mgmt. |
| | Airports | Airports Database, U.S. Dept. of Transportation |
| Land Use | Land cover | National Land Cover Database, USGS |

*See Appendix for full source citations

4.2.2 Data Retrieval:

At the outset of the project, we expected that the methods for assembling the social and economic impact data would be fairly straightforward, involving downloading national datasets from various federal government websites and converting them into formats that could be visualized in a Tethys-based web application. To show flood impacts at a human scale, we sought to use the highest resolution data possible. Most of these datasets are not updated frequently (i.e., annually or less) so we decided to store them directly in the server rather than automate the data retrieval. While we ultimately succeeded in compiling the targeted data, the process was complex and time consuming given the very different retrieval and formatting protocols of each source agency and dataset. The process was further complicated by the fact that we were building our prototype on a single computer which required us to limit the size of data files in order to minimize backend processing time. In addition, metadata was often insufficient to provide complete and accurate understanding of the sources and field definitions for all of the data file contents.

4.2.3 Data Formatting

To create a modular system design that would allow for different data sources to be used in the future, we chose GeoJSON as the standard file format for all of the geospatial data. The GIS shapefiles that are available from many agencies can be readily converted to GeoJSON. However, we found that the graphical user interfaces available to download the shapefiles can be difficult to locate and cumbersome to use, particularly when the data retrieval must be narrowed down to a sub-state study area. Many agencies do now offer APIs that can be used to expedite retrieval into JSON or CSV formats, but each web service has a different retrieval method, research is required to identify the correct codes for desired data fields, and often the geographic location information is not located in the same file. In general, this work would benefit from a more standardized cross-agency approach to data formatting and retrieval.

All of these challenges point to the importance of incorporating state and local datasets in the FloodImpact application since they are often more detailed and accurate. For example, data on critical disaster response information such as the location of emergency shelters or local public transit lines, are not available at the national level. We therefore decided to add a function in the design for the FloodImpact application to allow users to upload their own map layers. Although we didn't have sufficient time to fully implement this function, we did incorporate one such dataset from Texas in our prototype for demonstration purposes.

4.2.4 Data Visualization Methods

For each dataset, we determined the symbols, colors, transparency, and labels that would be simplest for the user to understand. The flood visualization scheme draws on best practices recommended by the USGS and NOAA⁽³⁾, using a blue color scheme graduated from light to dark to represent shallow to deep flood waters. Each social impact data type is represented by a different single color, with continuous datasets, e.g., population counts, divided into no more than five unique categories and displayed using a graduated color scale of the same primary color.

4.2.5 Summary Impact Analysis

To effectively convey the potential social and economic impact of a flood event, it is important to use both visual images and quantitative measures. A simple approach, included in our application design, is to sum the counts of people, homes, schools, medical centers, etc. that are located within the inundation zone to the greatest level of accuracy possible (i.e., counts based on census data will overestimate impacts because block totals are included even when only a portion of the block area is flooded). We had initially intended also to provide calculations of potential economic damage, such as the cost to repair damaged buildings, by using Hazus, a FEMA-developed, GIS-based, software package. However, most of the relevant data in Hazus is out of date and would have produced very inaccurate results that could not be quickly recalculated within the web application for variations in the flooded area. Given that inaccuracy and time restrictions, we were not able to include economic damage estimates in this version of FloodImpact. We also considered developing one or more indices to display aggregate social vulnerability across multiple factors in a single map layer. There is a rich literature on social vulnerability indexing to draw from and this is another feature that could be pursued with additional time and resources.

4.3 Data Processing and Management

To connect the flood inundation forecasts and social impact data, we built a set of scripts to create files containing the data on social impacts within a given flood inundation zone. The scripts perform a spatial query for each pre-stored social dataset, testing for overlap, and then extracting all the records that overlap with the inundation extent polygon(s). Those extracted datasets are then converted into GeoJSON format. We used GDAL tools for both spatial overlap testing query as well as to convert shapefiles into GeoJSON format. Finally, after the conversion process is complete, the processed files are stored in a GitHub repository which can be accessed by our Tethys-based web application.

4.4 Tethys-based Web Application

To create a publicly accessible user interface we used Tethys Platform. As described earlier, our goal was to create a clean and simple interface that would be easy for the general public to navigate and would focus on the most pertinent information for the user to comprehend the flood impact. The web application uses OpenLayers, a JavaScript library, to pull the flood extent and flood impact datasets from the GitHub repository and display them as layers on top of the basemap. OpenLayers is also used to set the options for toggling among layers. Different transparency settings aid visualization and allow the user to see the social impacts relative to the flood inundation extent.

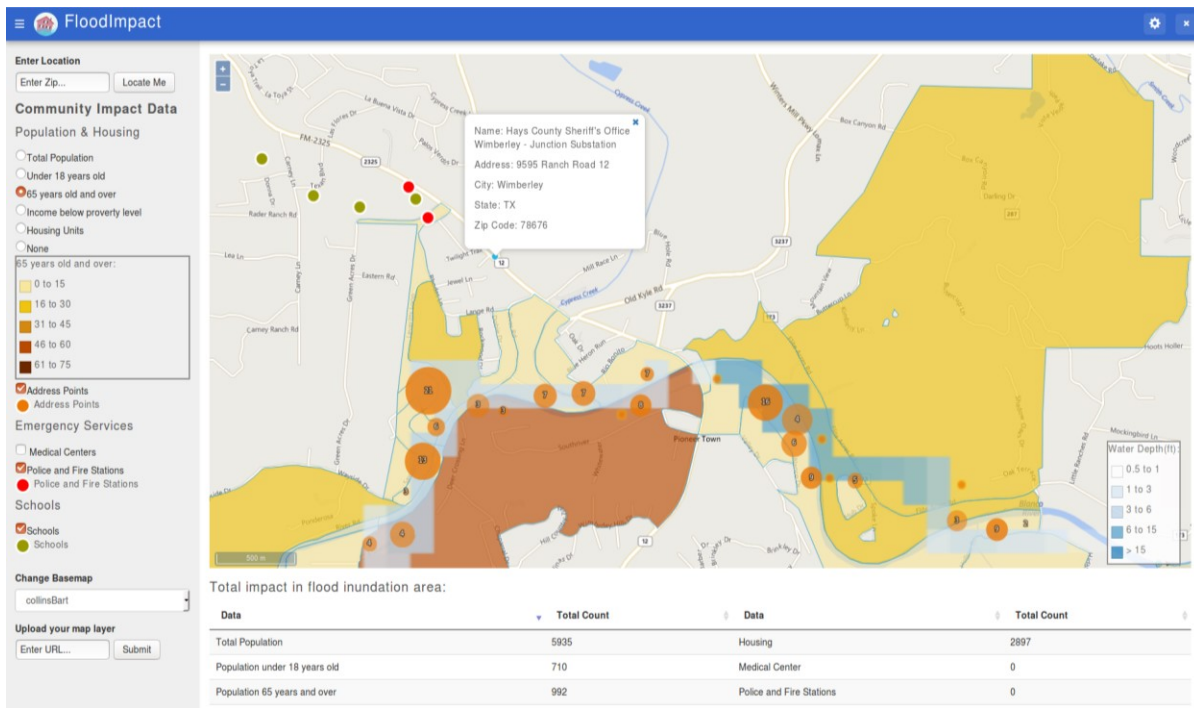


Figure 2. Application Screenshot

As shown in **Figure 2** below, the application contains the following functionalities:

- **Location Selector:** The user may enter an address location which will serve as the center of the area shown in the map view. The user may then pan across and zoom in and out within the extent of the watershed.
- **Map View of Flood Inundation Area:** Bing Maps serves as the basemap which allows the user to toggle between road and satellite view maps. The forecasted flood inundation area is also automatically displayed on the basemap, along with a legend indicating flood depth. The application will not display any data when there is no flood forecast for the user's area. County boundary lines are also prominently displayed since counties are often the first line of defense for flood response.
- **Menu of Flood Impact Data Layers:** The left side of the screen provides a menu allowing the user to toggle layers and view the data for different social and economic impacts. Layers related to population and housing are shown on the map by census block or block group area and each layer must be viewed individually. Other data, such as schools, fire stations, or airports are shown as color coded points and may be displayed simultaneously with a population or housing layer. For each layer, the map view highlights the impacted area for the user by displaying only the data that is immediately in or adjacent to the flooded area. Color coded legends pop up to show the data definitions for each selected map layer.
- **Pop-up Data Labels:** When the user clicks on a point or shape (e.g., census block) on the map, a window will appear providing the name and other available data (e.g., school address, total population count in the block area) for that location.
- **Summary Statistics:** A chart at the bottom of the screen provides total counts of the social and economic indicators within the given inundation zone.

- *Custom File Upload:* The interface includes a placeholder for a function to allow a user to upload their own map layer. Due to time constraints this function was not fully built out.

5. Case Study: May 2015 Blanco River Flood

To develop a prototype of the FloodImpact application we identified a historical flood event that could be used a case study. We established three main criteria for the case study selection:

- Primarily rainfall driven flooding, with no coastal or snow melt driven inundation
- A mid-size urban area with socio-economic variability
- Variation in topographic relief

The Blanco River basin in Texas fulfilled all these criteria. The watershed contains both rural and urban areas, and has over 200 m of topographic relief from the upper basin to the mouth of the Blanco River. The basin also has a history of flash flooding due to sudden and intense rainfall. In particular, we were interested in applying FloodImpact to the 2015 Memorial Day Weekend Floods which caused major damage in the Wimberley area.

On May 23, 2015, two high intensity storms released thirteen inches of rain over the course of two hours on the upper Blanco River Basin, west of Wimberley, Texas. A forty-foot flood wave flowed down the Blanco River toward Wimberley, swept away a vacation house and resulted in the deaths of eight people. The population of Wimberley, which had nearly doubled due to the Memorial Day weekend, had little advanced warning of the impending flood. The basin west of Wimberley had no upstream gages at the time, and relied almost exclusively on ground-spotters and blanket flood watches issued by the National Weather Service⁽⁴⁾. To help mitigate such disasters, communities such as Wimberley require a way to quickly process real-time precipitation forecasts into meaningful estimates of flood risk.

Dr. Hatim Sharif at the University of Texas in San Antonio provided our team with a GSSHA model of the Blanco River basin at 150 m resolution. The model included data from the National Elevation Dataset, National Land Cover Database, and the Natural Resources Conservation Service STATSGO soil dataset. Using NEXRAD data, we simulated the May 2015 event from 2015-05-23 00:00:00 until 2015-05-25 00:00:00, and extracted maximum flood depths across the entire basin. We were able to display flood depth information with potential community impacts, as well as provide preliminary summary statistics. However, because our inundation forecast was limited to the area inside the single Blanco River basin, our application did not capture all of the impacts from the May 2015 storm event which affected many neighboring basins.

6. Conclusion

The scope of this project was quite ambitious for the time available at the Summer Institute. The web application required knowledge of hydrological modeling, socioeconomic datasets, web-development, and GIS. Our primary challenges were rapid model development, rectifying the various datasets, and

putting everything in a format usable by the interface. Overall, we were successful in implementing a basic workflow around automation and developing core functionalities, but were limited in terms of scale by available resources.

We found that freely available, well-documented tools, such as GDAL and GSSHA, were relatively straight-forward to learn and deploy quickly. However, complications arose while trying to access, store, and process the various socioeconomic datasets. Furthermore, while the datasets we could acquire were relevant at relatively fine resolutions, the hydrological model output was not. Ultimately, we could not resolve our immediate need for modeled-data at hyper-resolution with our remaining time for implementation. We also discovered that deploying the application interface while retaining our backend functionality was more cumbersome than expected. Our final demonstration was limited to a local machine to retain all functionality. Access to a web-hosting service might have solved this problem.

In terms of future development, we think the model and user interface can be improved. A canned model approach using hyper-resolution flood forecasts might be more ideal for this type of on-the-fly impact estimation. A future modeling component might be based on a database like that used by Canned GSSHA, a previous Summer Institute project. Trying to capture all the complexities of runoff generation in a database might be an application for machine learning. The user interface would benefit from direct testing and feedback from our intended users to ensure the visualization schemes are customized to meet their highest priority information needs. For example, it might be preferable to develop multiple versions of the application to best meet the different needs of emergency responders and the general public. Based on limited feedback, it appears a mobile version is desirable. However, a mobile platform brings additional design challenges involving navigation and visualizations for a small screen. The impact estimates could also be expanded to include economic damage assessments, indices aggregating social vulnerability across multiple measures, and summary statistics by flood depth.

Supplementary Materials: Source code available at <https://github.com/amsainju/FloodImpact>

References

1. Downer, C. W., & Ogden, F. L. (2004). GSSHA: Model to simulate diverse stream flow producing processes. *Journal of Hydrologic Engineering*, 9(3), 161-174.
2. Cutter, S. L. (2016). Social Vulnerability and Community Resilience Measurement and Tools. Retrieved from <http://www.cnid.cl/wp-content/uploads/2016/09/SUSAN-CUTTER.pdf>.
3. Integrated Water Resources Science and Services Consortium (2015). Design for the National Flood Inundation Mapping Services. Unpublished.
4. Thomas, J. (2016). When the River Rises: The Wimberley Floods of 2015. Available online: <http://features.texasmmonthly.com/editorial/wimberley-floods-memorial-day-weekend-2015/>. Accessed 20 July 2017.

Appendix:

Sources of Social, Economic and Physical Vulnerability Data Indicators

2010 Census, U.S. Census Bureau, <https://www.census.gov/2010census/data/>
American Community Survey 5-Year Data (2009-2015), U.S. Census Bureau,
<https://www.census.gov/programs-surveys/acs/data.html>

2016 TIGER/Line Shapefiles, TIGER Products, U.S. Census Bureau,
<https://www.census.gov/geo/maps-data/data/tiger.html>
National Land Cover Database, 2014, U.S. Geological Survey,
<https://www.sciencebase.gov/catalog/item/4f70a43ce4b058caae3f8db3>
National Structures Dataset, 2010-2016, U.S. Geological Survey,
<https://www.sciencebase.gov/catalog/item/4f70b240e4b058caae3f8e1b>
National Transportation Dataset, 2014, U.S. Geological Survey,
<https://www.sciencebase.gov/catalog/item/4f70b1f4e4b058caae3f8e16>
Airports Database (2017), National Transportation Atlas Database, U.S. Dept. of Transportation,
http://osav-usdot.opendata.arcgis.com/datasets/0e872765538d499a883850e3f2ba0848_0
Texas Address Database and Maps, 2017, unpublished data developed for the Texas Dept. of Emergency Management.

Data and Technological Resources for Modeling and Application Development

Canned GSSHA,
https://github.com/CI-WATER/tethysapp-canned_gssha/blob/master/tethysapp/canned_gssha
Vixie-cron, <ftp://isc.org/isc/cron/>
Geospatial Data Abstraction Library, <http://www.gdal.org/>
Dropbox, <https://www.dropbox.com>
Textbelt, <https://textbelt.com/>
GSSHA, www.gsshawiki.com/
OpenLayers, <https://openlayers.org/>
Bing Maps REST Service, <https://msdn.microsoft.com/en-us/library/ff701713.aspx>
National Weather Service - Weather Prediction Center - Quantitative Precipitation Forecasts,
<http://www.wpc.ncep.noaa.gov/qpf/qpf2.shtml>
National Elevation Dataset, <https://lta.cr.usgs.gov/NED>
Natural Resources Conservation Service STATSGO Soil Dataset,
<https://catalog.data.gov/dataset/statsgo>
NEXRAD, <https://www.ncdc.noaa.gov/nexradinv/>

Appendix

1. Summer Institute Leaders



David R. Maidment
Technical Director
University of Texas, Austin



Edward P. Clark
Director, National Water Center
NOAA



Fred Ogden
University of Wyoming
NOAA Senior Scientist



Sagy Cohen
University of Alabama



Jim E. Nelson
Brigham Young University



Sarah Praskiewicz
University of Alabama

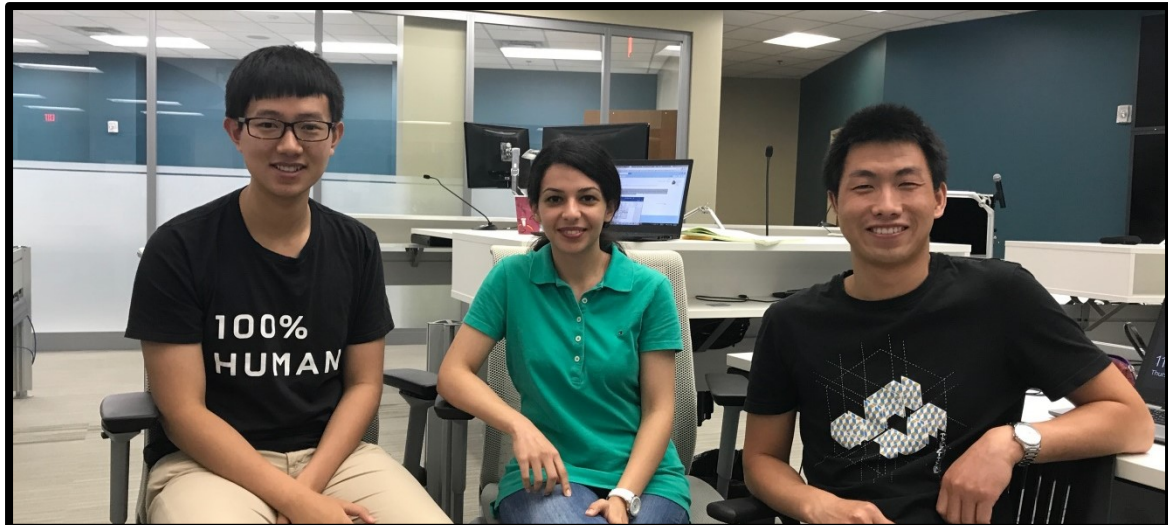
2. Summer Institute Course Coordinators



Jim Coll, University of Kansas
Mike Johnson, University of California Santa Barbara

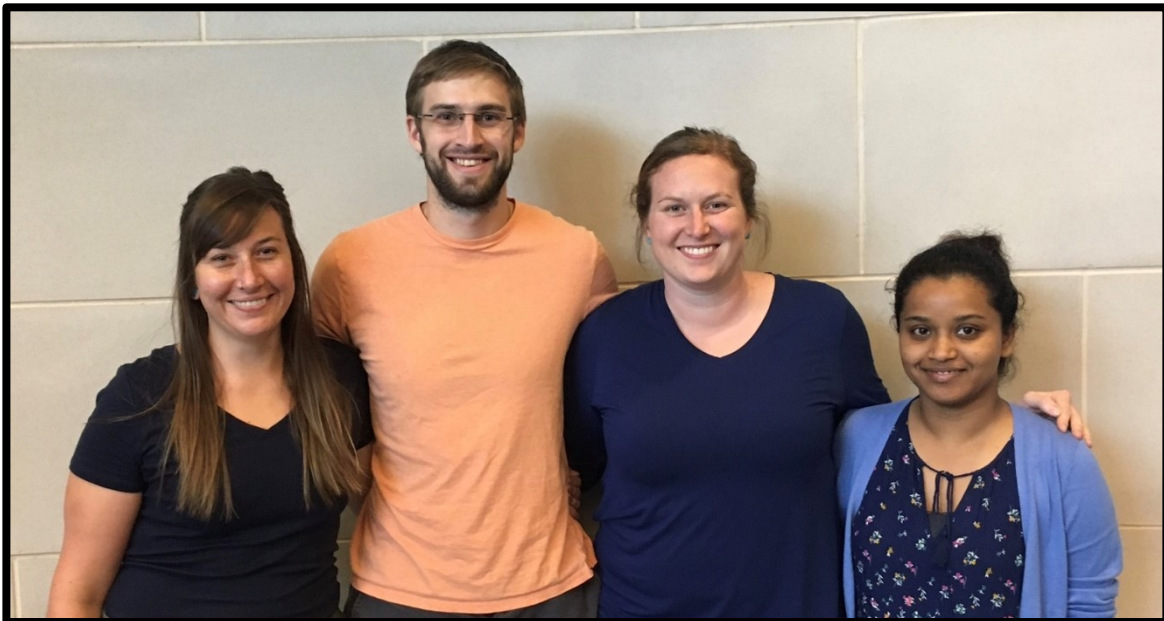
III. Summer Institute Research Fellows

Chapter 2: Comparison of Coarse and High-Resolution Hydrologic Modeling in Mountainous Areas



Qicheng Tang, The Pennsylvania State University
Irene Garousi-Nejad, Utah State University
Siwei He, University of Wyoming

Chapter 3: Unstructured Mesh Resolution in an Urban Watershed



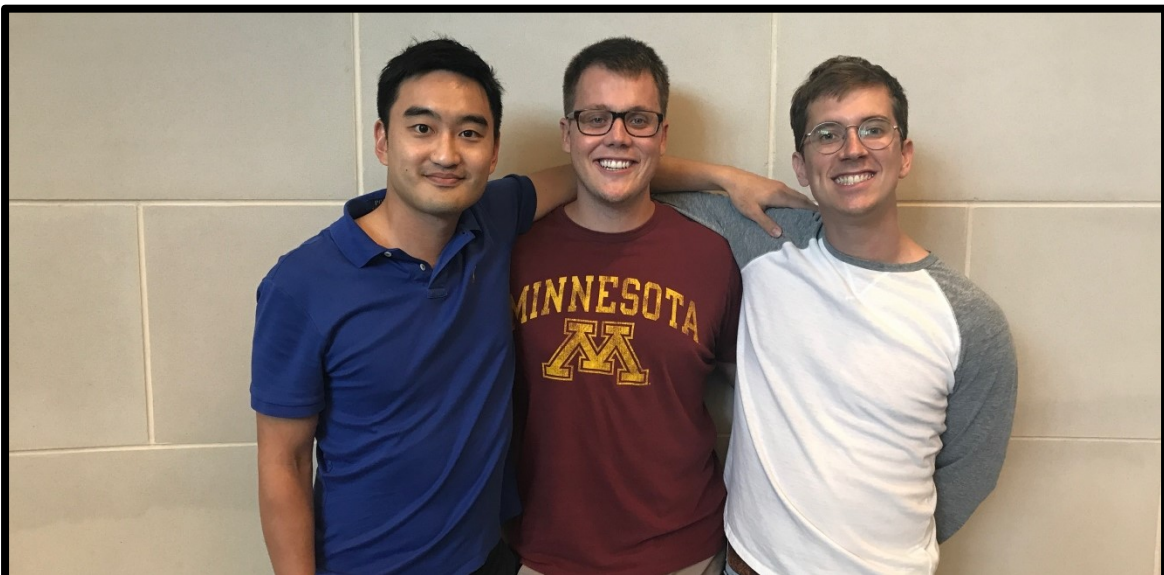
Danielle Tijerina, Colorado School of Mines

Eddie Teirnan, University of Texas, Austin

Lauren Grimley, University of Iowa

Mariam Khanam, University of Alabama

Chapter 4: Assessing the Importance of Different Channel Routing Schemes



Seungwoo Jason Chang, University of Florida

Tyler Madsen, Iowa State University

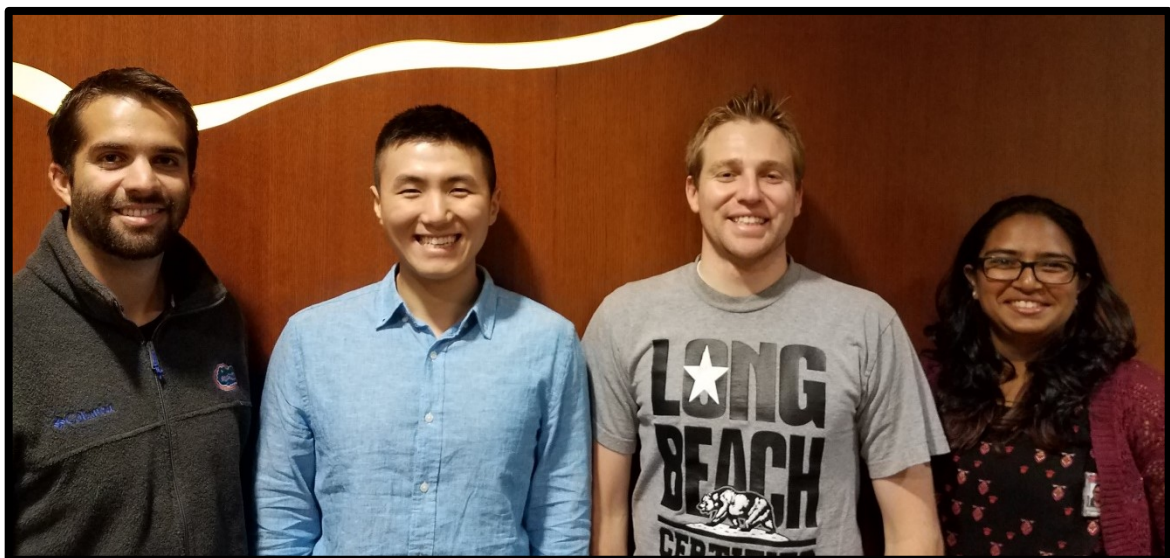
Chris Turnipseed, Louisiana State University

Chapter 5: Integrity Check of Synthetic Rating Curves for HAND Inundation Mapping



Jeff Zheng, University of Texas, Austin
Oludamilola Eyelade, University of California, Santa Barbara
Lukas Godbout, University of Texas, Austin
Sayan Dey, Purdue University

Chapter 6: Comparing NWM Inundation Predictions with Hydrodynamic Modeling



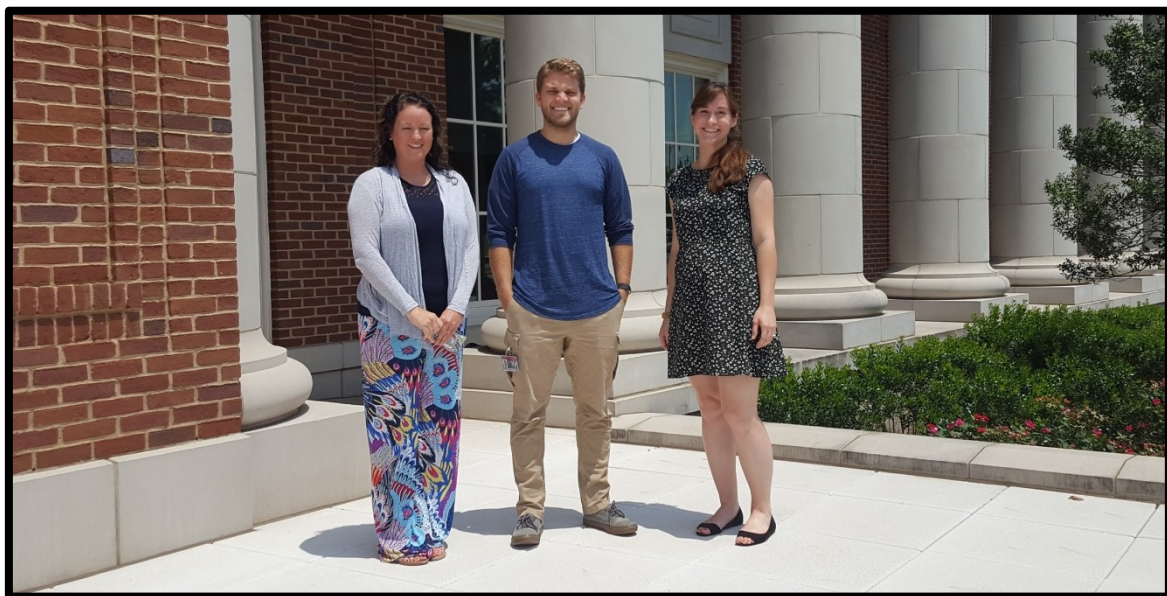
Fernando Aristizabal, University of Florida
Cehong Luo, University of Alabama
Ryan Egbert, Brigham Young University
Apoorva Shastry, The Ohio State University

Chapter 7: Statistical Framework for Analysis of NWM Streamflow Product



Kerim Dickson, Carnegie Mellon University
Aaron Heldmyer, University of Colorado, Boulder
Neelam Jahan, University of Texas at El Paso

Chapter 8: Using the National Water Model Forecasts to Plan for and Manage Ecological Flow and Low-Flow During Drought



April Nabors, University of Alabama at Birmingham
Spencer McDonald, Brigham Young University
Carly Hansen, University of Utah
Javad Shafiei Shiva, Syracuse University (not pictured)

Chapter 9: Using Public Input to Create a Better Online Flood Mapping Framework



Courtney Jackson, The Pennsylvania State University
Brad Carlberg, Iowa State University
Kathleen Eubanks, Louisiana State University

Chapter 10: FloodImpact: A Web Application to Identify Flood Extent and Community Vulnerabilities for real-time Weather Forecasts



Arpan Sainju, University of Alabama
Jason Regina, University of Wyoming
Chiamaka Oyekwe-Madumelu, University of Texas at Dallas
Suzanne Goldstein, San Francisco State University